Biomechanical Approach on Corrective Force Acting on Spine in Scoliosis Deformity Surgery

DOCTORAL THESIS

Remel Alingalan Salmingo
Laboratory of Biomechanical Design
Research Group of Biomechanics and Robotics
Division of Human Mechanical Systems and Design
Graduate School of Engineering
Hokkaido University

学 位 論 文 内 容 の 要 旨
DISSERTATION ABSTRACT

博士の専攻分野の名称　　博士（工学）
Title of Degree　　Doctoral (Engineering)

氏名　　サルミンゴ・レメル・アリンガラン
Name　　Remel Alingalan Salmingo

学 位 論 文 題 名
Title of dissertation submitted for the degree

Biomechanical Approach on Corrective Force Acting on Spine in Scoliosis Deformity Surgery

Scoliosis is a complex pathology characterized as a three-dimensional (3D) deformity of the spine combined with rotation of the vertebrae. The treatment for severe scoliosis is achieved when the abnormally deformed spine is surgically corrected and fixed into a desired shape by application of corrective forces using implant rods and screws. Understanding the magnitude of corrective forces carried by the implant rods is important because overloading can lead to implant rod and bone fracture. The deformation of implant rod is an inevitable consequence of the corrective forces developed by the inherent resistance of the scoliotic spine to correction. The main aim of this study was to analyze the scoliosis corrective forces from implant rod deformation using Finite Element Analysis. The changes of implant rod geometry before the surgical implantation and after surgery were measured to analyze the postoperative corrective forces. A numerical method to measure the intraoperative three-dimensional geometry of implant rod and rod deformation using two cameras is proposed. The intraoperative deformation of implant rod during scoliosis corrective surgery was measured by the dual-camera system and consecutively the intraoperative forces using the proposed method based on Finite Element Analysis. The effect of screw placement configurations, i.e. number of screws and screw density to the corrective forces and degree of scoliosis correction was also investigated. The postoperative corrective forces acting on the vertebrae of the spine were significantly lower than the intraoperative corrective forces. The increase in number of screws tended to decrease the magnitude of corrective forces but did not provide higher degree of scoliosis correction. Although higher degree of scoliosis correction was achieved with higher screw density, the corrective forces increased at some levels indicating that higher screw density is not guaranteed as the optimal surgical strategy. Scoliosis correction is not only dependent on the corrective forces but also with various parameters such as screw placement configuration and implant rod shape.

Chapter 1 briefly introduces the background of the study. The previous studies section discusses the related literatures on corrective forces acting on the implant rod and spine during the scoliosis treatment and the delimitations in relation to the current level of research in the area. The main objectives of this study are also presented.

Chapter 2 provides a general background, biomechanical and clinical aspect of scoliosis as a disease. This chapter presents also the principles of management of scoliosis, i.e. how it is being treated by implant fixation, and the existing problems in which this research study is trying to address from a biomechanics point of view.

Chapter 3 presents a method to analyze the corrective forces acting on the implant rod and vertebra using finite element modeling. The implant rod before the surgical implantation was reconstructed using an elasto-plastic finite element model. This chapter also presents the three preliminary clinical cases that were used to conduct finite element deformation analysis.

Chapter 4 deals with the development of a dual-camera system and numerical method to measure the three-dimensional implant rod geometry intraoperatively for scoliosis deformity surgery. The results of the validation experiment to establish the accuracy of the dual-camera system using the actual implant rod utilized during scoliosis surgery are presented.

Chapter 5 presents the effect of various screw placement configurations on the magnitude of corrective forces and degree of scoliosis deformity correction. This chapter discusses the consequences of using more screws and putting screws nearer to each other (screw density) to the magnitude of corrective forces and degree of scoliosis correction. The magnitude of forces did not have significant relationship with the degree of scoliosis correction. The corrective forces tended to reduce when more screws were used indicating that the loads acting on the spine were more distributed. The magnitude of corrective forces increased with higher screw density.

Chapter 6 presents the deformation behavior of implant rod using the changes of implant rod geometry before surgical implantation and after surgery. The influence of the changes of implant rod curvature on scoliosis correction was also presented. A significant relationship was found between the degree of rod deformation and implant rod curvature before surgical implantation indicating that the rod curvature after surgery or the clinical outcome could be predicted from the initial implant rod shape. The changes of implant rod curvature greatly influenced the scoliosis correction because the spine curve can be over or under corrected after scoliosis surgery.

Chapter 7 deals with the clinical application of the dual-camera system to measure the intraoperative three-dimensional geometry of implant rod during scoliosis surgery. The three-dimensional geometry of implant rod at the different phases of scoliosis treatment (i.e. preoperative, intraoperative and postoperative) was measured. The intraoperative forces were also computed.

Chapter 8 summarizes the findings and conclusions of the work, their clinical and biomechanical significance are also discussed.

The work presented in this thesis provides clinicians and bioengineers a new method to measure the magnitude of corrective forces acting on the vertebrae of the spine and implant rod using finite element modeling. The dual-camera system that has been developed gives in-depth insights on the deformation behavior of implant rod at the different phases of scoliosis treatment, i.e. from preoperative, intraoperative, and postoperative phases. The effects of screw placement configuration to the magnitude of the corrective forces and degree of correction will help clinicians to objectively decide which surgical strategy is likely to attain a desirable outcome. The deformation behavior of the implant rod observed in this study revealed that the postoperative implant rod geometry could be predicted from the initial implant rod shape. This is essential for the preoperative planning of the surgical parameters such as decision-making of the initial implant rod geometry. This study brings forward new insights on the effects of spinal instrumentation to the biomechanics of scoliosis correction.

Table of Contents

List of Tables

List of Figures

1

Introduction

1.1 Background

Biomechanics came from the Greek words bios, i.e. “life” and mēchanikē, i.e. “mechanics”), is the study of the structure and function of living organisms such as humans, animals, plants, organs, and cells by application of the mechanical principles. Biomechanics is focused on solving biological problems from a mechanics point of view. The subfields include musculoskeletal, cardiovascular, and respiratory systems, hard and soft tissues, fluid, sport, biotribology, cell and orthopaedic biomechanics.

Orthopaedic biomechanics covers a wide range of topics including mechanics of fracture and fracture fixation, mechanics of implants and implant fixation, mechanics of bones and joints, wear of natural and artificial joints. The collaborative work between the orthopaedic surgeon and bioengineer has turned the artistic nature of orthopaedic surgery into a more established domain of scientific research. The latest research in biomechanics, whether experimental and/or modeling through computer simulation, provides a scientific explanation of the causes of musculoskeletal disorders and evaluation of the treatment methods. The need for advancement of knowledge to provide the best scientific evidence in making decisions about the care of individual patient strengthened the role of doing research in biomechanics. This is true with the poorly understood and inadequately managed orthopaedic diseases e.g. Perthes’ disease, osteoarthritis, musculoskeletal pain, osteoporosis, carpal tunnel syndrome, scoliosis and many more. For the past decades, computer simulation has become an indispensable tool in biomechanics since human experimental investigations can be sometimes unethical, impossible and practically difficult to implement. This is because musculoskeletal research requires human subjects most of the time, e.g. in this study, forces acting on the spine in vivo. Musculoskeletal research includes investigation of the pathologies in bones, ligaments, tendons, muscles, cartilage, joints and connective tissues. Abnormal deviations from its physiological form and function, e.g. spine deformity or scoliosis, significantly affect the quality of life (QOL) of an individual.

Scoliosis is a complex spinal pathology in which a human spine is abnormally deformed in three dimensions combined with vertebral rotation. The most common type of scoliosis is idiopathic scoliosis in which the etiology or cause of the disease remains unknown. Epidemiological studies indicate that scoliosis prevails during the adolescent period and common among females than males. The standard treatment of scoliosis is achieved through surgical treatment. Surgical treatment is attained by application of corrective forces to deform and bring back the scoliotic spine into a straight curve on the frontal plane using implant rods and screws. Several implant designs have evolved and became more advanced in applying the corrective forces three-dimensionally. However, until now, reports on the complications of implant fixation systems such as implant rod breakage, screw pull-out, bone fracture and implant loosening still exist. These could be due to the high amount of corrective forces acting at the spine carried by the implant rod and screws. Indeed, our clinical data revealed a significant deformation of the implant rod when its geometry before implantation and after surgery was compared. The analysis of corrective forces acting on the deformed implant rod is important to understand the magnitude of in vivo loads acting at the vertebrae of the spine.

The main phases of scoliosis treatment include the preoperative, intraoperative and postoperative phases i.e. before surgery, during surgery and after surgery, respectively. Intraoperative tracking of the truck motion has been conducted to gain better understanding of the effects of instrumentation systems on movement or deformation of spinal segments during scoliosis corrective surgery. However, tracking of the changes of implant rod three-dimensional geometry which could primarily affect the correction of spine deformity has never been studied before. To the best of our knowledge, there has been no report on the measurement of the intraoperative implant rod three-dimensional geometry and deformation during scoliosis surgery. Likewise, although analysis of corrective forces acting on the deformed rod before implantation and after surgery is important in understanding the magnitude of postoperative loads, analysis of the intraoperative forces brought by the

orthopaedic surgeons during scoliosis surgery may also provide useful information on the mechanism of correction by studying the in vivo loads carried by the implant rods during surgery.

Several instrumentation systems and surgical strategies were developed to correct scoliosis and prevent surgical treatment complications. However, determining the type of instrumentation system, surgical techniques and strategies remain disputed until now. This is due to the fact that the decision-making of the surgical parameters such as the levels of instrumentation or fixation, types of implants, number of implants, shape and length of implant rod is still dependent on surgeon's experience. The optimal surgical outcome is not achieved due to the variability of surgeon's individual preferences and correction objectives. The number of screws, level of screw placement and implant rod shape should be investigated to establish the effect of these surgical parameters on the biomechanics of scoliosis correction.

Scoliosis corrective surgery requires an in-depth planning of the surgical parameters which will be implemented during the operation. These parameters such as the implant rod shape and screw fixation level are important in achieving the optimal clinical outcome. Unfortunately, there is no consensus on what possible implant rod shape is optimal that could lead to a certain clinical outcome until now. Moreover, since implant deformation is an inevitable consequence of correcting the spine deformity by application of corrective forces, changes in rod shape could alter the sagittal curve and also the clinical outcome. This has also led to the investigation on the deformation behavior of the implant rod during the surgical treatment of scoliosis.

1.2 Previous studies

The goal of this research is to calculate the corrective forces acting on the spine using the deformation or changes of implant rod geometry in scoliosis deformity surgery. It is therefore necessary to review how corrective forces acting on the spine were previously measured.

The corrective forces can be easily explained using the brace treatment method. Figure 1.1 shows a scoliotic patient corrected with a brace. The corrective forces required to deform the scoliotic spine into straight line in the frontal plane are represented as arrows. These forces should be maintained using supports (i.e. brace pads). In this case, the corrective forces are equal to the opposite/reaction forces acting to the braces. Interface corrective force measurement using pressure pads (Pedar, Novel, Munich, Germany) attached to the Boston brace was also conducted in sixteen idiopathic scoliosis patients. They found out that in all positions the mean corrective force at the lumbar brace pad was larger than the mean corrective force at the thoracic brace pad (van den Hout et al., 2002).

Hirsch and Waugh (1968) imbedded the strain gages into the distraction tool and Harrington rod to measure the corrective forces during distraction (tension). The instrumented distraction tool was used to distract the lamina of both lumbar and thoracic post-mortem specimens to measure its ultimate load. It was concluded that the corrective or distraction force should not exceed to 30 kilopond (294 N) as the ultimate load of thoracic lamina. The real-time data of in vivo force was taken within twenty four (24) hours after surgery. The highest axial force found throughout the day during voluntary sitting and standing was only 20 kilopond (196 N).

Nachemson and Elfström (1969) improvised the Harrington rod spreader using a leaf spring and a pointer scale. The modified spreader provides reading of the corrective force from zero to forty kilopond (0-392 N). Although the device does not provide real-time force measurements, it has been used in about sixty consecutive operations without having surgically induced fractures. The instrumented Harrington rod spreader was apparently a useful tool to prevent bone fractures during surgery.

The in vivo force during the surgical procedure has already been measured in Harrington system. Such knowledge is necessary to decide how patients should be managed during the postoperative period. Nachemson and Elfström (1971) developed the wireless telemetry system to measure the in

vivo axial forces acting on the Harrington rod. The rod was modified such that the force gauge Pressductor can be fitted inside (Fig. 1.2). The force gauging system was attached and removed about two to three weeks after the surgical operation. The distraction forces during the surgical operation ranged from 20 to 40 kilopond (196 to 392 N) resulted to 55 to 70% reduction of the Cobb angle. The force declined with time rapidly in the beginning and slowly after three days. After ten days, the recorded corrective force stabilized at about one-third of the maximum force measured during the surgical operation. It was confirmed that the spine (i.e. through adaptation or fusion of bone) takes over a portion of the axial load from the implant rod through time. This implies that through in vivo corrective force measurements, the time of treatment can be well approximated up to when the treatment can be safely discontinued.

Lou et al. developed an electronically instrumented rod rotating device to monitor the torque applied by the surgeons during the derotation maneuver (Lou et al., 2002). The maximum torque applied by the surgeon to the lever arm ranged from 4-12 Nm (equivalent to 20-60 N). A premature trend due to the limited cases confirmed that a higher amount of correction (i.e. preoperative Cobb angle minus postoperative Cobb angle) requires also a higher amount of torque. The acquired torque values strengthened the idea that a significant amount of corrective loads were acting on the implant rod because if the corrective forces don't exist, there will be no torque readings at all. They have shown that too much high corrective forces could cause bone and implant fracture. They concluded also that insufficient forces may not attain the required correction.

Direct measurement of corrective forces acting at the vertebrae of spine is basically unethical and practically difficult to implement. An alternative approach through computer simulation by finite element modeling is essential to understand the magnitude of corrective forces being applied to the spine. Several studies have investigated the biomechanics of scoliosis correction by application of patient-specific finite element models (Aubin et al., 2003, 2008; Lafon et al., 2009; Wang et al., 2011a). These studies were successful in

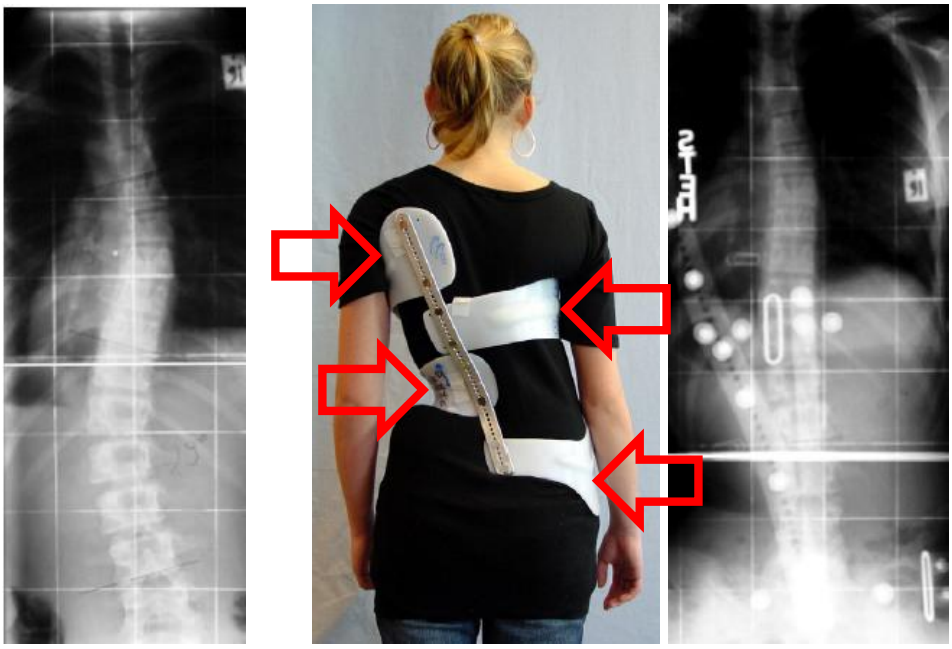

(a) (b)

Figure 1.1 Scoliotic spine corrected with brace. (a) Spine deformity exists before bracing (b) Corrective forces induced by braces after bracing (Redrawn from Weiss et al., 2007).

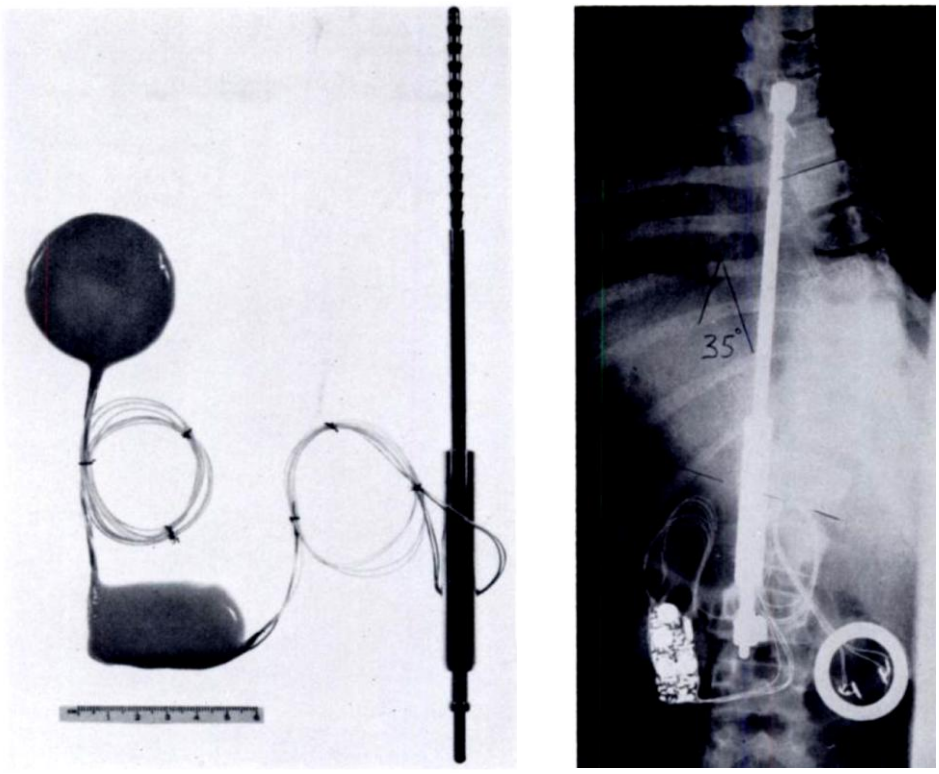

(a) (b)

Figure 1.2 (a) Wireless telemetry system attached to the Harrington rod for measurement of axial corrective forces. (b) Wireless telemetry system attached to the spine of a scoliosis patient (Nachemson and Elfström, 1971).

computing the forces acting on the implant rod-vertebra interface (Fig. 1.3). They also estimated the possible clinical outcome using finite element modeling. Some studies also performed simulation of surgeon's preferences and correction objectives using Finite Element Analysis (FEA) to model the various surgical steps and strategies since the decision-making of surgical parameters such as the levels of instrumentation or fixation, types and number of implants, shape and size of implant rod is still dependent on the individual surgeon's experience and preferences (Wang et al., 2011a, 2011b; Desroches et al., 2007; Majdouline et al., 2009). These studies were conducted to examine the possible advantages and disadvantages between the different instrumentation systems and strategies by comparing the distribution of corrective force acting on the vertebrae of scoliosis patients (Fig. 1.4). However, the magnitude of the forces obtained by these studies might not be so realistic because the analysis was focused only on the elastic deformation of the rod. Elasto-plastic deformation analysis should have been considered. Moreover, the three-dimensional implant rod geometry acquisition methods were limited because they did not measure the actual initial geometry of the implant rod. They just approximated the implant rod geometry from the postoperative radiographs and videos. Thus, it was not possible to obtain the real initial and final three-dimensional geometry of the implant rod and consequently the corrective forces using their methods.

In an attempt to gain better understanding on the effects of instrumentation systems and surgical strategies on the intraoperative correction of spine deformity, electromagnetic system and infrared cameras combined with markers mounted to the trunk were used to monitor the real-time trunk motion or deformity correction during scoliosis surgery (Mac-Thiong et al., 2000; Duong et al., 2009). However, these methods require placement of devices and markers to the trunk which may lead to increased time of the surgical procedure. The intraoperative change of implant rod shape which is one of the primary factors that governs the correction of spine deformity has never been reported before. Thus, a method to measure the

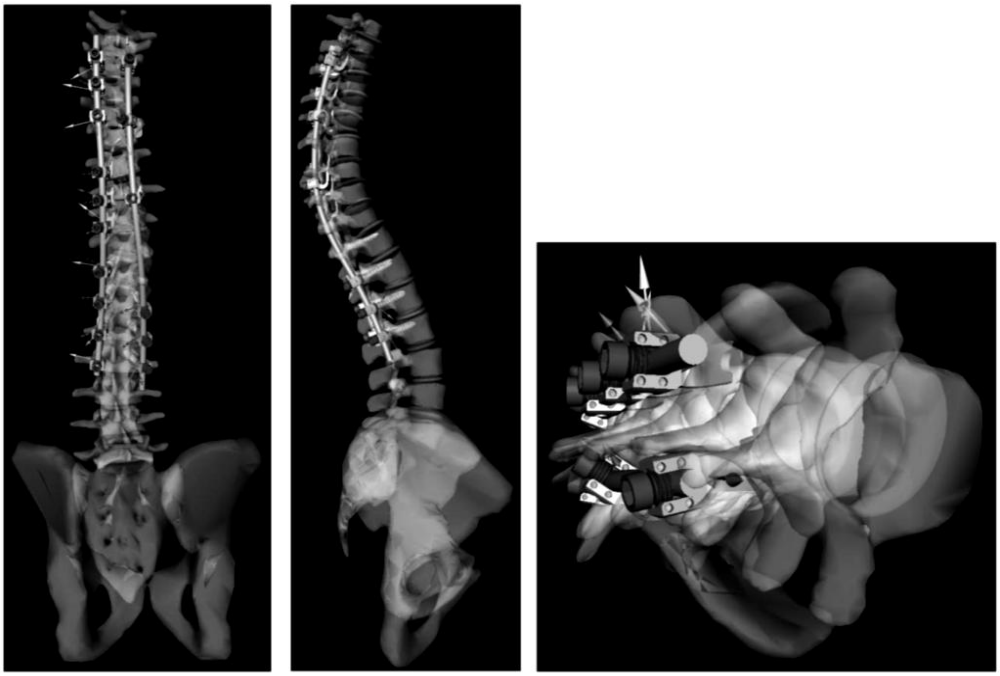

Figure 1.3 Biomechanical finite element modeling of scoliosis surgery. Posterior view (left). Lateral view (middle). Top view (right). The arrows represent the level of the corrective forces between the implant and vertebrae of the spine (Aubin et al., 2008).

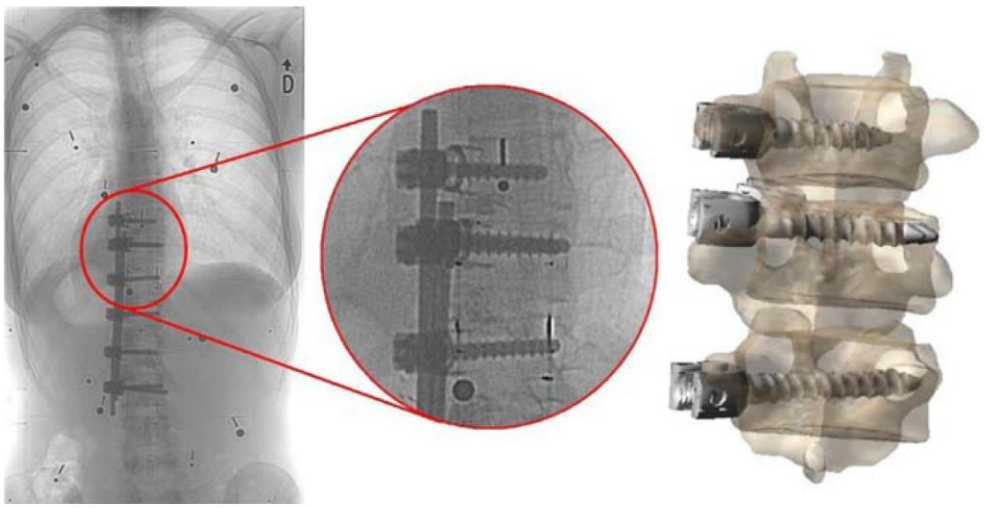

Figure 1.4 X-ray showing fixation of scoliosis deformity by implant rods and screws (left). Finite element model of the spine and implants to analyze the distribution of corrective forces using various instrumentation strategies (right) (Desroches et al., 2007).

intraoperative three-dimensional geometry of the implant rod during surgery is important to understand the biomechanical basis of scoliosis correction mechanism.

1.3 Aims of this study

The direct experimental measurement of the corrective forces acting on the spine in vivo is basically unethical and practically difficult to implement. An alternative method by computer simulation of rod deformation forces through finite element modeling is necessary to be developed. The knowledge that we will obtain can be used for further improvement of the clinical management of scoliosis deformity. The first objective of this study was to propose a method using Finite Element Analysis to compute the three-dimensional forces acting on the spine from implant rod deformation in scoliosis deformity surgery.

The second aim of this study was to develop a new method to reconstruct the intraoperative three-dimensional geometry of the spinal rod using two cameras. This will be used to measure the real-time in vivo three-dimensional geometry of implant rod and deformation during scoliosis corrective surgery. This will help us understand the intraoperative effects of the instrumentation system on the correction of scoliosis deformity.

The optimal clinical outcome is not always achieved because the decision-making on what placement configuration of screw is best to correct the scoliosis deformity remains disputed until now. The third aim of this study was to establish the relationship between the magnitude of corrective forces, degree of correction and screw placement configuration. We also aimed to investigate the effects of screw density on corrective forces and degree of correction.

Until now, there is no consensus yet on what initial implant rod shape could lead to a possible postoperative rod shape. Thus, the fourth aim of this study was to investigate and establish the deformation behavior of the implant rods during scoliosis surgery. This will be done by evaluating the degree of rod deformation from the changes of the implant rod curvature before

implantation and after surgery. The relationship between the degree of rod deformation and the implant rod shape before implantation was sought to establish whether it is possible to predict the postoperative outcome from the initial rod shape. Since the implant rod curvature constitutes also the spine curvature because it is directly attached to the spine through the screws, the postoperative implant rod angle of curvature was also used to evaluate the scoliosis correction at the sagittal plane.

The analysis of the intraoperative forces brought by the orthopaedic surgeons during scoliosis surgery may also provide useful information on the mechanism of deformity correction. The fifth aim of this study was to measure the intraoperative three-dimensional geometry and deformation of implant rod during scoliosis corrective surgery. The previous method to calculate the corrective force from implant rod deformation was used to calculate the intraoperative forces acting on the implant rod and vertebra during scoliosis deformity surgery.

2

Scoliosis

2.1 Background

Scoliosis is characterized as a deformity of the spine in three-dimensions accompanied by axial rotation of the vertebrae. The occurrence of scoliosis as a disease has been recognized clinically for centuries. In fact, its treatment was clearly described in ancient Hindu religious literature around 3500 BC to 1800 BC (Kumar, 1996). The first description of scoliosis morphology was oversimplified, i.e. a two-dimensional deformity characterized by an abnormal lateral deviation of the spine as shown in Fig. 2.1(left). However, the advancement of medical imaging and computing systems redefined scoliosis as a spinal pathology in which the spine is abnormally deformed in three dimensions combined with vertebral rotation (Aaro and Dahlborn, 1981; Drerup, 1984; Hattori et al., 2011; Illés et al., 2011; McKenna et al., 2012; Perdriolle and Vidal, 1987; Stokes, 1994; Tadano et al., 1996).

Scoliosis reduces the quality of life involving pain, diminishing lung capacity and functional impairment due to restrained mobility and inability to work (Maruyama and Takeshita, 2008; Lou et al., 2005). It is classified into four categories: congenital, neuromuscular, degenerative and idiopathic. The first three classifications can be recognized and diagnosed easily as it started from birth, caused by neuromuscular disorders, and effects of aging for congenital, neuromuscular, and degenerative scoliosis, respectively. Congenital scoliosis starts from birth and it is caused by the failure of the vertebrae to individually form or to separate from each other. It is easily recognized as one or more abnormally formed vertebrae as seen from plane radiographs (Erol et al., 2002). Neuromuscular scoliosis is caused by a variety of neuromuscular disorders which include cerebral palsy, spinal cord injuries, syringomyelia, poliomyelitis, duchenne muscular dystrophy (DMD) and myelomeningocele (Berven and Bradford, 2002; Mehta and Gibson, 2003). It is well established that the mechanical properties of the human spine (especially the intervertebral disc) decrease along with age. A type arising from the negative effects of age-related changes in the spine is called as degenerative scoliosis. Likewise, degenerative diseases including osteoporosis

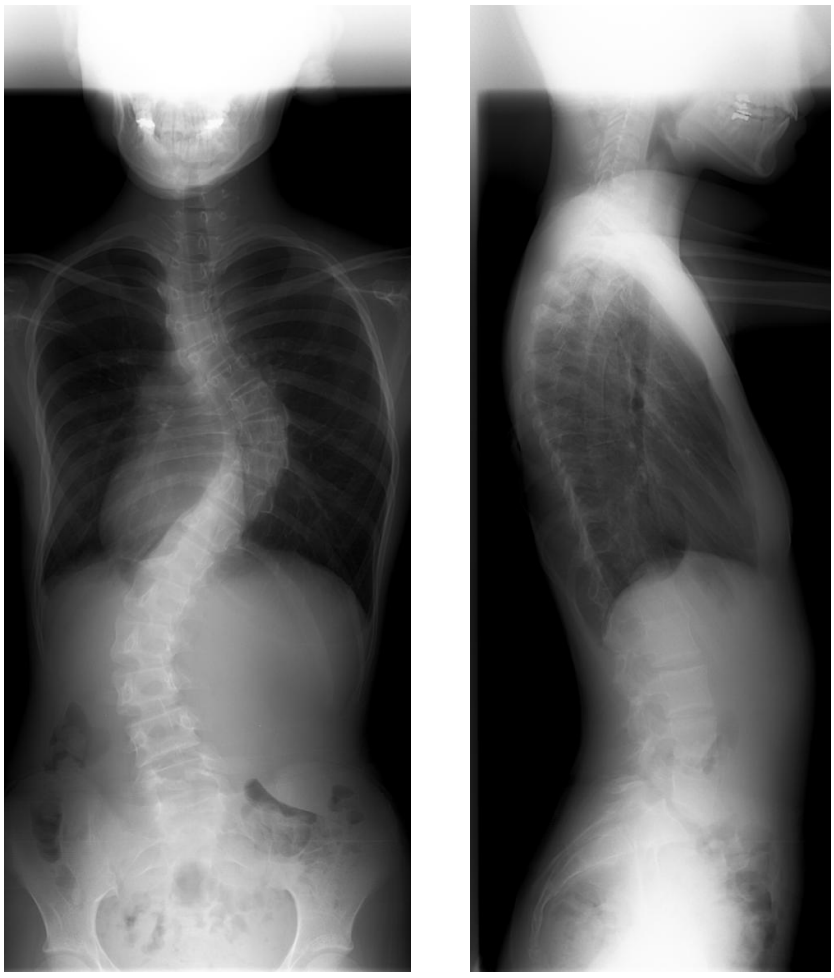

Coronal view (Back) Sagittal view (Right side)

Figure 2.1 Radiographs showing scoliosis.

or a combination with intervertebral disc disease can contribute to the development of degenerative scoliosis (Tribus, 2003). All of the previous three categories are different than idiopathic scoliosis. In idiopathic scoliosis, the etiology or cause of the disease remains unknown. This is the most common type of scoliosis involving 70-80% of the scoliotic patients (Patwardhan et al., 1986; Schroth, 1992). Recently, research has focused on multiple areas since the etiology has not yet been fully understood. The current consensus is that a multi-factorial process is occurring. These include genetic, abnormal biomechanical forces, abnormal neurophysiologic process, connective tissue abnormality and biochemical changes during puberty (Lowe et al., 2000).

2.2 Prevalence and risk factors

In the United States, scoliosis affects 2-3% of the population (Salehi et al., 2002). It affects all ages, gender and races irrespective of socio-economic status. Although scoliosis may occur as early as the age of less than three (Arkbania, 2007), a study showed that the primary age of onset is from 12 to 14 years of age (Riseborough and Davies, 1973). Their study established that the prevalence was associated with age (i.e. during the adolescent period) and gender (i.e. mostly females) (Fig. 2.2). A significant gender dependent ratio was also found between female and male patients seeking medical help at the Katharina Schroth Spinal Deformities Centre in Germany. The female to male ratio of the scoliotic patients was 7:1 (Schroth, 1992). It is now well understood that the onset of scoliosis is during puberty where rapid height growth occurs and females are at higher risk than males.

2.3 Diagnosis and treatment

Diagnosis

Several studies were conducted to diagnose and monitor the progression of scoliosis using noninvasive diagnostic techniques (Bunnel, 2005) to reduce the cancer-related risks of multiple radiation exposures (Doody et al., 2000;

Ronckers et al., 2008). These include moiré topography (Adair et al., 1977; Daruwalla and Balasubramaniam, 1985), Adam's forward bend test (Pierre et al., 1998) and inclinometry or measurement of the angle of trunk rotation observed with the patient in the forward bent position (Grossman et al., 1995). Although these techniques are very useful for early screening and detection, x-rays are still required to accurately establish the diagnosis, severity and progression of the spine deformity (Angevine and Kaiser, 2008).

If the result of the early screening indicates scoliosis, an x-ray imaging is necessary to accurately measure the severity of the scoliotic curve. Generally, the severity of the curve can be quantitatively measured using the Cobb angle (Goldberg et al., 2001). The Cobb angle is defined as the maximum tangent angle between two lines drawn parallel to the end plates of vertebrae in the scoliotic curve (Fig. 2.3).

Treatment

All scoliosis patients that cannot be treated successfully with conservative method (i.e. brace treatment) often need surgical intervention (Dickson and Weinstein, 1999). A consensus was established by the North American Spine Society whether what type of treatment is necessary pertaining to the severity of the curve using the Cobb angle (Table 2.1). Generally, patients with curves between 0-20 degrees don't need any type of treatment. These patients are just observed and followed periodically using x-rays to note any progression of the curve. If curve progression occurs while the person's height growth continues, bracing is recommended for patients with curves of 20-40 degrees (Fig. 2.4). The concept of bracing is well understood that it will not correct the curve but may prevent further curve progression (Bilgic et al., 2010). The successful bracing depends on the amount of time the patient wears the brace. The brace is worn until skeletal maturity for 16 to 23 hours a day. For severe cases, surgical treatment through implant fixation is usually indicated (i.e. curves greater than 50 degrees) and curves that still progress despite of the bracing treatment.

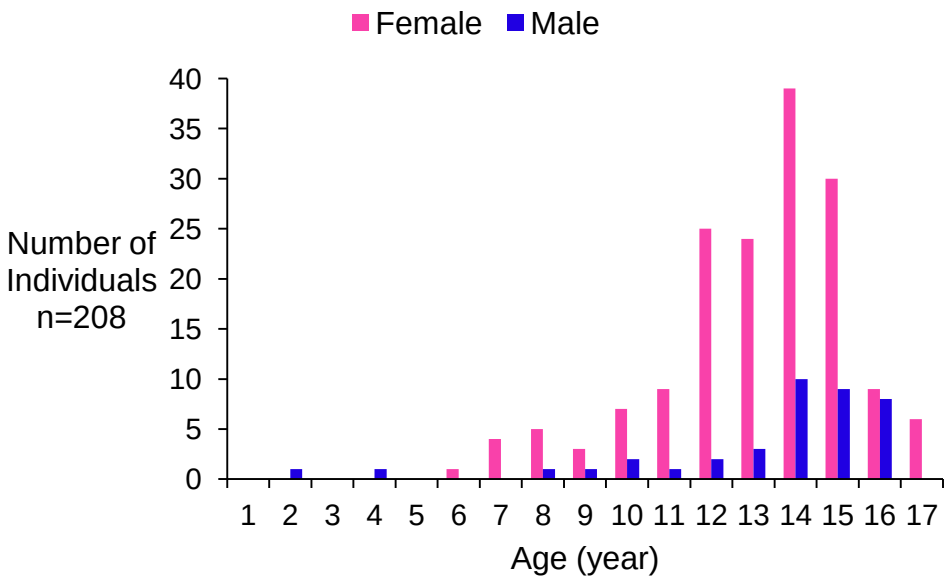

Figure 2.2 Age of onset of idiopathic scoliosis (Redrawn from Riseborough and Davies, 1973).

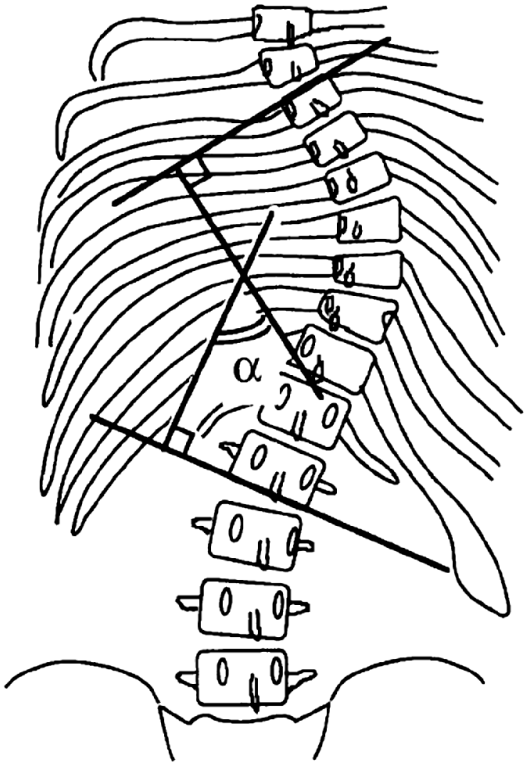

Figure 2.3 The Cobb angle α (Tadano et al., 1996).

(a) (b)

Figure 2.4 Scoliotic spine corrected with brace. (a) Before bracing. (b) After bracing (Weiss et al., 2007).

Table 2.1 Severity of the scoliotic curve expressed in Cobb angle and its corresponding treatment (North American Spine Society).

Curve in degrees (Cobb Angle α)	Treatment
0-20	Observe for progression
20-25	Brace if progression is documented and substantial growth remaining
25-30	Brace if progressive and growth remains
30-40	Brace if growth remains
40-50	Brace if growth remains vs. surgery
>50	Surgery

2.4 Implant rod fixation

Surgical treatment of severe scoliosis requires fixation of implantable devices such as metallic screws, hooks, wires and rods. These devices are implanted and directly fixed into the spine using a surgical technique dependent on the type of fixation system being used. For the past decades, several surgical fixation systems and their corresponding techniques have emerged. These will be discussed in the succeeding sections.

Harrington spinal fixation system

In 1960s, Harrington revolutionized the treatment of scoliosis by introducing the first widely used spinal implant fixation system (Harrington, 1962). A scoliosis case was corrected using the Harrington system as shown in Fig. 2.5. The Harrington system consists of distraction rods and hooks. The c-shaped clamp of the hook is attached (hooked) onto the lamina of the vertebra while the body of the hook is fastened to the rod through its grooves (Fig. 2.5(right)). The hooks in the concave side (left rod) are distracted (i.e. pulled in tension) while hooks in the convex side (right rod) are compressed optionally. As a result, a significant reduction of the scoliotic curve can be observed. The hooks are then fixed into the rods. The hooks carry the distraction (tensile) and compression forces. These implants fix the spine to remain in the corrected shape to prevent the spine from going back to its previous scoliotic or deformed shape. However, during longer follow-ups, the Harrington system demonstrated poor results. Due to its inherent design limitation, (i.e. a two-dimensional correction system) sufficient correction of the rotational and sagittal curve were not attained (Willers et al., 1993). Major complications of the Harrington system include mechanical failure such as rod breakage and dislodgement of hooks from the lamina (McAfee and Bohlman, 1985). The technical difficulties on the use of the system were raised, particularly in securing the hook on the rod at the superior end. The hook at the superior end migrates down the rod resulting in loss of fixation leading to failure of scoliosis correction (Gertzbein et al., 1982). Furthermore, problem

on laminar fracture was raised, it was confirmed that the hook forces were concentrated at the lamina as revealed from the fracture patterns of the cadaver specimens (Freedman, 1986).

The Harrington spinal instrumentation system addressed scoliosis as a two-dimensional deformity. Currently, the mindset has changed. Scoliosis is now referred to as a three-dimensional deformity of the spine with vertebral rotation. Despite of the design limitations and problems, the Harrington spinal instrumentation system has been used for decades. This system has enlightened surgeons and bioengineers to the possibility of using an internal correction system such as metallic devices to correct the scoliosis deformity.

Pedicle screw fixation system

A more sophisticated implant fixation system that can be placed throughout the thoracic and lumbar vertebrae has been developed using pedicle screws and rod. Its name is literarily derived from the part of the vertebra "pedicle", where the screw is inserted into the medullary or central area of the pedicle.

Various methods or surgical techniques on how to fix the pedicle screw to the rod have been proposed (McLain et al., 1993; Schlenk et al., 2003; Schlenzka et al., 1993; Steinmetz et al., 2008). However, the fundamental surgical technique of pedicle screw fixation is almost the same and will be discussed here. The pedicle screw is inserted inside the pedicle through the vertebral body using a screw driver as shown in Figs. 2.6(a)(b). Once the screws are in place, surgeon bends the implant rod to attain a certain curvature corresponding to the severity of the scoliosis case. The implant rod is attached into the head of the screw as shown in Fig. 2.6(c). In this time, the implant rod may still translate or rotate. The setscrews are then attached and tightened in the top part of the screw head of the pedicle screws as shown in Fig. 2.6(d). Thus, the problem on the possibility of implant migration (hook migration) to the spinal canal is not possible in this system. Furthermore, the forces will be more distributed since the implants can be fixed in each vertebra or many vertebrae than the Harrington system (Fig. 2.5).

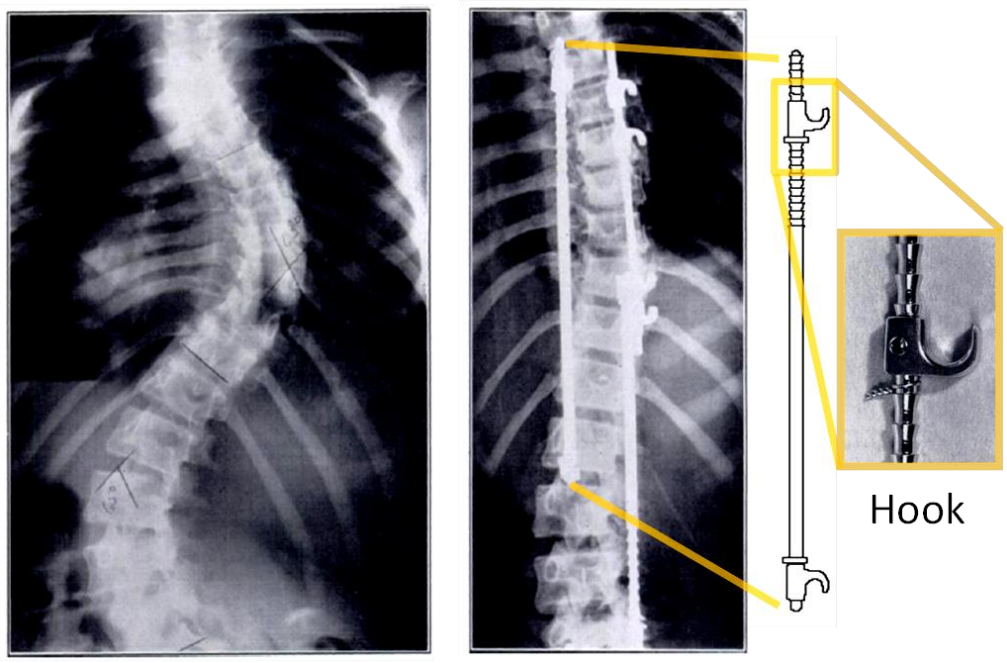

Figure 2.5 Scoliotic spine (left). Scoliosis correction by Harrington spinal instrumentation system (right) (Harrington, 1962).

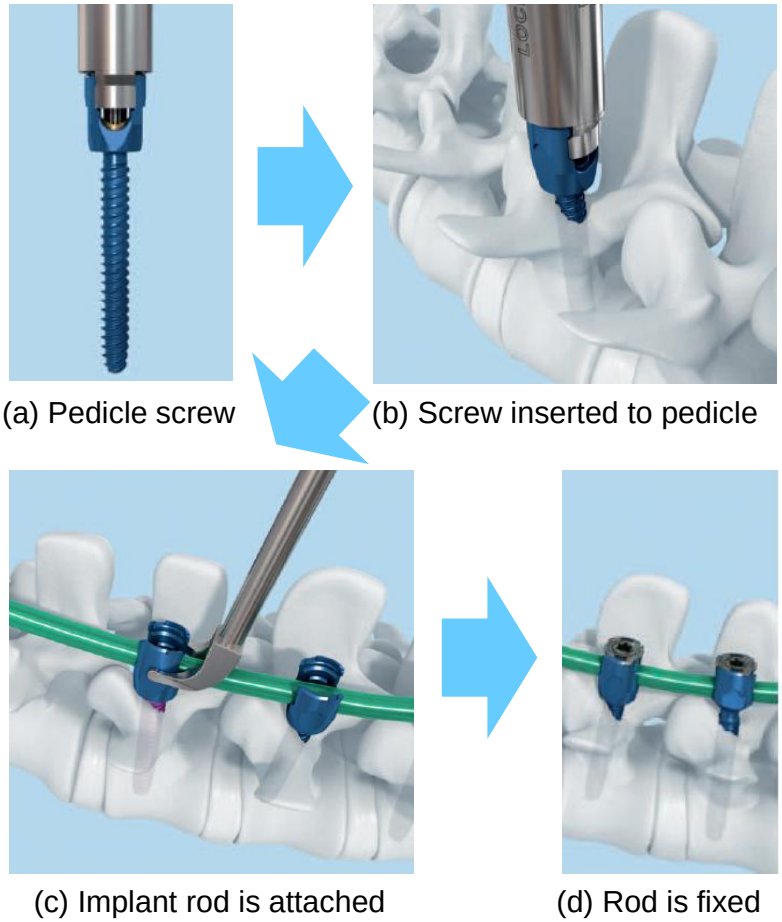

Figure 2.6 General procedure for pedicle screw fixation (Pangea System Technique Guide, Synthes®).

Rod rotation technique

The design capability of the pedicle screw fixation system to correct the deformity of the spine in three-dimensions has set off several correction systems including the famous Cotrel-Dubousset system. In 1980s, Cotrel and Dubousset introduced a new spinal instrumentation system called the CD system that allows the use of rod rotation techniques (Cotrel and Doubousset, 1988). The system includes monoaxial pedicle screw or rigid pedicle screw (i.e. the screw head design doesn't allow temporary screw head movement), polyaxial pedicle screws (i.e. the screw head is designed to allow temporary head movement), laminar hooks and rod. The screws are attached to the posterior spinal elements as shown in Fig. 2.7(a). Scoliosis correction is initiated by attaching a rod to the pedicle screws or hooks at the concave side (left side) of the deformity. Initially, the rod can still move or rotate. A rod rotating device is used to hold and rotate the rod (about 90 degrees). The rotation maneuver corrects the deformity by bringing the scoliotic spine to the midline in the coronal plane as shown in Fig 2.7(b).

Although better curve correction has been attained in the CD system, complications including mechanical failures were still being reported. Guidera et al. (1993) reported a total of 17 complications, including hook pullout, hardware prominence, infection, pseudarthrosis and two cases of broken CD implant rods. This indicates that a single-rod system will not work in all scoliosis cases. Furthermore, four cases of intraoperative laminar fractures and five cases of postoperative hook dislodgement were reported during the use of the CD system (Schlenzka et al., 1993). The undeniable imperfections of the current CD system which may be due also to the fact that the spine itself is still too complex to understand has led to continuous search for better instrumentation system and correction technique.

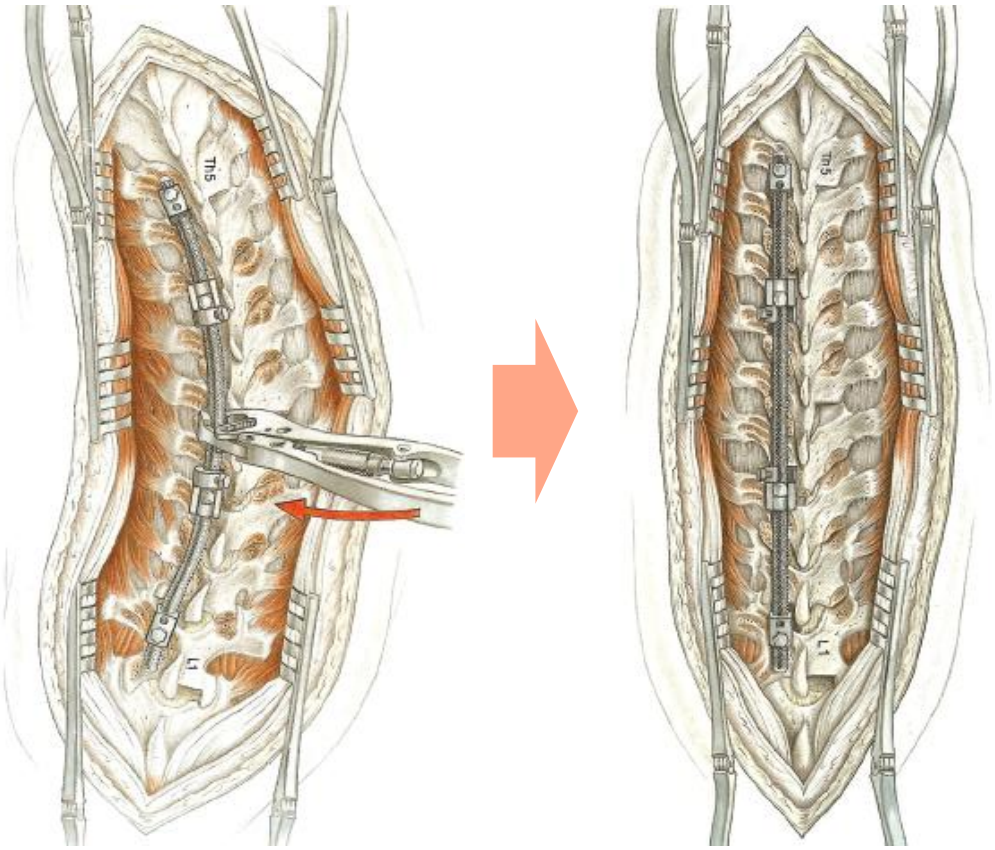

(a) Before rod rotation (b) After rod rotation

Figure 2.7 Illustration of the posterior rod derotation technique using the Cotrel-Dubousset system. (a) A rod rotating device is used to hold and rotate the rod that is temporarily untightened. (b) Curve correction is attained after rotation (Cheng et al., 2008).

2.5 Simultaneous double rod rotation technique (SDRRT)

Due to the existing problems found in the CD system, a surgical correction technique is currently being developed by the Department of Orthopaedic Surgery, Hokkaido University (Ito et al., 2010). The surgeons propose the use of two rods instead of one in order to augment its strength and prevent rod breakage which is currently an existing mechanical problem in the CD system.

The ultimate goal of the surgical technique is to attain the normal curvature of the spine through simultaneous rotation of implant rods. The procedure of the surgical technique using a wood model is shown in Fig. 2.8. Similar to CD system, the polyaxial pedicle screws are inserted first into the vertebra (wood blocks) of the spine. Since the screws are polyaxial, the head of the screw can temporarily rotate if it is not yet fully tightened. This mechanism can be seen because the heads of the screws are oriented at different directions (Fig. 2.8(a)). The implant rods are then inserted into the head of the screws as shown in Fig. 2.8(b). In this time, the implant rods can still translate or rotate because the screws are not yet fully tightened. A rod rotating device is used to hold and rotate the rods. The rods are simultaneously rotated up to 90 degrees. As a result, the previous lateral curvature of the bent rod is transferred into the sagittal plane while the straight profile was transferred into the coronal plane (Fig. 2.8(c)). Thus, the vertebrae are brought together at the same time in the corrected position through simultaneous rotation maneuver of rods.

The implant screws that hold the rods are fully tightened to fix and stabilize the corrected spine. Scoliosis deformity correction is now attained, however, analysis of the implant rod geometry before implantation and after surgery revealed a substantial degree of deformation of implant rod. This implies that the corrective forces developed during the rotation maneuver were high and deformed the implant rod during scoliosis corrective surgery. The biomechanical significance of rod deformation is discussed in the next section.

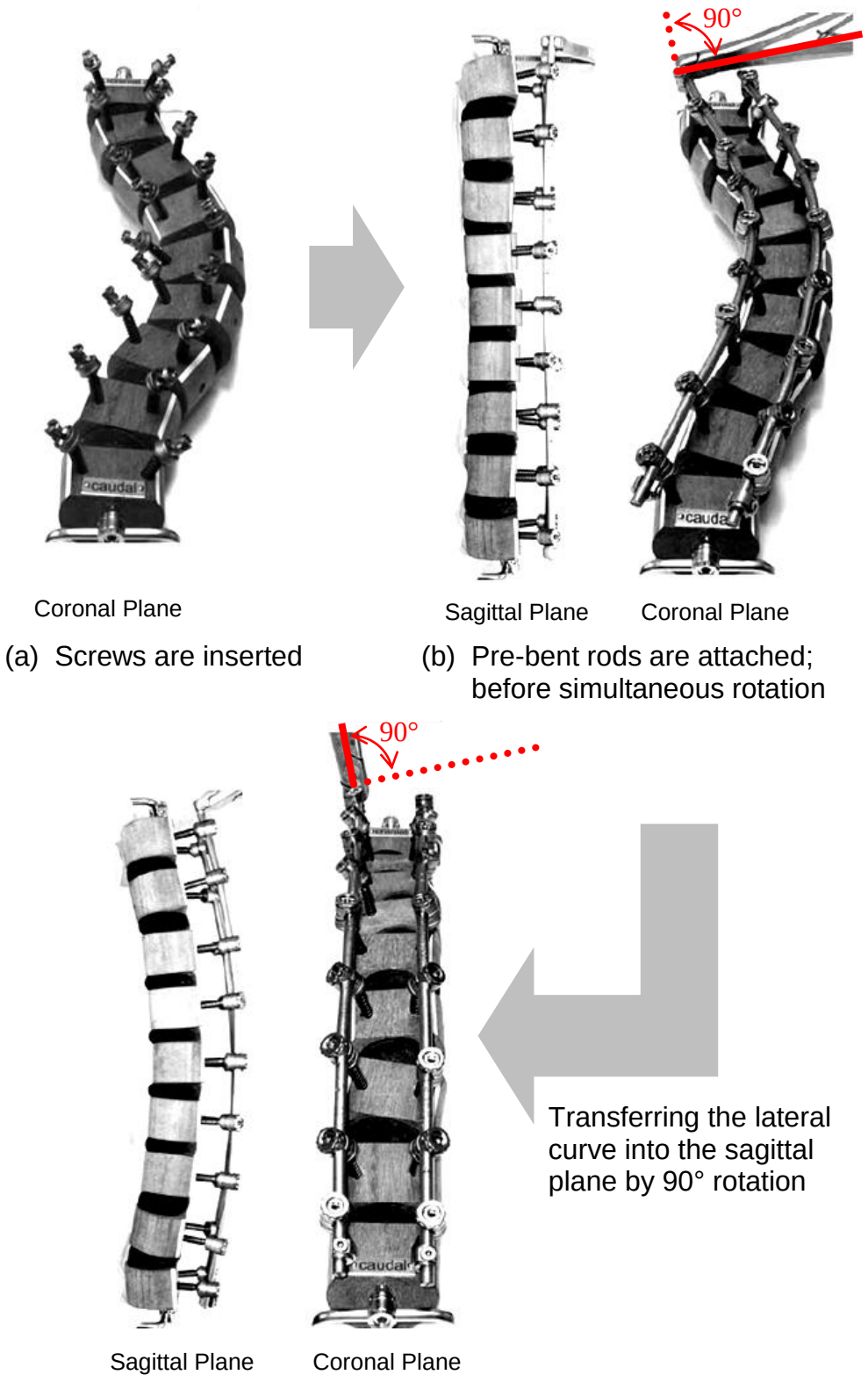

Figure 2.8 Wood model used to simulate simultaneous double rod rotation technique. (a) Polyaxial screws are inserted into the block of wood. (b) Pre-bent rods are attached into the head of the screws. (c) Curve correction is attained after simultaneous rotation of rods (Redrawn from Ito et al., 2010).

2.6 Implant rod deformation

The biomechanical basis of scoliosis correction is to apply suitable corrective forces by deforming the scoliotic spine into a desired shape. A significant amount of force is necessary to deform the scoliotic spine during scoliosis surgery because the inherent spine stiffness provides mechanical resistance to deformation correction. Scoliosis correction is attained by application of corrective force to the abnormally deformed spine using implant rods and screws (Figs. 2.9(a)(b)). The forcefully deformed or corrected spine should be fixed firmly in the corrected position and if not, the spine will go back to the previous scoliotic shape due to its inherent stiffness (Matsumoto et al., 1997; Lafon et al., 2010). Thus, the corrective forces are being carried by the implant rods throughout the fixation period.

In the surgical technique, the simultaneous rotation maneuver of rods is attained when a torque is applied to the rotating device to de-rotate the deformed spine. The torque required for the rotation maneuver corresponds to the corrective forces carried by the implant rod transferred to the spine through the screws. These forces are developed due to the inherent stiffness of the scoliotic spine which resists the deformation correction. The magnitude of the corrective force, however, was high which deformed the implant rod in scoliosis deformity surgery. Figure 2.9(c) shows the three-dimensional geometry of implant rod before surgery (implantation) and after surgery. The implant rod geometry before surgical implantation was measured by the surgeons. The implant rod geometry after surgery was measured by CT imaging. It can be seen that the implant rod was significantly deformed after the surgical treatment of scoliosis. Understanding the magnitude of corrective forces is important to prevent implant and bone overload. If corrective forces are known, its extent may provide surgeons an idea on how to improve the surgical procedures. Likewise, knowledge on the magnitude of corrective forces acting on the implant rods may provide an in-depth understanding of the biomechanics of scoliosis correction. The main objective of this study was to develop a method to calculate the corrective forces from implant rod deformation using Finite Element Analysis.

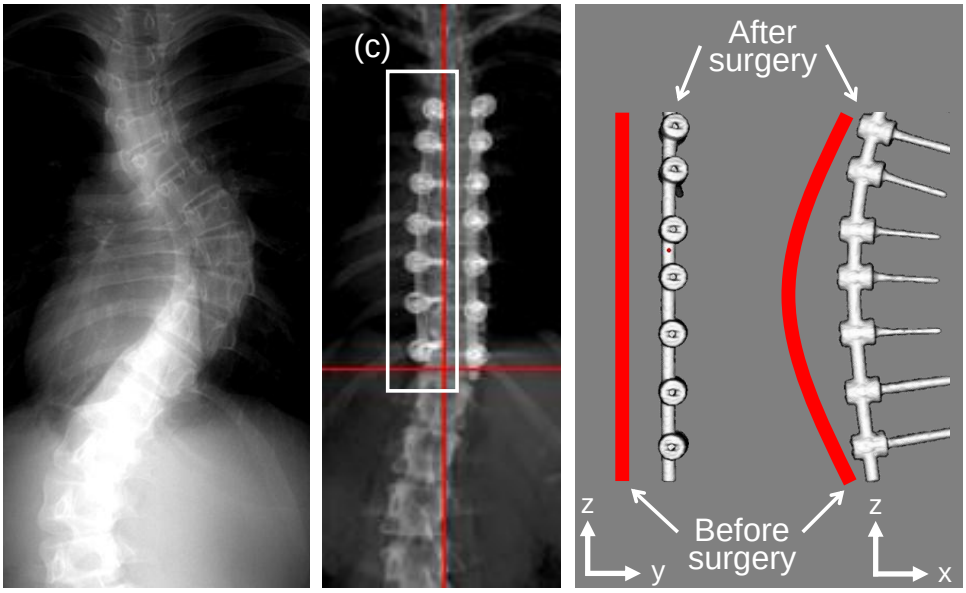

(a) Before surgery (b) After surgery (c) Implant rod deformation

Figure 2.9 Deformation of implant rod in scoliosis deformity surgery.

3

Corrective Force Analysis for Scoliosis From Implant Rod Deformation

3.1 Abstract

Surgical treatment of scoliotic spine is attained when it is fixed into a desired shape by implant rods and screws. Surgical correction was attained, however, the postoperative Computed Tomography (CT) image showed a significant deformation of implant rod indicating that there were corrective forces acting on it after the surgical treatment of scoliosis. A method to analyze the corrective forces acting at the deformed rod using the changes of implant rod geometry before implantation and after scoliosis surgery was proposed. The method was an inverse approach based on Finite Element Analysis (FEA). The geometries of implant rod before implantation and after the surgical treatment were measured three-dimensionally. The implant rod before the surgical implantation was reconstructed using an elasto-plastic finite element model. The three-dimensional forces were applied to the rod model through the locations of the screws. The forces were applied iteratively to the finite element model until the rod model was deformed the same after the surgical treatment of scoliosis. There were three (3) scoliosis patients involved in this preliminary study. The magnitude of corrective forces were obtained after a series of iterations and the maximum force acting at the screw of the three patients ranged from 198 N to 439 N. Based from previous studies, the magnitude of forces obtained in this study was clinically acceptable. We have found out that the maximum forces occurred at the lowest fixation level of vertebra of each patient. The three-dimensional forces acting at the deformed rod were analyzed from the changes of implant geometry using this method.

3.2 Introduction

Treatment of severe scoliosis deformities require surgical fixation of spinal devices such as rods, screws, hooks and wires. Various surgical techniques have evolved and became more sophisticated in applying the corrective forces to three-dimensionally deform the spine into desired shape using spinal implants. These surgical techniques are the rod rotation technique or popularly known as Cotrel-Dubousset (CD) technique, Simultaneous Double Rod Rotation Technique (SDRRT) and other techniques (Cheng et al., 2008; Cotrel et al., 1988; Guidera et al., 1993, McLain et al., 1993; Schlenk et al., 2003; Ito et al., 2010; Zielke, 1982).

Surgical correction of scoliosis deformity requires surgical technique or procedure. In this study, the SDRRT surgical technique was used to correct the scoliosis deformity. Two pre-bent rods were used and inserted into the polyaxial screw heads. The polyaxial screw heads remained untightened until the rod rotation was completed, i.e to permit rotation and translation of rod inside the screw head during the rod rotation maneuver. A rod rotating device was used to hold tightly and rotate the rod. A torque was applied on the rod rotating device to rotate the rod (approximately 90°). During this time, due to the inherent resistance of the spine, the corrective forces on rods are developed through the screws to deform the spine into the desired shape. Scoliosis correction was attained, however, the corrective forces acting on screws were high enough which deformed the implant rod after the surgical treatment of scoliosis. Investigation of the biomechanical changes, i.e. specifically the magnitude of corrective forces which caused the deformation of implant rod in vivo is important in understanding the biomechanics of scoliosis correction.

Several authors had analyzed the corrective forces during scoliosis correction using patient-specific finite element models (Lafon et al., 2009; Wang et al., 2011a). They were successful in analyzing the corrective forces occurring on the implant-vertebra interface. However, the magnitude of forces obtained might not be so realistic because their finite element models were only up to the elastic deformation of the implant rod. Elasto-plastic

deformation should have been considered in their analyses. Also, the rod geometry acquisition methods were limited because they did not quantitatively measure the actual initial geometry of the implant rod. The geometry of the implant rod was just approximated from the postoperative radiographs and videos. Thus, significant limitations still exist because they did not obtain quantitatively the initial and final three-dimensional geometry of rod, consequently the corrective forces using their methods.

The main objective of this study was to propose a method to analyze the three-dimensional forces acting at each screw from the changes of implant rod geometry after scoliosis surgery. These are the corrective forces developed at each screw transferred to the implant rod due to the resistance of spine during scoliosis correction surgery.

3.3 Methods

3.3.1 Force analysis from rod deformation

Figure 3.1(left) shows the posterior CT image of the spine after the surgical treatment. The spine is now fixed by implant rods and screws. The change of the implant rod geometry at the concave side of the deformity before surgery (i.e. before implantation) and after surgery indicate a significant deformation of the implant rod (Fig. 3.1(right)). The deformation of the implant rod was caused by the corrective forces acting on the implant screws. Since the finite element model was three-dimensional, the coordinate system proposed by the Scoliosis Research Society was used to standardize the three-dimensional axes of the implant rod (Yeung et al., 2003). The positive *x*-axis is directed anteriorly, the positive *y*-axis is directed toward the left lateral side and the positive *z*-axis is directed toward the superior direction.

Generally, when a material is deformed, forces occur in accordance to the deformation. Figure 3.2 is a schematic diagram showing the implant rod deformation before and after surgery. The origin (0,0,0) was set at the inferior end of the rod. The three-dimensional force $\vec{F}_i$ acting at the screw (*i-th* from

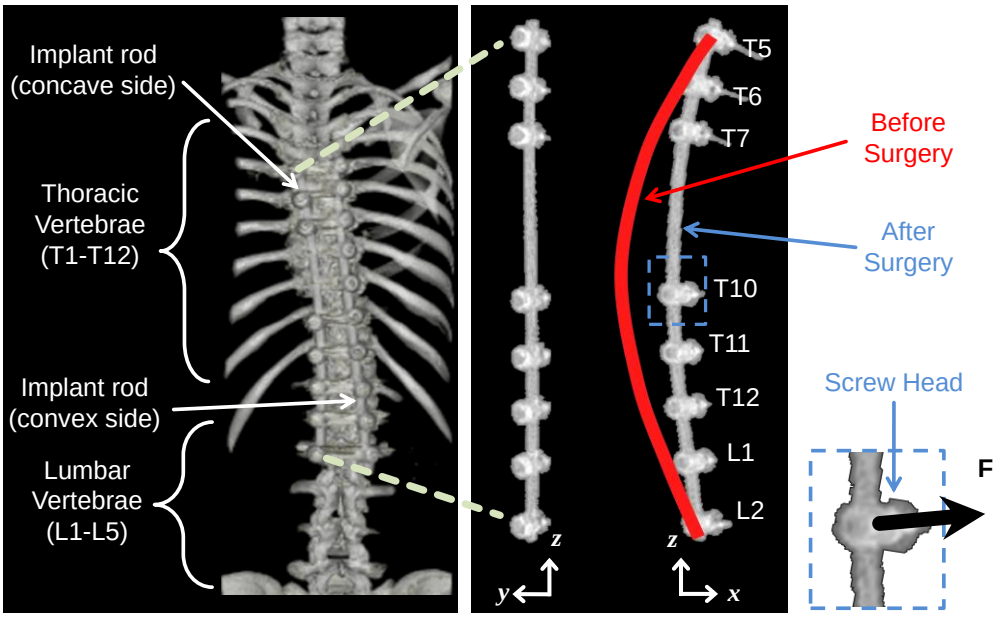

CT image of the spine and rods fixed by the screws

3D geometry of deformed rod and force at fixation point shown in frontal and sagittal view

Figure 3.1 Image showing the corrected spine after surgery (left). Implant rod deformation during the surgical treatment of scoliosis (right).

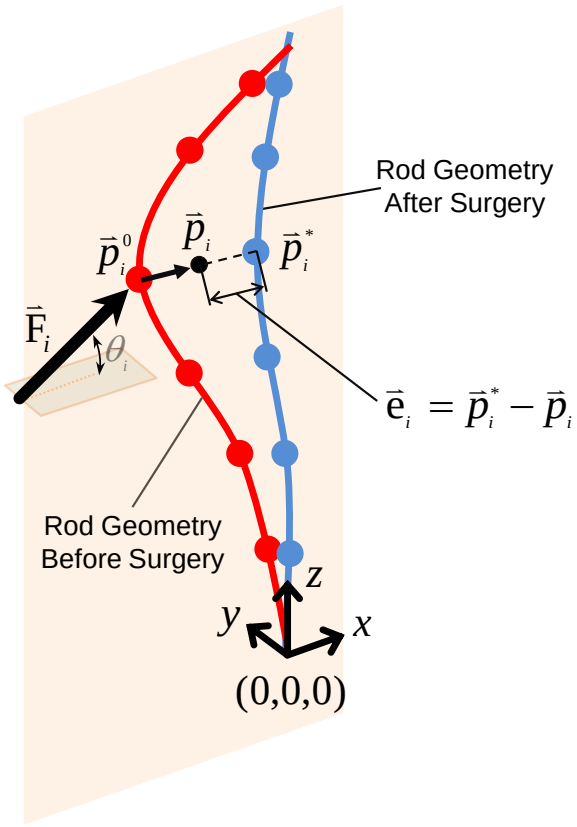

Figure 3.2 Schematic diagram of 3D rod geometry before and after surgery.

the bottom) which displaced the position of the screw before surgery $\vec{p}_i^{\,0}$ into after surgery $\vec{p}_i^{\,*}$ is required in the inverse analysis. Initially, zero force is applied to the screw $\vec{p}_i^{\,0}$; the rod geometry before surgery. The displacement $\vec{p}_i$ is calculated using FEA. To iteratively search the forces acting at the deformed rod after surgery, the difference $\vec{\mathrm{e}}_i$ which is defined as the distance between the screw location $\vec{p}_i^{\,*}$ on the rod geometry after surgery and displaced location $\vec{p}_i$ was used in the iteration process. The direction of the three-dimensional force $\vec{\mathrm{F}}_i$ created from the *x*-*z* plane is defined as the angle θ_i . The direction of force along *y*-*z* plane was neglected because CT acquisition could not accurately detect significant deformation along this side.

Figure 3.3 shows the inverse procedure to calculate the corrective forces from the implant rod deformation. The three-dimensional rod geometries before and after surgery were already known. The rod diameter was 6 mm and the rod length and curvature depends with each patient. The finite element model of the rod was made by a 10 node tetrahedral solid elements using finite element software ANSYS 11.0 (ANSYS, Inc., Pennsylvania, USA). The boundary condition was set considering the manner of rod fixation during the surgical treatment. The screws' coordinates were reoriented or rotated such that the most superior screw coincides with the *z*-axis (i.e. on top of the most inferior screw) because each patient has different implant rod orientation and fixation levels. The most inferior screw at the end of the rod was fixed in all translations but free to rotate while the most superior screw was also fixed except that it was free to move along the superior direction only.

Forces $\vec{\mathrm{F}}_i$ were set with initial negligible values. Elasto-plastic analysis was used because the implant rod was made from a titanium alloy (JIS T 7401-3), i.e. a typical elasto-plastic material. The deformation behavior of the rod in uniaxial tensile loading is shown in Fig. 3.4. In the elastic region $(0 \le \varepsilon \le \varepsilon_y)$, the stress-strain relation and E as the elastic modulus is expressed in Eq. (3.1).

$$\sigma = E\varepsilon \tag{3.1}$$

The stress-strain relationship in the plastic region ($\varepsilon_Y < \varepsilon$) is expressed in Eq. (3.2). The ε_Y is the yield strain which indicates the beginning of plastic deformation.

$$\sigma = E\varepsilon_Y + H(\varepsilon - \varepsilon_Y) \tag{3.2}$$

The material properties of the rod model were Elastic Modulus E, yield stress σ_Y, yield strain ε_Y and hardening coefficient H equal to 105 GPa, 900 MPa, 8.57x10^{-3} and 2.41 GPa, respectively. The von Mises stress was obtained to evaluate the stress distribution along the deformed implant rod.

The displacements from elasto-plastic deformation $\vec{p}_i$ were computed using FEA. The difference $\vec{e}_i$ at each screw location was calculated from the screw location after surgery $\vec{p}_i^*$. The evaluating function which was defined as the sum of the squares of differences on each screw is expressed in Eq. (3.3).

$$\sum_{i=1}^{n} \left|\vec{e}_i\right|^2 < \alpha \tag{3.3}$$

If the evaluating function is greater than α (where $\alpha = 0.5$), the value of the applied forces $\vec{F}_i$ are replaced using

$$\vec{F}_i \leftarrow \vec{F}_i + \beta\, \vec{e}_i \tag{3.4}$$

The constant coefficient β in Eq. (3.4) was introduced in every iteration step to attain a smooth and rapid convergence. The constant coefficient β is equal to 0.5 N/mm. The process repeats until the value of Eq. (3.3) is less than α. The forces at this iteration step are considered to be the optimal forces. These are the corrective forces transferred to the spine because the implant rod is directly connected to it through the screws. Furthermore, the stress or strain distributions of the deformed implant rod caused by the forces $\vec{F}_i$ were obtained in this study.

3.3.2 Clinical geometry measurements

The implant rod initial geometry was measured from the actual rod used before surgical implantation by the attending spine surgeons. The implant rod geometry after surgery was obtained a week (maximum) after the surgical

operation using Aquilion 64 CT scanner (Toshiba Medical Systems Corporation, Tochigi, Japan). The slice thickness was 0.5 mm. The images were imported into CAD software Solidworks (Dassault Systemes, Massachusetts, USA) to measure the 3D geometry and deformation. This procedure was approved by the research ethics committee of the Graduate School of Medicine and a proper informed consent was explained and obtained from all patients. The three patients were classified as severe Adolescent Idiopathic Scoliosis (AIS), i.e. with high Cobb angle that requires surgical treatment. The Universal Spine System (USS) II 6 mm diameter rods and polyaxial pedicle screws (Synthes GmbH, Oberdorf, Switzerland) were implanted using the SDRRT surgical technique. The clinical data of the patients used in this study is listed in Table 3.1.

In SDRRT, two implant rods are used for both the concave and convex side of the deformity. However, in all patients, the rod geometry images show that the rod at the convex side was not deformed (i.e. deformation was too small to be detected by CT imaging) after the surgical treatment of scoliosis. This implies that the corrective force acting on the rod at the convex side was negligible. On the other hand, the rod at the concave side was significantly deformed. The three-dimensional changes of rod geometry at the concave side of the three patients were used to analyze the corrective forces acting at the deformed rod after the surgical treatment of scoliosis.

3.4 Results

3.4.1 Corrective forces

The iteration process was stopped when the objective function was less than α and the applied forces at this iteration step was referred to as the optimal forces $\vec{F}_i$. Figure 3.5(top) shows the magnitude of three-dimensional forces acting at the vertebrae of Patient 1. These forces were acting at the deformed implant rod after scoliosis surgery. The direction of the three dimensional forces at each vertebra level along the *x*-*z* plane is defined by angle θ_i .

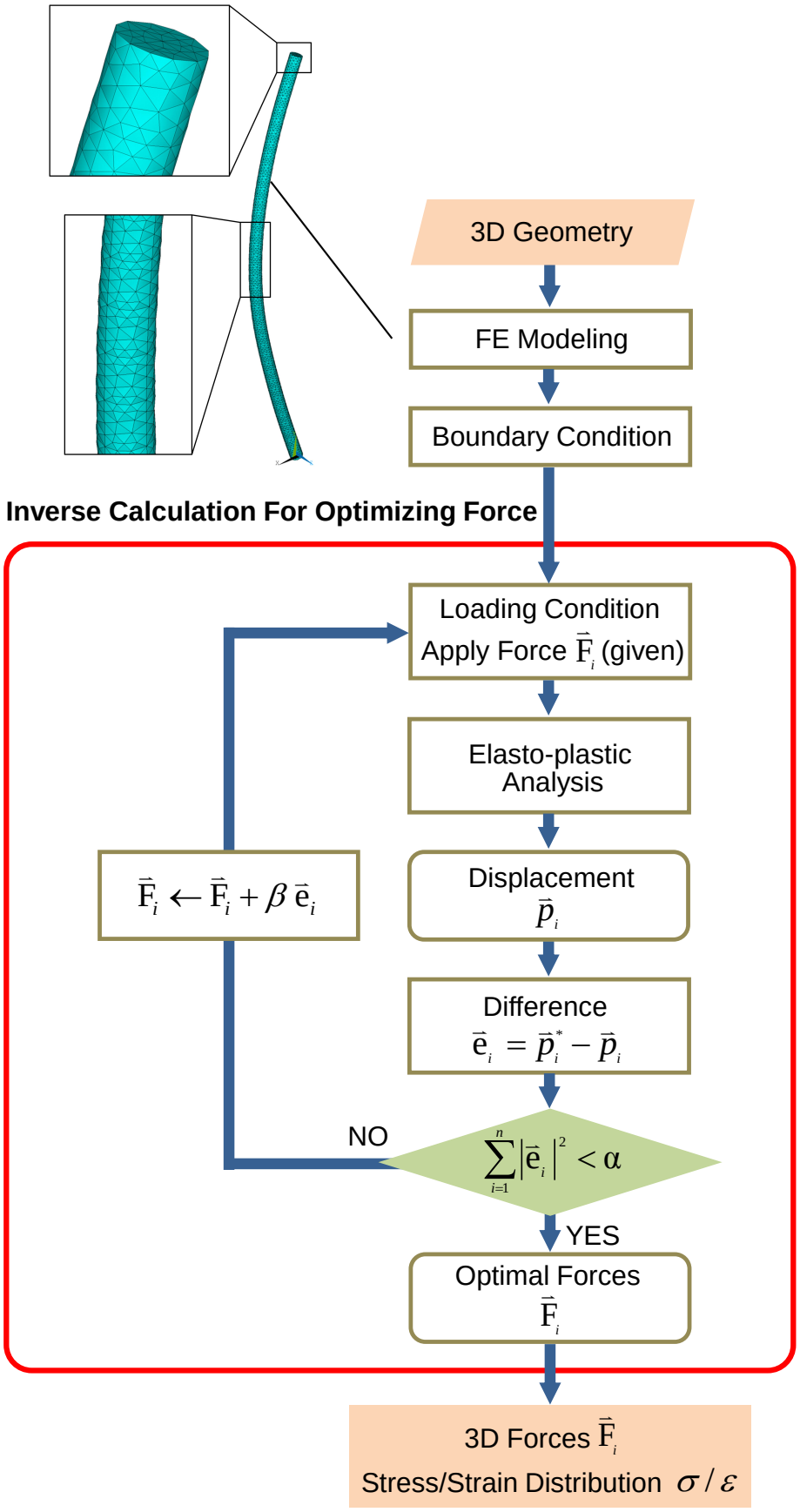

Figure 3.3 Procedure for corrective force analysis.

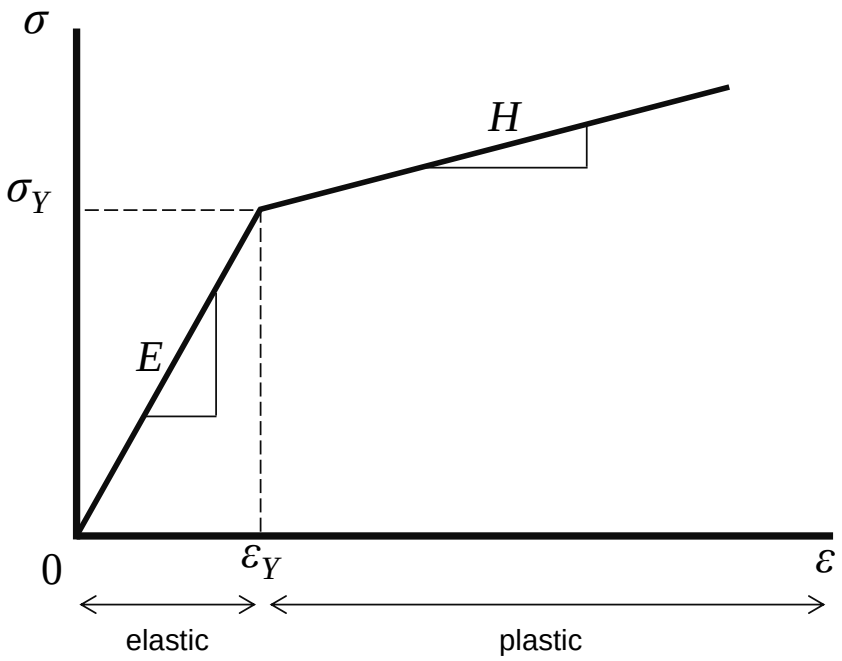

Figure 3.4 Bilinear elasto-plastic material model.

Table 3.1 Clinical data of the three scoliotic patients.

Patient	Gender	Age	Cobb angle before surgery	Cobb angle after surgery	Screw locations	Rod length (mm)
1	Female	16	57°	13°	T5, T6, T7, T10, T11, T12, L1, L2	226
2	Female	15	59°	28°	T6, T7, T11, T12	159
3	Female	14	68°	18°	T6, T7, T11, T12, L1	177

The direction of forces along the *y-z* plane was neglected since the rod was not deformed along that plane. Figure 3.5(bottom) shows the magnitude of forces that deformed the implant rod for Patient 2 and Patient 3. The maximum forces obtained were 248 N, 198 N and 439 N for Patient 1, Patient 2, and Patient 3, respectively.

3.4.2 Stress distribution

Since implant rod breakages have been reported previously by a number of studies, the possible location of rod breakage was also investigated. The von Mises stress distributions were obtained using FEA to find the possible location of rod breakage. Figure 3.6 shows the von Mises stress distributions when the implant rod was deformed after the surgical treatment of scoliosis. The maximum von Mises stresses were 726 MPa, 241 MPa, 905 MPa located about at T10 for Patient 1, T11 for Patient 2, T11 for Patient 3, respectively.

3.5 Discussion

The corrective forces acting at each screw were calculated using the changes of the implant rod geometry before and after surgery. The current maximum forces obtained in this study were located at the lumbar region 248 N, 198 N and 439 N for Patient 1, Patient 2, and Patient 3, respectively. These forces were developed at each screw when the scoliotic spine resisted the rotation of the rod. In effect, the forces deformed the rod after the surgical treatment of scoliosis.

Furthermore, the present method could be used also to analyze the post-operative corrective forces from the changes of implant rod geometry after many months or years. This is possible by detecting changes of the implant rod geometry using CT imaging of implant rod. Post-operative daily living activities such as standing, bending, walking and etc. may change the loads and rod shape in vivo. Such activities may cause the corrective forces to

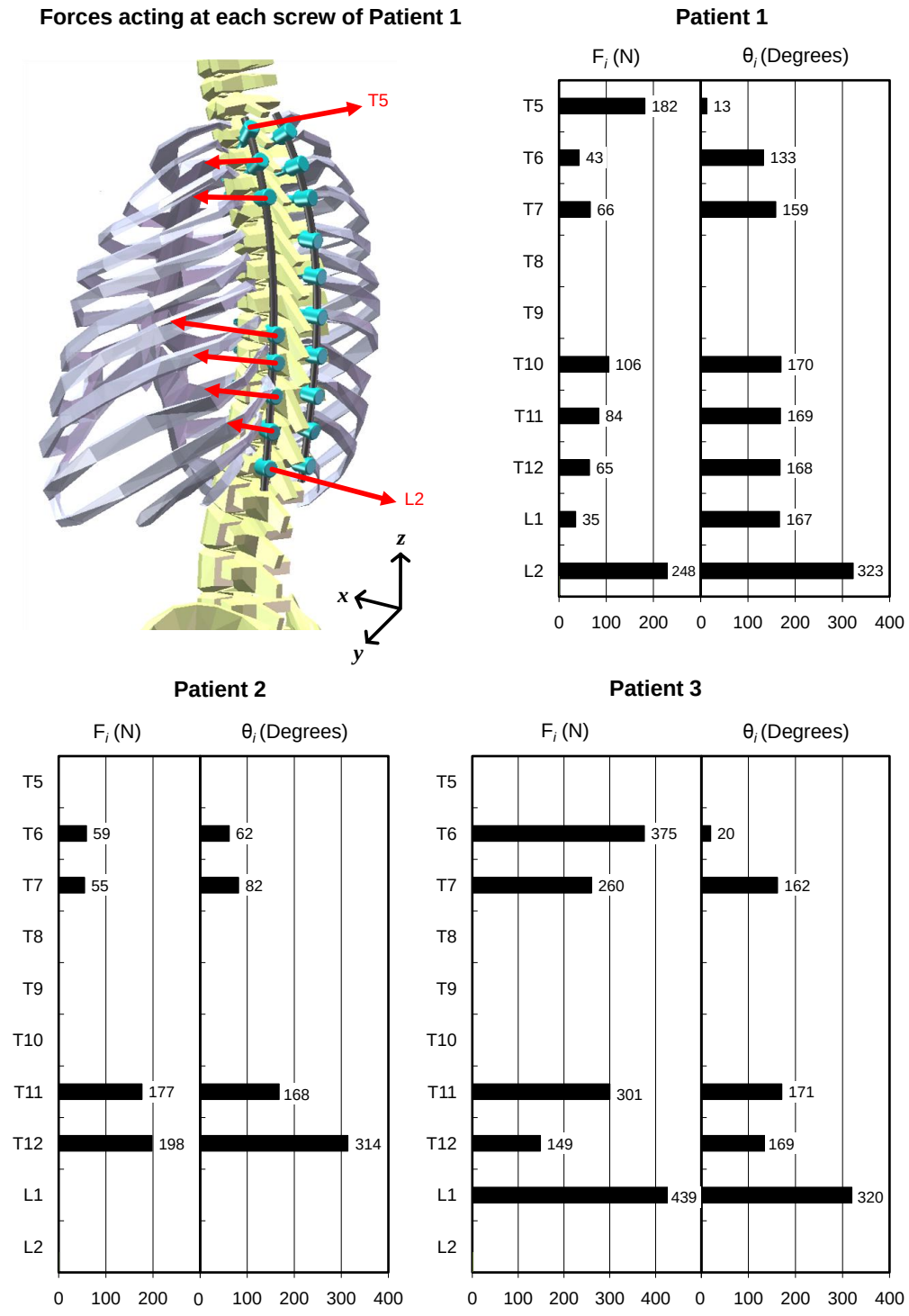

Figure 3.5 Magnitude of the three-dimensional corrective forces acting at each screw calculated from implant rod deformation.

increase or decrease which may affect the rigidity of the fixation. These activities could also develop high corrective forces which might be unsafe to the patient. The present method will be applied to investigate the magnitude of post-operative corrective forces from the changes of implant rod geometry during future patient follow ups.

The objective of optimal scoliosis correction is to deform and fix the scoliotic spine into the desired shape without damaging deformations and neurological complications. This could be attained by applying suitable corrective forces to the spine through implant rods and screws. However, the corrective forces required to correct the deformity must be sufficient enough to achieve the required correction. Previously, Lou et al. (2002) attached strain gages to the rod rotating device. They monitored the torsional force applied by the surgeon at the rotating device during the CD derotation maneuver. The measured torsional force ranged from 22-57 N. Although patients were limited, they found an increasing trend between the applied force and degree of correction. However, the corrective forces acting at each screw were difficult to measure since the rotating device is attached only to a single location along the implant rod. The magnitude of forces occurring at each screw is also important because overloading due to the rod rotation maneuver might occur (Little and Adam, 2010).

Another important issue during scoliosis surgery is the loss of feeling of the surgeon to feel the resistance of each corrected level (i.e. located at each screw). This is because the rod rotating device is attached to the rod at a single location only. The magnitude of corrective forces occurring at each screw could be excessive. Indeed, 15 cases of pedicle fractures were reported during the rod rotation maneuver due to excessive corrective forces (Di Silvestre et al., 2007). Although it is still difficult, however, it will be more useful clinically if we can directly establish the relation of the required torque to rotate the rod and the forces acting on each screw or vice versa. From this, the spine surgeons can decide intraoperatively whether the applied torque during the rotation maneuver is within the safe level of force.

Postoperative complications such as loosening and breakage of screws and rod breakage have been reported previously by many studies. Guidera et al. (1993) reported broken implant rods during the use of CD instrumentation. The breakage risk was investigated using von Mises stress. The von Mises stress distribution along the entire length of the deformed rod was obtained. The possible locations of rod breakage can be located. This also demonstrates the usefulness of the current method in locating possible locations of implant rod fracture by evaluation of the stresses distribution after the surgical treatment of scoliosis.

More accurate measurement of implant rod geometry before the surgical treatment is important to attain more accurate results. Currently, the surgeons manually traced the bent rods before surgical implantation. The traced geometry was scanned and reconstructed as an image file. The CT imaging can be used also to measure the rod geometry before surgical implantation. Although this has not been performed yet, we have to consider its viability in the clinical setting. Furthermore, a precise 3D geometry measurement method can be developed using cameras. Optical imaging using cameras is useful clinically because it can measure the shape of the rod without contact.

Optimal fixation level or configuration of implant screws should be also investigated in the future because the scoliosis cases presented here shows that the screws were not inserted at all vertebral levels. The corrective forces might change if more or lesser screws were used and there can be various screw placement configurations applicable for a certain scoliosis case. Some authors investigated the different screw placement configurations in anterior spine instrumentation using a biomechanical model (Desroches et al., 2007). They were successful in finding the optimal screw placement configurations before surgery as confirmed by the post operative results. Some screw placement configurations were not recommended because the calculated corrective forces exceeded the published pullout forces. Their study introduces the possibility to perform preoperative planning using the anterior approach. Further study considering not only the deformation of rod but also the effect of

various screw placement configuration to the corrective forces in SDRRT surgical technique shall be further investigated, i.e., to investigate the optimal number and placement of screws preoperatively.

Lou et al. (2002) also strengthened that too much high corrective forces can cause implant breakage or bone fracture which may lead to pullout of the screws from the vertebra. The magnitude of corrective forces is important during scoliosis surgery. Liljenqvist et al. (2001) performed pullout tests of pedicle screws using nine human cadaveric thoracic spines. The measured pullout strengths of the pedicle screws ranged from 532 N to 808 N. Although this value seems to be unsafe because it is close to the maximum calculated value of our study (i.e. 439 N), implant differences as well as specimen (osteoporotic vs. normal, age, sex) need to be considered for better comparison. The closest pullout experiment that can be compared to our results was conducted by Seller et al. (2007). They used calf vertebrae and the same implant screw that has been used in this study (i.e. USS II posterior screw). The average pullout force obtained was 2413 N and that was approximately 5.5 times higher than the maximum calculated force of our study (2413 N / 439 N $\approx$ 5.5). This indicates that the forces acting on the screws of the current scoliosis patients are still safe and far below than the pullout force threshold. Again, differences in bone quality and implant configurations such as implant insertion depth might affect the current comparisons. It is highly suggested that actual pullout experiments shall be conducted to validate these findings. Nevertheless, problems involving screw pullout did not occur as confirmed by the spine surgeons.

Two implant rods were used for each scoliosis patient, i.e. for the concave and convex side of the deformity. The geometry of implant rod attached on the concave and convex side of Patient 1 is shown in Fig. 3.7. It was noticed that the rod geometry of all patients at the convex side did not change (undetectable deformation by CT imaging) after the surgical treatment. Further investigation must be done in order to elucidate the mechanism of these findings. Conversely, the rod at the concave side indicates that it has a significant mechanical role during correction of scoliosis deformity.

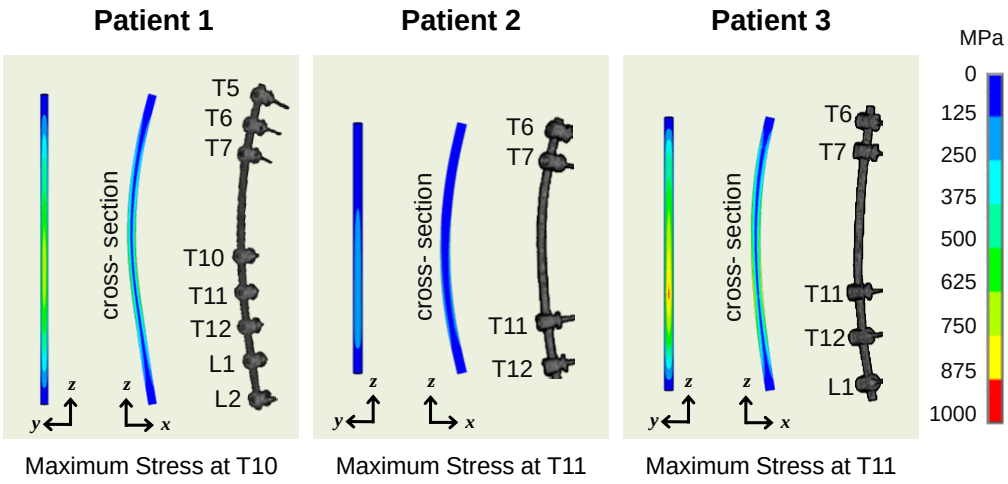

Figure 3.6 von Mises stress distribution of the deformed implant rod after the surgical treatment.

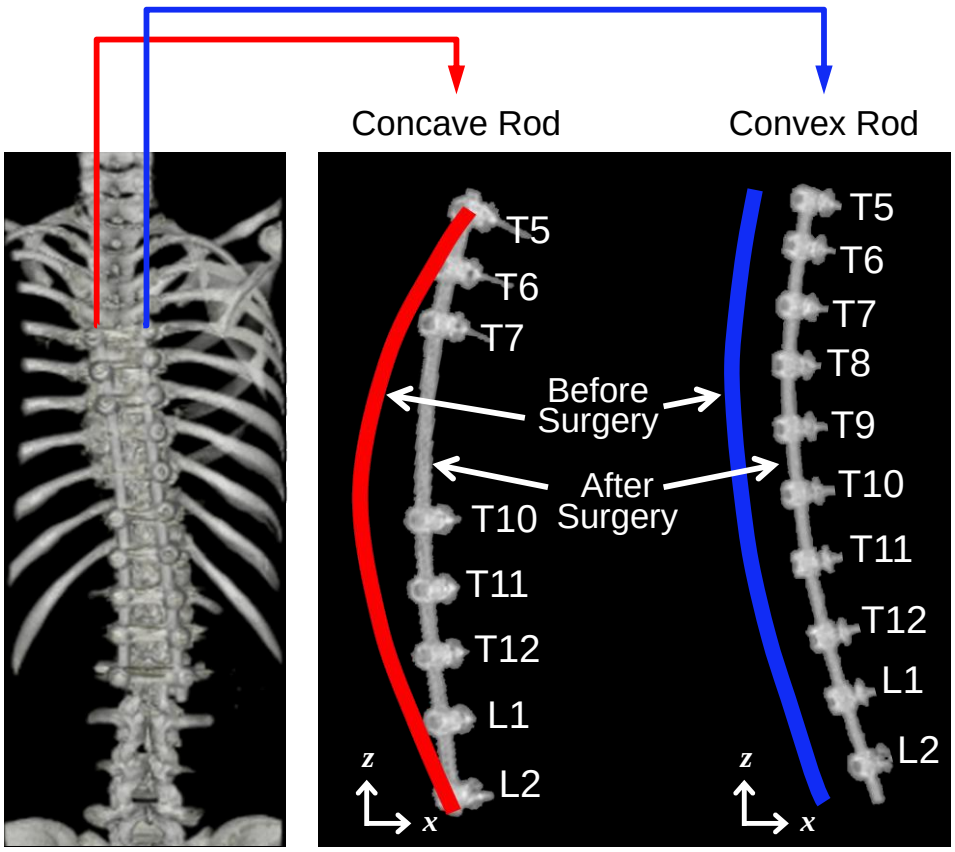

Figure 3.7 Rod geometries in the concave and convex side before and after the surgical treatment of Patient 1.

The implant rods and screws are fixed into the spine for a long period of time. The bone of the spine is continuously remodeling or adapting its structure during the fixation period. At this time, the forces acting on the rod might change due to adaptation of spine. The changes of rod geometry will be further investigated using CT imaging during future follow ups.

4

Numerical Method for In Vivo Measurement of Implant Rod Three-Dimensional Geometry During Scoliosis Surgery

4.1 Abstract

Implant rods and screws are used for the treatment of severe scoliosis to stabilize and support the forces applied during the correction of spinal deformity. Several studies measured the scoliosis corrective forces developed during the surgical procedure using biomechanical finite element modeling. These studies approximated the clinical outcome and measured the corrective forces acting on the screws. However, they were not able to measure the intraoperative three-dimensional geometry of implant rod. Thus, the results of biomechanical modeling might not be so realistic and the corrective forces during the surgical correction procedure could not be measured intraoperatively. Techniques in projective geometry had shown to be successful in three-dimensional reconstruction of shapes using the images obtained from different views. In this study, we propose a numerical method to measure the intraoperative three-dimensional geometry of implant rod in vivo based on two cameras. The reconstruction method only requires few parameters, i.e. the included angle θ between the two cameras, actual length of rod in mm and location of points for curve fitting. The spinal rod that is being utilized during scoliosis surgery was used to evaluate the accuracy of the current method. The three-dimensional geometry of rod was measured using a conventional scanner and compared to the proposed method based on two cameras. The average error ranged from 0.32 to 0.45 mm. The numerical method presented here demonstrated the possibility of measuring the intraoperative three-dimensional geometry of spinal rod during scoliosis surgery.

4.2 Introduction

Treatment for severe scoliosis deformity often leads to surgical intervention using implant rods and screws. These spinal devices are used to stabilize and support the forces applied during the correction of spinal deformity. Previous studies involving patient specific biomechanical models of spine and implants were useful in estimating the clinical outcome and corrective forces acting on the rods. However, these studies lack accurate method to measure the three-dimensional geometry of implant rod during scoliosis surgery. The implant rod geometry was just approximated from the postoperative radiographs (Aubin et al., 2003; Desroches et al., 2007; Lafon et al., 2009; Wang et al., 2011a). Thus, they have to assume that the rod does not deform during the surgical treatment of scoliosis or being a rigid body model. As a consequence, too high forces were obtained due to overly constrained displacements (Aubin et al., 2008). The reported values of corrective forces were so high that should have deformed the spinal rod during scoliosis surgery. The deformation of implant rod during scoliosis correction surgery using Simultaneous Double Rod Rotation Technique (SDRRT) was reported by Salmingo et al. (2012a) and Ito et al. (2010). They measured the corrective forces from implant rod deformation, however, they were not able to measure the intraoperative deformation of rod during the surgical treatment of scoliosis. Intraoperative deformation of rod is also directly related to the intraoperative forces acting on the spine during scoliosis surgery. Thus, it is necessary to develop a method that can measure the intraoperative three-dimensional geometry of spinal rod during scoliosis surgery.

Stereographic images obtained by cameras at different views can be mathematically described into three-dimensions using projective geometry techniques (Hartley and Zissermann, 2003). The first objective of this study was to propose a numerical method to measure the three-dimensional geometry of spinal rod using two cameras with only few parameters (i.e. included angle between the cameras, length of implant rod and location of points for curve fitting). The second objective was to evaluate the accuracy of

the numerical method using the actual implant rod used during scoliosis surgery.

4.3 Methods

4.3.1 Implant rod 3D geometry reconstruction

Figure 4.1 shows how two points in three-dimensional space can be represented into two stereographic planes or two views. The image plane of each camera was oblique with each other by an included angle θ (Fig. 4.1(a)). To establish the reference and standardize the three-dimensional coordinate system, the coordinate system of Camera 1 was used. The optical axis is the imaginary line passing through the center of the lens of Camera 1. The optical axis is set parallel to the *x*-axis. The *y*-axis concurs with the *u*-axis and the *z*-axis lies with the *v*-axis of Camera 1. The two cameras were positioned allowing *v* and *h* axes to be parallel. The location of the other point from the origin (0,0,0) obtained by image projections were measured in pixels as (u_1, v_1) and $(w_1^{'}, h_1^{'})$, left image (Camera 1) and right image (Camera 2), respectively.

Since *v*-axis and *h*-axis are parallel, height v_1 should be equal to $h_1^{'}$ in theory. However, the actual values of both coordinates obtained by the two cameras do not perfectly result into this relation due to the differences in intrinsic parameters of each camera (e.g. focus, positioning error). To compensate the difference, a scaling factor $f_s = v_1 / h_1^{'}$ was used to transform the location of points in Camera 2 using equations

$$h_1 = v_1 = f_s h_1^{'} \tag{4.1a}$$

$$w_1 = f_s w_1^{'} \tag{4.1b}$$

The points when projected above could be described by Fig. 4.1(b). The geometric relation of points yields to

$$\beta = 180° - \theta \tag{4.2}$$

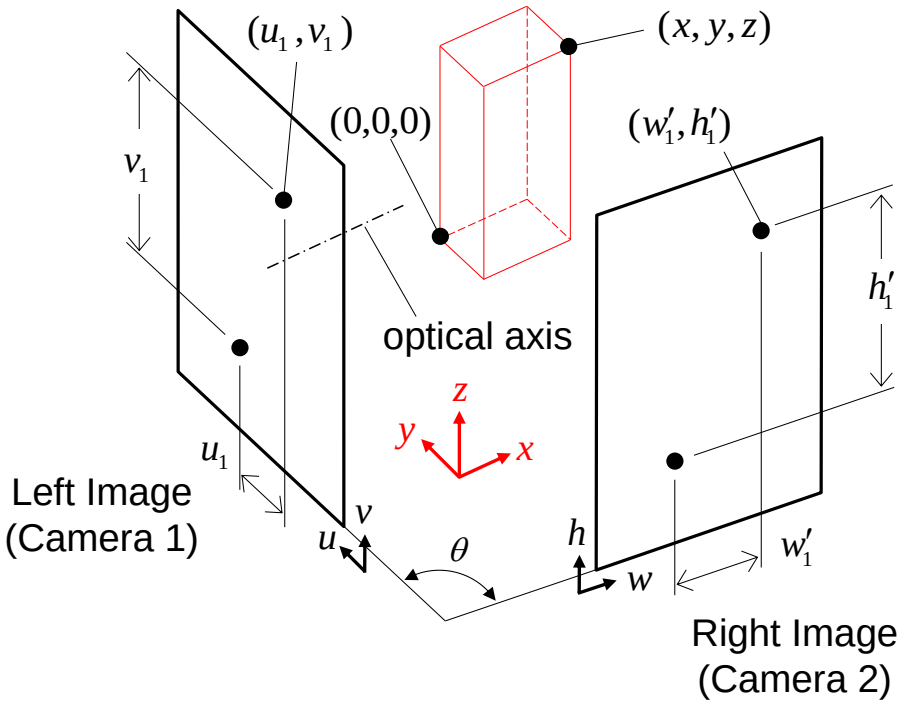

(a)

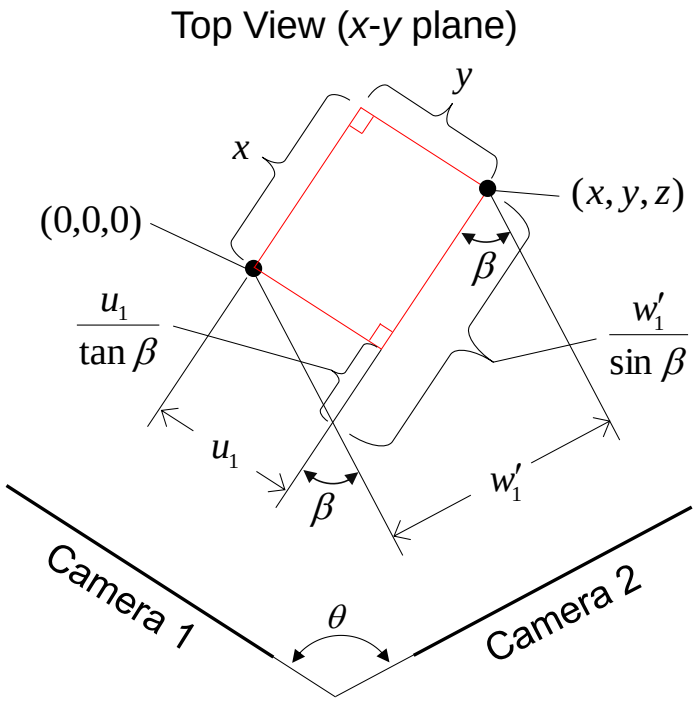

(b)

Figure 4.1 Three-dimensional reconstruction from different views. (a) Projection of points in image plane of each camera at different views (b) Geometric relation of points when viewed from the top.

The distance of point along *x*-axis from the origin (0,0,0) can be computed using equation

$$x = w_1/\sin\beta - u_1/\tan\beta \tag{4.3}$$

Since the positive *y*-axis and *z*-axis coincide with *u*-axis and *v*-axis respectively, the three-dimensional location of two points can be computed using the generalized matrix

$$\begin{bmatrix} x \\ y \\ z \end{bmatrix} = \begin{bmatrix} -1/\tan\beta & 1/\sin\beta & 0 \\ 1 & 0 & 0 \\ 0 & 0 & 1 \end{bmatrix} \begin{bmatrix} u_1 \\ w_1 \\ v_1 \end{bmatrix} \tag{4.4}$$

Figure 4.2(a) shows a schematic model of spinal rod in three-dimensional space where left and right images are projected at different views. The locations of points (cross marks) were arbitrarily selected from the inferior to superior endpoints along the central axes of rod, Fig. 4.2(b). The selected points in the left image were fitted by least-square method using quintic polynomial function proposed by Kanayama et al. (1996) and Tadano et al. (1996) expressed as

$$u(v) = a_1 v + a_2 v^2 + a_3 v^3 + a_4 v^4 + a_5 v^5 \tag{4.5}$$

The coordinates of superior endpoints were obtained to compute the distance using the scaling factor f_s. The scaling f_s in Eq. (4.1) was computed for the right image to transform the location of selected points in Camera 2. The transformed points in the right image were also fitted as

$$w(h) = b_1 h + b_2 h^2 + b_3 h^3 + b_4 h^4 + b_5 h^5 \tag{4.6}$$

The transformed superior endpoint $h_{\max}$, i.e. also equal to $v_{\max}$ after transformation was divided by *n*-divisions. Equations (4.5) and (4.6) were evaluated for *n*-divisions equal to $v_{\max}/n \to v_{\max}$ or $h_{\max}/n \to h_{\max}$. Thus, the previous generalized matrix for spinal rod at *n*-divisions becomes

$$\begin{bmatrix} x_n \\ y_n \\ z_n \end{bmatrix} = \begin{bmatrix} -1/\tan\beta & 1/\sin\beta & 0 \\ 1 & 0 & 0 \\ 0 & 0 & 1 \end{bmatrix} \begin{bmatrix} u(v_{\max}/n) \\ w(h_{\max}/n) \\ v_{\max}/n \quad \text{or} \quad h_{\max}/n \end{bmatrix} \tag{4.7}$$

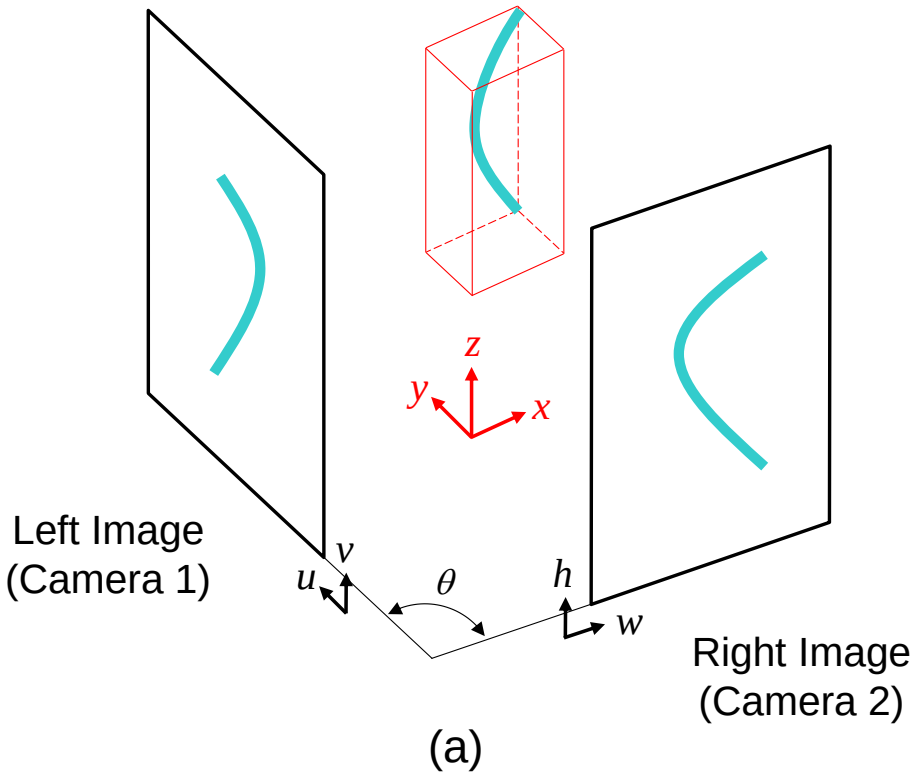

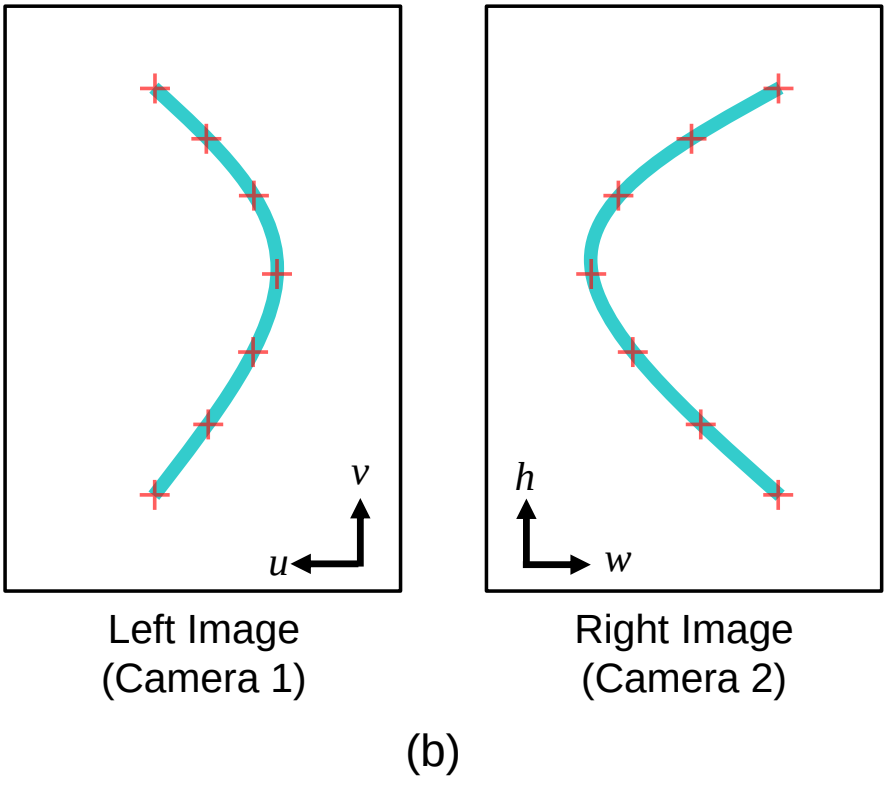

Figure 4.2 (a) Curved implant rod in space projected at different views. (b) Selected points (arbitrary) from inferior to superior endpoint in left and right images of rod for quintic polynomial curve fitting.

The locus of the three-dimensional points can be computed in three-dimensions having coordinates (x_n, y_n, z_n) expressed as *n*-divisions by Eq. (4.7). To mathematically express the three-dimensional coordinates (x_n, y_n, z_n) of rod using parametric equations, they were fitted again by quintic polynomial functions as

$$x = c_1 z + c_2 z^2 + c_3 z^3 + c_4 z^4 + c_5 z^5 \tag{4.8a}$$

$$y = d_1 z + d_2 z^2 + d_3 z^3 + d_4 z^4 + d_5 z^5 \tag{4.8b}$$

In general, three-dimensional geometry of implant rod can be represented by parametric equations

$$x(t) = c_1 t + c_2 t^2 + c_3 t^3 + c_4 t^4 + c_5 t^5 \tag{4.9a}$$

$$y(t) = d_1 t + d_2 t^2 + d_3 t^3 + d_4 t^4 + d_5 t^5 \tag{4.9b}$$

$$z(t) = t \tag{4.9c}$$

Calibration is necessary to convert pixels into mm because the units of the previous equations are still in pixels. We know that deformation of rod caused by bending does not significantly change the length of the rod (i.e. measured at the neutral axis or central axis of implant rod). The actual length of rod L_{actual} expressed in mm before bending can be used for calibration because it is measureable prior to/before surgical implantation. The actual rod length was measured before bending and the curve length of rod in pixels was numerically integrated using trapezoidal method as

$$L_{pixel} = \int_0^t \sqrt{\left(x'(t)\right)^2 + \left(y'(t)\right)^2 + \left(z'(t)\right)^2}\, dt \tag{4.10}$$

The calibration scale *k* was computed using Eq. (4.11). This also represents the resolution of the dual-camera system expressed in mm/pixel.

$$k = L_{actual} / L_{pixel} \tag{4.11}$$

Thus, the parametric equations in Eq. (4.9) can be represented as a vector function in pixels as

$$\mathbf{r}_p = \langle x(t), y(t), z(t) \rangle \tag{4.12}$$

For values of *t*, the 3D coordinates of rod can be converted into mm by equation

$$\mathbf{r} = \mathbf{r}_p \cdot k \tag{4.13}$$

4.3.2 Method validation

The USS II implant rod (Synthes GbmH, Oberdorf, Switzerland) which is being utilized during scoliosis surgery was used for the validation of the current method. To establish reference, the spinal rod was bent only in *X*-*Z* plane and scanned using a conventional scanner, in Fig. 4.3. Arbitrary points (cross marks) were selected from the inferior to superior endpoint along the central axis of rod. A scale was used for image calibration. Image processing algorithm was programmed using MATLAB software (Mathworks, Massachusetts, USA). The scanned three-dimensional geometry of rod was also expressed using quintic polynomials as

$$X(t) = e_1 t + e_2 t^2 + e_3 t^3 + e_4 t^4 + e_5 t^5 \tag{4.14a}$$

$$Y(t) = 0 \tag{4.14b}$$

$$Z(t) = t \tag{4.14c}$$

The bases of the two digital cameras Nikon D60 (Nikon Corporation, Tokyo, Japan) were fixed on the same plane for the reconstruction of the three-dimensional implant rod geometry. The included angle θ was set at 120 degrees. The bent implant rod was attached to the spine sawbone using three different positions (Fig. 4.4). These positions correspond to the possible implant rod orientation during scoliosis surgery using rod rotation technique (i.e. SDRRT). The first position indicates the position of rod after the rotation maneuver. The second and third positions show the rod position before the rod rotation maneuver. This is when scoliosis deformity still exists and corrective force has not been applied yet. To make sure that the three positions have the same 3D geometry during measurements, the implant rod was fixed such that it could not be deformed by the spine model. Both left and right images were obtained from the three positions. Selected points (7 points each) were fitted using the least square method. Curve fitting measurements for each position

was repeated using three trials. Since the rod was bent at a single plane, coordinate rotation was performed such that the coordinate axis of the two-camera and scanner reconstruction method coincides because the orientation of each rod differs from each other.

For all measurements, t was evaluated for n-divisions (set to 50 divisions). The error was computed as the difference between the corresponding coordinates (x_n, y_n, z_n) of two-camera and scanner method as

$$e(t) = \sqrt{(\Delta x(t))^2 + (\Delta y(t))^2 + (\Delta z(t))^2} \tag{4.15}$$

4.4 Results

4.4.1 Implant rod three-dimensional geometry

The implant rod three-dimensional geometry reconstructions were conducted using the dual-camera system. The actual length of rod was 199.51 mm. The average resolution (i.e. equal to k) obtained by the scanner and dual-camera method was 0.04 mm/pixel and 0.12 mm/pixel, respectively. A sample of three-dimensional image reconstruction using the dual-camera method is shown in Fig. 4.5 (evaluated by t for n-divisions; 50-divisions). The results agree well with the geometry of the actual spinal rod because it was not deformed along the Y-axis direction.

4.4.2 Error validation

The average error for each measurement trial is listed in Table 4.1. The total mean error ranged from 0.32 to 0.45 mm and mean maximum error was 0.64 to 0.78 mm. The average three-dimensional coordinates of the three trials for each position were also computed. To evaluate whether the geometries of the rod in different positions were the same, a coordinate rotation was performed such that the coordinate axis of each position coincides with each other. An error $e(t)$ between the three different positions was also obtained. The mean error between the different positions was 0.37 mm, as listed in Table 4.2. The mean maximum error was 0.57 mm.

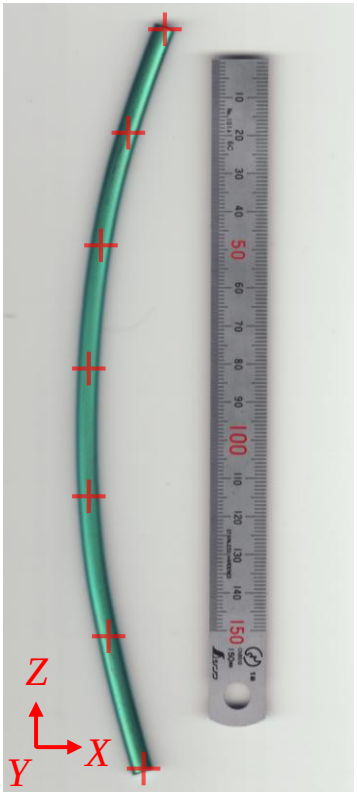

Figure 4.3 Scanned image of spinal rod with scale for validation of the dual-camera method. Cross marks are selected arbitrary points for curve fitting.

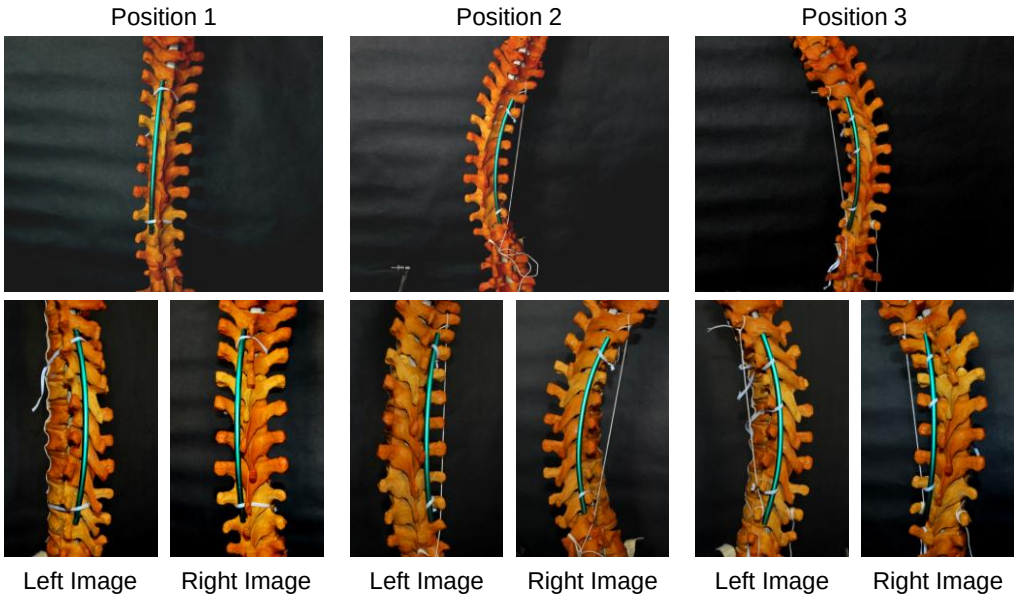

Figure 4.4 Left and right images of the three different positions obtained by the two cameras at different views (upper pictures are taken from the center of both left and right views).

Table 4.1 Error $e(t)$ between the dual-camera and scanner reconstruction method.

Trial	1st Position		2nd Position		3rd Position	
	Ave. Error $e(t)$ (mm)	Max. Error $e(t)$ (mm)	Ave. Error $e(t)$ (mm)	Max. Error $e(t)$ (mm)	Ave. Error $e(t)$ (mm)	Max. Error $e(t)$ (mm)
1	0.39	0.83	0.42	0.84	0.35	0.90
2	0.50	0.82	0.32	0.55	0.33	0.58
3	0.45	0.70	0.45	0.72	0.29	0.45
Mean	0.45	0.78	0.40	0.70	0.32	0.64
SD	0.05	0.07	0.07	0.14	0.03	0.23

Table 4.2 Error $e(t)$ between the three different positions obtained by the dual-camera reconstruction method.

Position	Error between different positions	
	Ave. Error $e(t)$ (mm)	Max. Error $e(t)$ (mm)
1st vs. 2nd	0.46	0.71
1st vs. 3rd	0.28	0.45
2nd vs. 3rd	0.36	0.56
Mean	0.37	0.57
SD	0.09	0.13

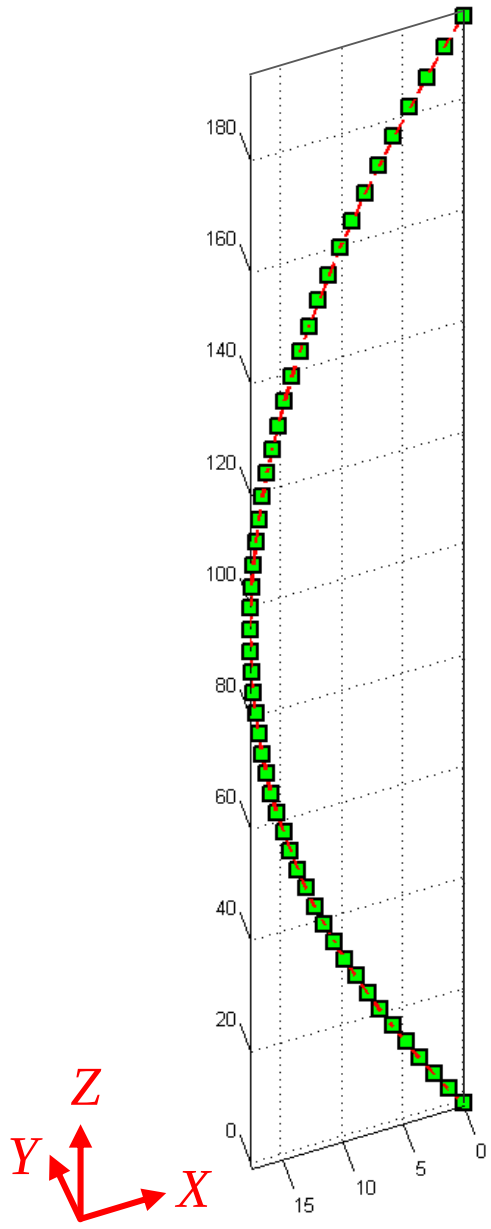

Figure 4.5 Typical reconstructed three-dimensional geometry of spinal rod using dual-camera system. It can be seen that the distance of points in *y*-axis is almost zero. This is in agreement with the actual spinal rod geometry.

4.5 Discussion

Previous studies showed that the implant rod three-dimensional geometries were just approximated from 2D videos and images (Aubin et al., 2003, Aubin et al., 2008; Desroches et al., 2007; Lafon et al., 2009; Wang et al., 2011a, 2011b). A method that can measure the three-dimensional geometry of implant rod in vivo is necessary to help understand the deformation behavior of rod as well as the biomechanics of scoliosis correction. The advantage of this study is that the actual implant rod length was used for calibration instead of calibration markers. Calibration markers could interfere and may add complexity during the surgical procedure. Also, the value of rod length in pixels is always higher than the actual rod length in mm. Thus, an error on measurement of actual rod length does not greatly affect k (Eq. 4.10). The proposed method is useful when plastic deformation exists because small changes in length will not significantly effect k. The included angle θ, actual length of rod in mm and location of points for curve fitting are the only parameters required to reconstruct the three-dimensional geometry of the spinal rod. Thus, the method presented here is relatively simple and does not require many parameters. Although quintic polynomial functions were used, functions such as B-splines could also be adapted to our method for more complex geometries and other applications. However, the results indicate that the accuracy was practically acceptable because it is within less than of a millimeter. The three possible rod positions during the scoliosis surgery were examined at different times. Although this represents the intraoperative setting, clinical validation studies should be conducted in the future to better evaluate the accuracy of the method during scoliosis corrective surgery.

5

Relationship of Forces Acting on Implant Rods and Degree of Scoliosis Correction

5.1 Abstract

Various surgical techniques for the correction of severe scoliotic deformity have evolved and became more advanced in applying the corrective forces. The objective of this study was to investigate the relationship between corrective forces acting on deformed rods and degree of scoliosis correction. Implant rod geometries of six adolescent idiopathic scoliosis patients were measured before and after surgery. An elasto-plastic finite element model of the implant rod before surgery was reconstructed for each patient. An inverse method based on Finite Element Analysis was used to apply forces to the implant rod model such that it was deformed the same rod geometry after surgery. Relationship between the magnitude of corrective forces and degree of correction expressed as the change of Cobb angle was evaluated. The effects of screw configuration on the corrective forces were also determined. Corrective forces acting on rods and degree of correction were not correlated. Increase in the number of implant screws tended to decrease the magnitude of corrective forces but did not provide a higher degree of correction. Although greater correction was achieved with higher screw density, the forces increased at some level. The biomechanics of scoliosis correction is not only dependent on the corrective forces acting on the implant rods but also associated with various parameters such as screw placement configuration and spine stiffness. Considering the magnitude of forces, increasing screw density is not guaranteed as the safest surgical strategy.

5.2 Introduction

Optimal scoliosis surgical treatment is not achieved due to the variability of surgeons' preferences and different correction objectives. Decision-making on the levels of instrumentation/fixation, types and number of implants, shape and size of implant rod is still dependent on individual surgeon's experience (Desroches et al., 2007; Majdouline et al., 2009). Several studies were conducted to simulate various surgical steps and strategies to determine the advantages and disadvantages among the different instrumentation systems by comparing the distribution of corrective forces acting at the vertebrae (Wang et al., 2011a, 2011b). Also, preoperative surgical planning was made possible using patient-specific finite element models (Aubin et al., 2003, 2008). These studies estimated the suitable surgical strategy for scoliosis surgical treatment, however, the results might be unrealistic because rod deformation was not considered in their analyses (Aubin et al., 2003, 2008; Desroches et al., 2007; Lafon et al., 2009). The implant rod geometry was approximated only from the postoperative data. In fact, the reported magnitudes of force (range from several hundred and even thousand Newton) were apparently high that should have deformed the implant rod during the surgical treatment. Hence, the postoperative geometry of rod could not be used as a substitute for the initial implant rod geometry. Careful investigation on the geometrical changes of rod and corrective forces acting on it are also important to fully understand the scoliosis correction mechanism (Salmingo et al., 2012a, 2012b). Moreover, relationships between the magnitude of corrective forces, number of screws, screw placement configuration and degree of correction need to be established or elucidated. Understanding the relationships between these parameters could enhance the management of spinal deformities.

The first objective of the study was to analyze the corrective forces acting on the deformed implant rod after the surgical treatment of scoliosis. The relationships between the magnitude of corrective forces, degree of correction, screw density, and absolute number of screws were determined.

5.3 Methods

5.3.1 Patients and implant rod deformation

Six scoliosis patients diagnosed as severe adolescent idiopathic scoliosis were enrolled in this study. All patients were surgically operated in the same orthopaedic department after the completion of requirements set by the ethics committee of the university hospital. Implant rods having 6 mm diameter and polyaxial pedicle screws of USS II Polyaxial system (Synthes GmbH, Oberdorf, Switzerland) were used. The implant rod length varies with each scoliosis patient. All rods were pre-bent only at a single plane. Implant rods and screws were surgically implanted following the Simultaneous Double Rod Rotation Technique (SDRRT) procedure as discussed in the previous chapters and study of Ito et al. (2010). The implant rod deformation was measured using the implant rod geometry. Figure 5.1(a) shows the radiograph of the corrected spine after the surgical treatment of scoliosis. The initial geometry of rod was measured before surgical implantation (Fig. 5.1(b)). The final geometry of rod was measured a week (maximum) after surgery by Aquilion 64 CT scanner (Toshiba Medical Systems Corp., Tochigi, Japan). The coordinate system proposed by the Scoliosis Research Society was used (Yeung et al., 2003). The positive *x*-axis, *y*-axis, and *z*-axis are directed toward the anterior, left lateral side and superior direction, respectively. For all cases, force analysis of rod at the convex side was neglected because the CT imaging could not significantly detect deformation of rod along that side. On the other hand, the rods at the concave side were significantly deformed after the surgical treatment of scoliosis. The changes of implant rod geometry at the concave side of each patient was obtained and used in this study.

5.3.2 Force analysis procedure

The procedure for calculating the corrective forces using Finite Element Analysis (FEA) is shown in Fig. 5.2. FEA was performed using ANSYS 11.0 software (ANSYS, Inc., Pennsylvania, USA). The elasto-plastic finite element model of the implant rod before surgery was reconstructed using a 10 node

tetrahedral solid element. The forces were applied iteratively to the location of screws until the implant rod was deformed the same after surgery.

The elasto-plastic material model was based from the implant manufacturer specifications. Material properties were elastic modulus (E), yield stress (σ_Y), yield strain (ε_Y) and hardening coefficient (H) equal to 105 GPa, 900 MPa, 8.57×10^{-3} and 2.41 GPa, respectively.

5.3.3 Degree of correction

Cobb angle measurements were performed from frontal radiographs that were taken before and after surgery. The degree of correction $\Delta\theta$ was defined as the difference between the preoperative Cobb angle θ_1 and postoperative Cobb angle θ_2 (Table 5.1). The degree of correction was also expressed as correction rate computed as the ratio of the degree of correction over the preoperative Cobb angle $\Delta\theta/\theta_1$.

5.3.4 Screw density

To investigate the effects of various screw configurations, the screw density was calculated as the number of pedicle screws used divided by the number of pedicle screws that could have been used within the implant rod length. This was expressed as percentage. Since the implant rod at convex side was not significantly deformed after the surgical treatment of scoliosis, the screw density at that side of the deformity was excluded.

5.3.5 Pullout and push-in force

The computed forces correspond also to the pullout and push-in forces acting at the vertebrae to correct the scoliosis deformity. The magnitudes of pullout and push-in forces were also computed from the computed forces. In this study, the pullout or push-in force was defined as the pulling or pushing force acting parallel to the endplate of the vertebra at the sagittal plane (Fig. 5.1(c)). This was computed using the reaction force vector (i.e. acting at the spine in

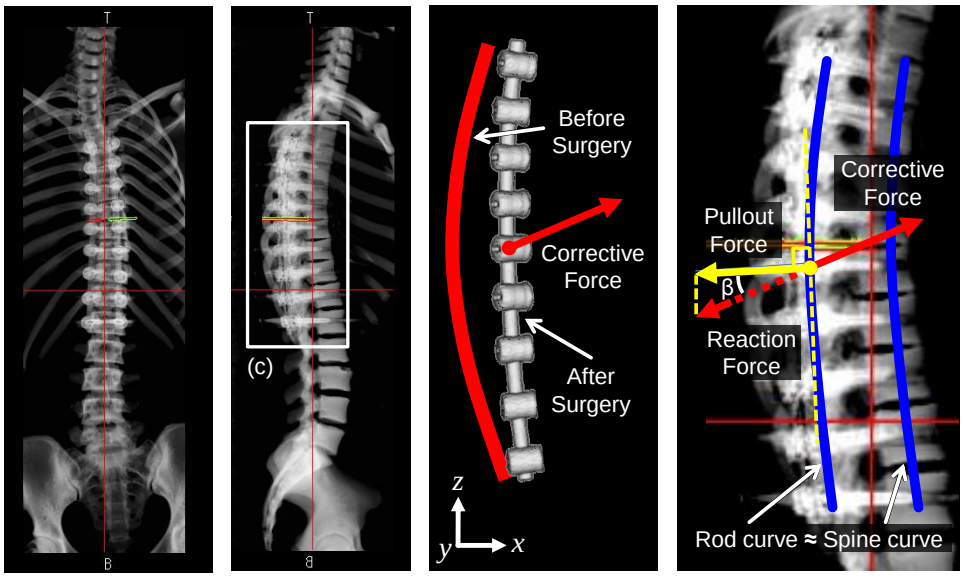

Figure 5.1 (a) Postoperative radiograph of operated scoliotic spine. (b) Corrective force acting at the screw of deformed rod. (c) Pullout force computed from the reaction force of corrective force.

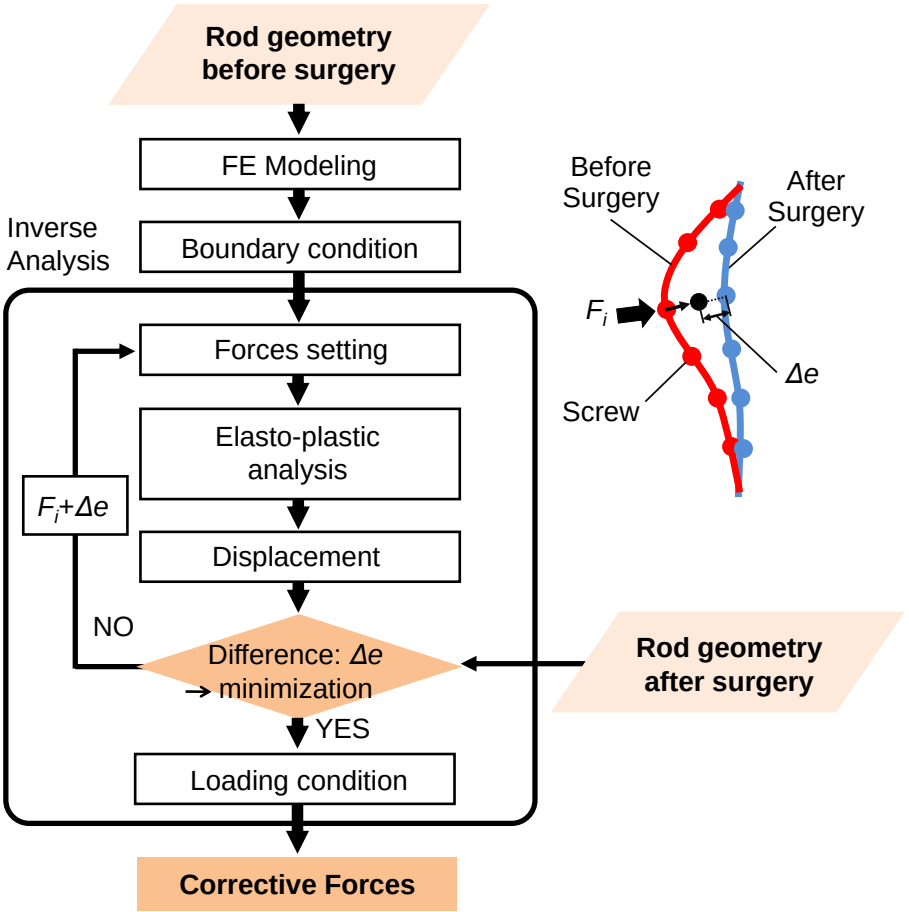

Figure 5.2 Procedure for corrective force analysis using FEA.

the opposite direction) of the computed corrective force that deformed the rod during scoliosis surgery. Since the rod curvature constitutes the spine curvature after the surgical treatment of scoliosis, it was used as the reference to define the direction of the pullout or push-in force. The rod geometry was fitted by quintic polynomial function described in the previous study of Salmingo et al. (2012b). The tangent angle (broken line) which is orthogonal to the axis of pullout or push-in force was computed by evaluating the first derivative of quintic polynomial function at the location of each screw. The reaction force was resolved into force component (Reaction force × Cosβ), i.e. equal to the magnitude of pullout or push-in force acting at the corresponding vertebra level.

5.4 Results

The magnitude of corrective forces obtained by FEA acting on each screw is listed in Table 5.2. The corrective force acting at the apical vertebra was also obtained. Along the apical vertebra, the corrective forces tended to increase. This indicates that the apical vertebra needs higher corrective forces. For cases where the screw was not placed in the apical vertebra, the closest force acting at the apex was used or whichever was higher in case that the closest force could not be determined, i.e. Patient 6. This supports the fact that vertebrae near the apex needed higher corrective force. The maximum forces were located at the extreme fixation levels mainly at the lumbar side. The absolute number of screws, screw density and magnitude of corrective forces were summarized in Table 5.3.

5.4.1 Degree of correction

Table 5.1 shows the correction rate of each scoliosis patient. The correction rate mean was 69% (SD 11%). The results show that Patients 6 and 5 gained the lowest and highest correction rates, respectively. The increase in absolute number of screws did not significantly correlate with the degree of correction

Table 5.1 Clinical data of scoliosis patients.

Patient	1	2	3	4	5	6
Preoperative Cobb angle, θ_1 (deg.)	76	75	57	68	83	59
Postoperative Cobb angle, θ_2 (deg.)	27	26	13	18	14	28
Degree of correction, $\Delta\theta = \theta_1 - \theta_2$ (deg.)	48	49	44	50	69	31
Correction rate, $\Delta\theta/\theta_1$ (%)	64	65	77	73	83	53

Table 5.2 Magnitude of corrective forces acting at each vertebra level.

Vertebra Level	Patient					
	1	2	3	4	5	6
T2	49	270				
T3	33	58				
T4	33	74				
T5	31	115	182			
T6	36	139	43	375	263	59
T7	–	–	66	260	34	55
T8	–	–	–	–	82	–
T9	*93	*–	–	–	96	*–
T10	39	151	*106	*–	*99	–
T11	63	89	84	301	85	177
T12	56	399	65	149	63	198
L1	28		35	439	39	
L2	29		248		253	
L3	192					

*Apical vertebra Units in Newton

($r = 0.48$, $p > 0.05$) (Fig. 5.3). On the other hand, the screw density correlated well with degree of correction ($r = 0.81$, $p < 0.025$) (Fig. 5.4). Figure 5.5 shows the relationship between the average force and degree of correction. A significant correlation could not be found between the average force ($r = 0.03$, $p > 0.05$) and the degree of correction. In total, the magnitude of forces did not correlate well with the degree of correction.

5.4.2 Effect of increase in number of screws

The relationships between the absolute number of screws and magnitude of forces are shown in Fig. 5.6. A decreasing trend was found between the number of screws and average force, however, the correlation was not significant ($r = 0.63$ and, $p > 0.05$) (Fig. 5.6(top)). Conversely, there was a significant negative correlation between the force acting at/near the apical vertebra ($r = 0.73$, $p < 0.05$) with number of screws (Fig. 5.6(bottom)).

5.4.3 Effect of screw density

The screw density at the concave side of each patient was obtained. The summation of forces and maximum force did not correlate well with increasing screw density ($r = 0.04$ and $r = 0.28$, $p > 0.05$ respectively) (Figs. 5.7(top) and 5.7(bottom)). Likewise, a trend could not be established for both relationships. It was also noticed that for some patients the summation of forces and maximum forces are relatively lower than patient who had 100% screw density. Thus, having higher implant density is not guaranteed as the safest surgical strategy if we consider the magnitude of forces.

5.4.4 Magnitude of pullout and push-in force

The pullout or push-in forces acting at the vertebrae of scoliosis patients were computed (Fig. 5.8). The results show that almost all patients had push-in force at the most inferior and superior level, whereas the apical region had

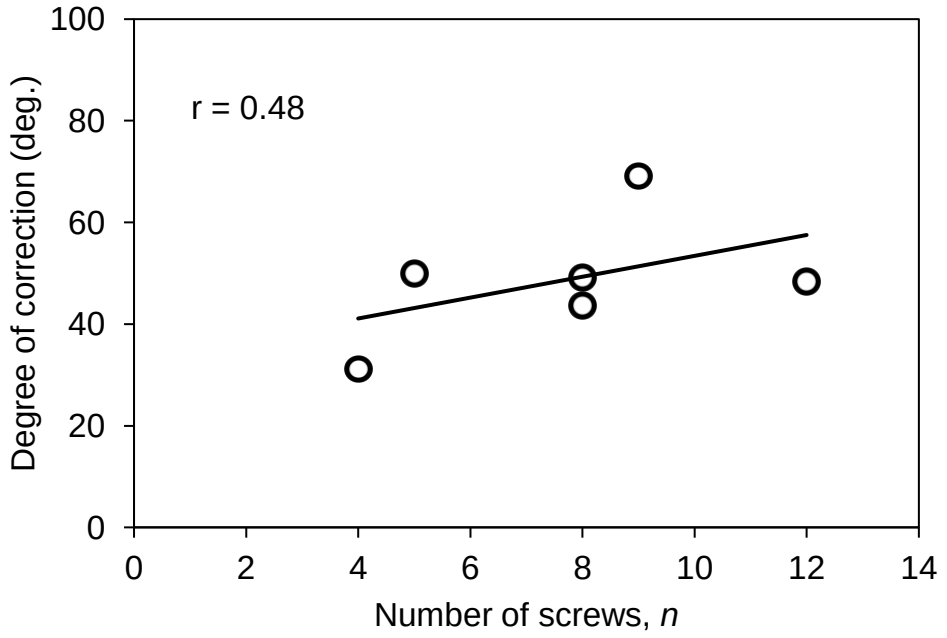

Figure 5.3 Relationship between the number of screws and degree of correction.

Table 5.3 Summary of number of screws, screw density and magnitude of forces of each patient.

Patient	1	2	3	4	5	6
Number of screws, *n*	12	8	8	5	9	4
Screw density (%)	86	73	80	63	100	57
Summation of forces, Σ*F* (N)	682	1295	829	1524	1014	489
Average force, Σ*F*/*n* (N)	57	162	104	305	113	122
Maximum force, F_{max} (N)	192	399	248	439	263	198
Force at/near apex (N)	93	151	106	301	99	177

pullout forces. Furthermore, the values of pullout forces indicate that the magnitude is increasing at the apical region suggesting that significant forces are required in this region to correct the spinal deformity.

5.5 Discussion

Patient-specific finite element models aided the approximation of possible clinical outcomes of different surgical strategies through preoperative planning. However, these studies lack detailed modeling of implant rod because the initial rod geometry was not measured before surgery. Until now, relationships of various parameters such as the magnitude of corrective forces, number of implants used, degree of correction and implant placement configuration are not yet well understood. It well understood that too high corrective forces can cause implant breakage or bone fracture which may also lead to pullout of screws from the vertebra (Mehta et al., 2012; Paxinos et al., 2010). Thus, analysis of corrective forces acting on deformed rod is important to understand the biomechanics of scoliosis correction.

In this study, the degree of scoliosis correction did not depend on the absolute number of screws. Implant placement configuration such as screw density contributed to higher degree of correction. This suggests that vertebrae can be easily manipulated if more implants are attached nearer to each other. Apparently, Patient 6 (having lowest screw density) and Patient 5 (having the highest screw density) gained the lowest and highest correction rate, respectively. The findings in this study are in agreement with the previous study of Clements et al. (2009), although implant and screw density was defined differently. We defined screw density as the percentage of number of pedicle screws used divided by the number of pedicle screws that could have been used within the implant rod length, whereas they defined implant density as the ratio of implants used over the number of available implants sites within the measured Cobb angle. This is because we believe that the implants sites within the implant rod length have significant role in deformity correction than

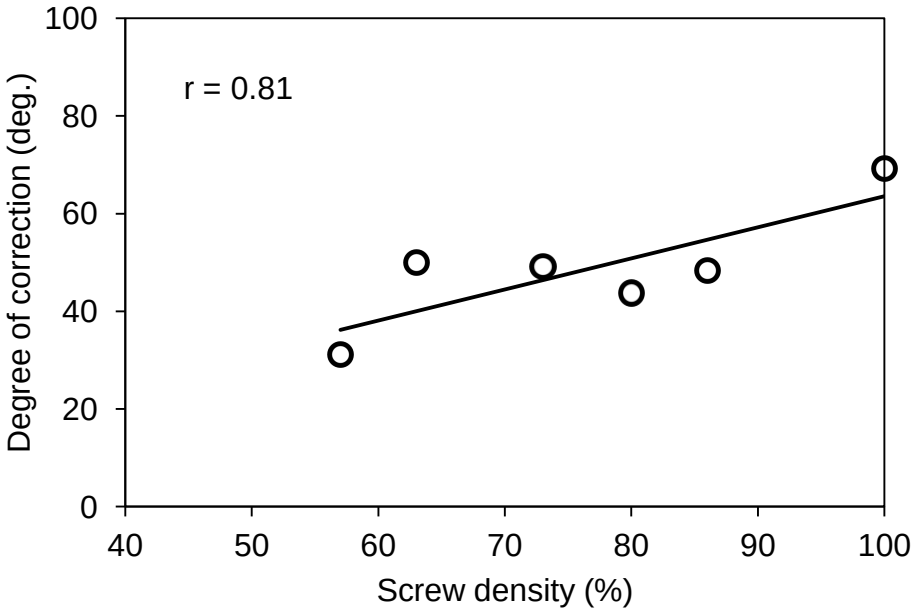

Figure 5.4 Relationship between the screw density and degree of correction.

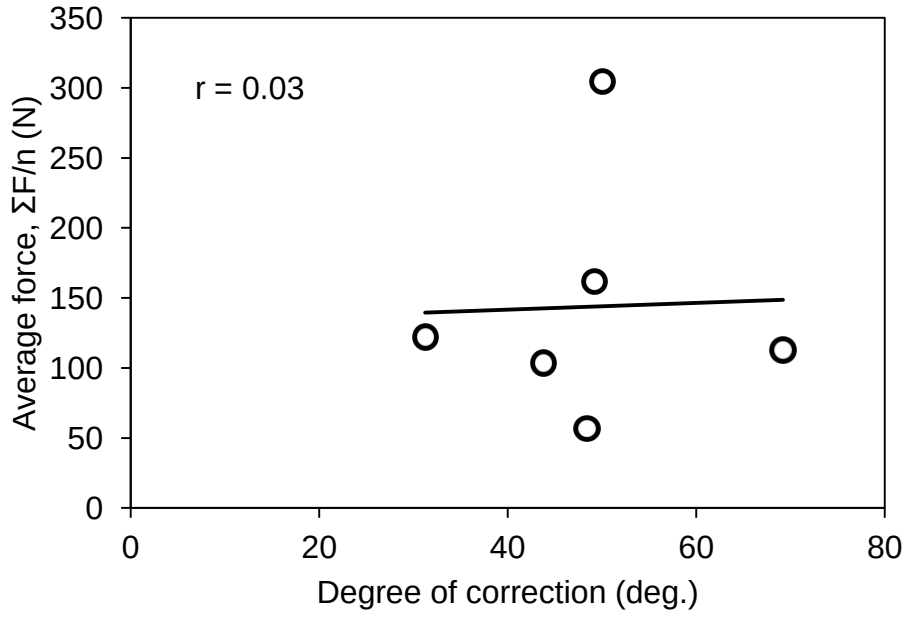

Figure 5.5 Relationship between the degree of correction and average force.

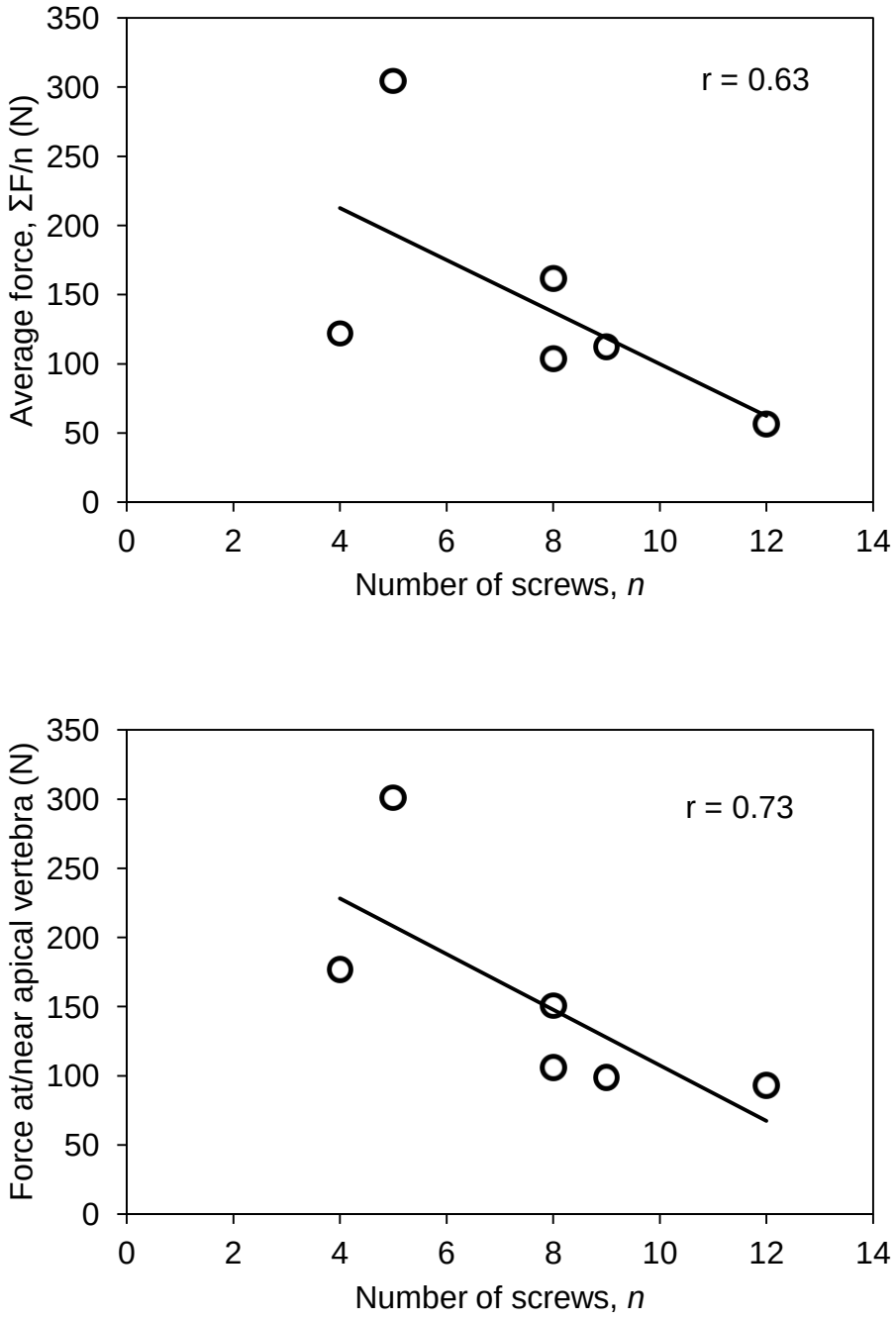

Figure 5.6 Relationships between the number of screws and magnitude of forces. Number of screws vs. average force (top). Number of screws vs. force at/near apical vertebra (bottom).

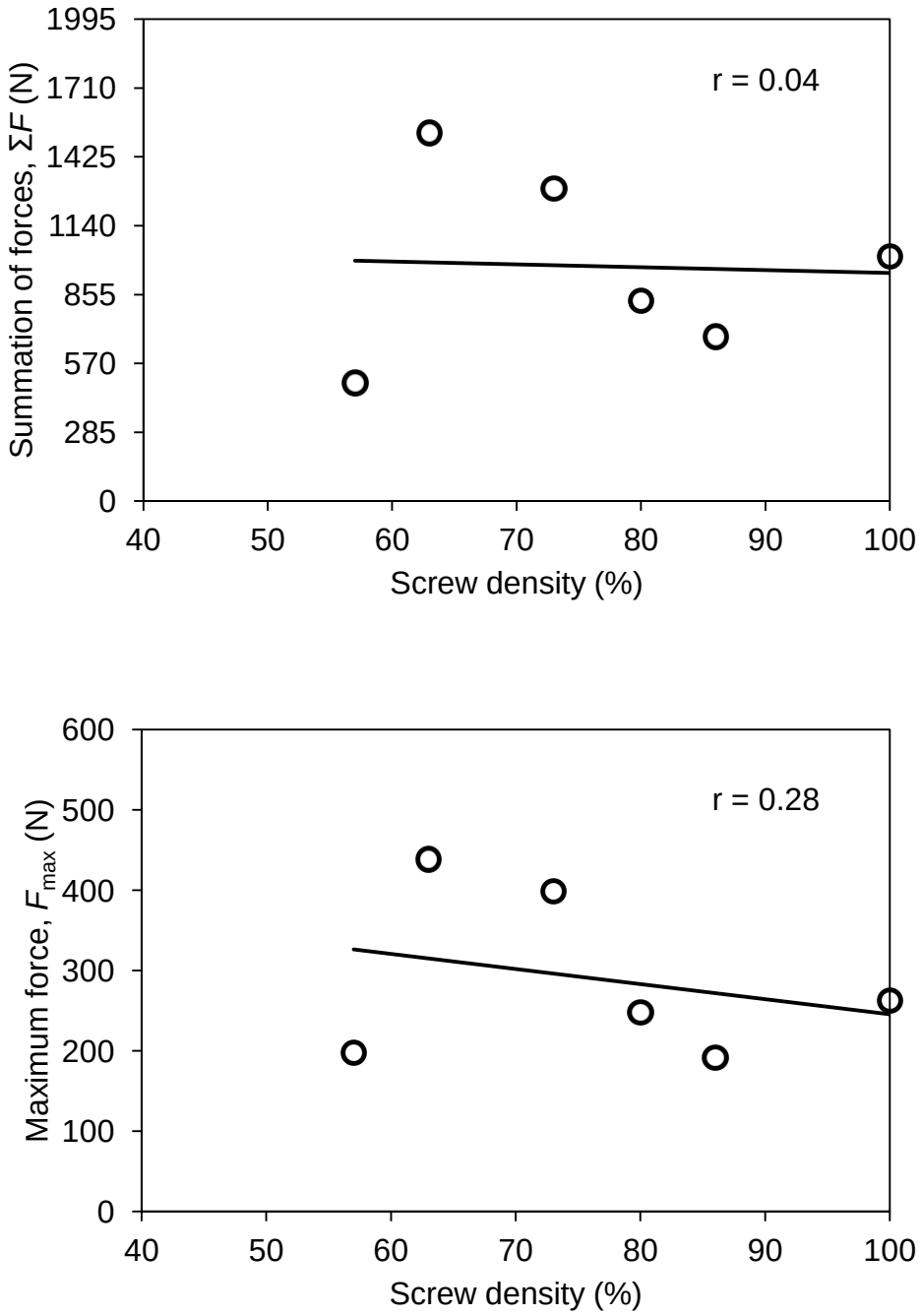

Figure 5.7 Relationships between the screw density and magnitude of forces. Screw density and summation of forces (top). Screw density and maximum force (bottom).

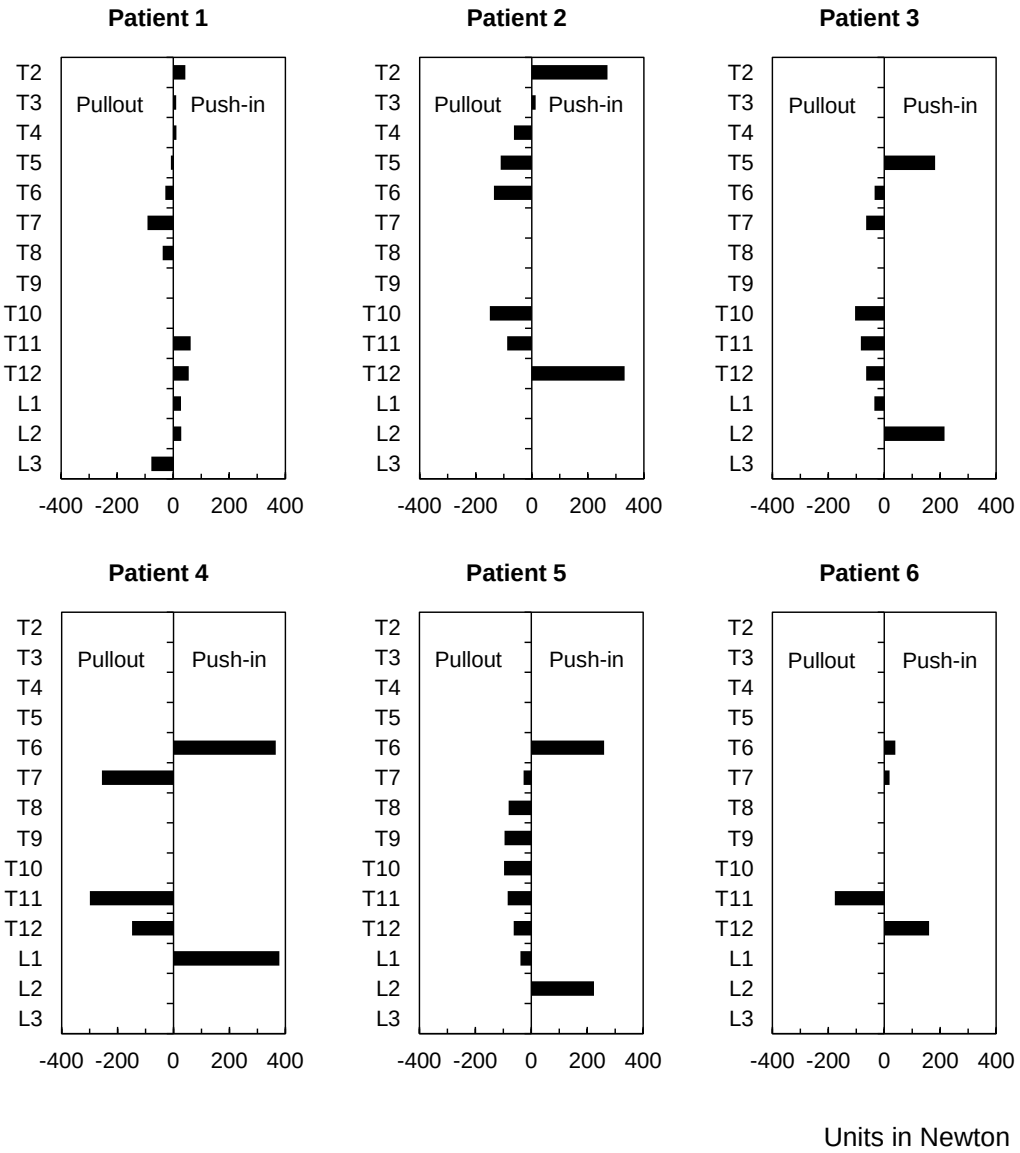

Figure 5.8 Pullout and push-in forces acting at the vertebra of each patient.

the implants sites beyond the implant rod length. Screw density at the convex side was not also included because the implant rod was not deformed after surgery. The rod at the convex side might have limited role in derotation maneuver but provides additional strength after it has been fixed by the screws.

The magnitude of forces did not correlate well with the degree of correction. The results suggest that scoliosis correction mechanism is not only dependent to the corrective forces. Some parameters such as flexibility or stiffness of the scoliotic spine need to be considered. Intuitively, patients having stiffer scoliotic spines need higher corrective forces than patients who have more flexible scoliotic spines. The current magnitude of forces must have been affected by patient's flexibility or stiffness. Spine's flexibility or stiffness is one of the major factors that influence the outcome of the clinical operation. Little et al. (2012) showed that flexibility is a primary factor which governs the degree of deformity correction and there is still much to be understood about the complex relationships that determine the individual patient's flexibility.

Although not statistically significant, a decreasing trend was found between the magnitude of forces and number of screws. The magnitude of corrective forces tended to be more distributed with increasing absolute number of screws. Conversely, increase in number of screws increases the surgical time that could also result to increase in blood loss and morbidity (Rose et al., 2009). Nevertheless, the previous relationship showed that the increase in number of screw did not result to higher curve correction.

The maximum and summation of forces indicate that having 100% screw density does not result to optimal clinical outcome. It was observed that some patients have much lower values of maximum and summation of forces than the patient who had 100% screw density. Further studies involving various screw placement configurations including the distribution of instrumented and non-instrumented levels could decrease the magnitude of forces while achieving similar outcome of curve correction.

6

Influence of Implant Rod Curvature on Sagittal Correction of Scoliosis Deformity

6.1 Abstract

A retrospective analysis was conducted to quantitatively measure the changes of implant rod angle of curvature during surgery and establish its influence on the sagittal correction of scoliosis deformity. No previous study had investigated the influence of the changes of implant rod angle of curvature on the sagittal deformity correction during scoliosis surgery. Twenty adolescent idiopathic scoliosis patients underwent surgical operation. Two implant rods were attached to the concave and convex side of the deformity. The implant rod geometry before the surgical implantation was measured during scoliosis treatment. The postoperative implant rod geometry after surgery was measured by CT scan. The implant rod angle of curvature was determined from the implant rod geometry at the sagittal plane. The spine sagittal curvature of healthy adolescents obtained by previous studies was used to assess the sagittal deformity correction. The difference between the postoperative implant rod angle of curvature and normal spine sagittal curvature of the corresponding instrumented level was used to evaluate over or under correction of the sagittal deformity. As a result, the implant rods at the concave side of deformity of all patients were significantly deformed after surgery. A significant relationship was found between the degree of rod deformation and the rod angle of curvature before surgical implantation. The results indicate that the postoperative sagittal outcome could be predicted from the initial rod shape. The changes in the implant rod angle of curvature may lead to the over or under correction of the sagittal curve. The rod deformation at the concave side suggests that the corrective forces acting on that side are higher than the convex side.

6.2 Introduction

Scoliosis deformity is usually evaluated using the Cobb angle. However, scoliosis is a complex deformity that needs to be assessed in three-dimensions. Several authors had proposed mathematical expressions in order to evaluate the morphology of scoliotic spines in three dimensions as well as the rotation of vertebrae (Kanayama et al., 1996; Tadano et al., 1996; Stokes et al., 1987). The correction of scoliosis deformity in frontal, sagittal and axial planes has been widely studied since then (Delorme et al., 2000; Smith, 2001; De Jonge et al., 2002; Rhee et al., 2002; Lee et al., 2004; Storer et al., 2005; Vialle et al., 2005; Kim et al., 2006; Lowenstein et al., 2007; Cheng et al., 2008).

The evaluation of the sagittal plane deformity correction involves a complex analysis of the spine segments as contrary to the Cobb angle measured at the frontal plane. The spine normally has thoracic kyphosis and lumbar lordosis curves in the thoracolumbar region. Neglecting to correct these curves could produce pain, intervertebral disc degeneration, bone-implant fracture, flat back and joint degeneration (Knott et al., 2010; Vrtovec et al., 2012). Lowenstein et al. (2007) proposed a method to measure the sagittal correction using the thoracic sagittal kyphosis from the superior endplate of T4 to the inferior endplate of T12 and lumbar lordosis measured from L1 to L5. Furthermore, a more complex evaluation involves the determination of sagittal balance. Although several papers discussed the various indicators for the measurement of sagittal balance, the Scoliosis Research Society (SRS) defined that the normal sagittal alignment is achieved when the plumb line drawn from the center of the cervical vertebra C7 lies within ±2 cm of the sacral promontory (Legaye et al., 1998; Berthonnaud et al., 2005a, 2005b; Boulay et al., 2006; Ondra and Marzouk, 2007; Roussouly and Nnadi, 2010). These methods have advanced the understanding of the sagittal plane correction. However, the fundamental limitation of visualizing and using the key anatomical landmarks still exists. Some studies reported inter and intra observer differences during measurements of sagittal spine curvatures (Labelle et al., 1995; Berthonnaud et al., 2005b, Dimar et al., 2008). These differences are due to the anatomical variants that are inherent to the spine morphology

which alter its normal symmetry from side-to-side (Liljenqvist et al., 2002; Rajwani et al., 2004). Asymmetry is primarily demonstrated by vertebral wedging in adolescent idiopathic scoliosis. Thus, failure to visualize the anatomical variants could lead to measurement errors. On the other hand, the postoperative lateral radiographs from previous studies show that the implant rod shape or curvature constitutes also the postoperative sagittal curve of the spine within the implant rod length, similar to Fig. 6.1(a) (Benli et al., 2007; Lowenstein et al., 2007; Clement et al., 2008; Asher et al., 2010; Ito et al., 2010; Patel et al., 2010; Hwang et al., 2012). These indicate that the implant rod curvature could be also used for the evaluation of sagittal curve correction. This also shows the use of implant rod to correct the deformity because the spine has to follow the rod shape during and after scoliosis surgery.

Due to the variability of surgeons' preferences and different correction objectives, optimal surgical treatment of scoliosis is not always attained (Desroches et al., 2007; Majdouline et al., 2009). Indeed, until now, there is no consensus yet on what possible initial shape of rod could lead to a certain sagittal outcome. Biomechanical models of the spine and instrumentation were developed to simulate various correction objectives, surgical steps and strategies (Aubin et al., 2003, 2008; Lafon et al., 2009). Some suitable surgical strategies for scoliosis patients were determined. However, the results might be unrealistic because rod deformation was not considered in their analyses (i.e. rigid body model). They estimated the preoperative implant rod geometry from postoperative data. The reported magnitude of forces (in several hundred or even thousand Newton) were apparently high that should have deformed the implant rod during the surgical treatment (Salmingo et al., 2013). Careful investigation on the changes of implant rod geometry is important because implant rod deformation could alter the sagittal alignment and consequently the clinical outcome.

The objective of this study was to measure the changes of implant rod angle of curvature before surgical implantation and after surgery, preoperative and postoperative, respectively. The difference between the preoperative and postoperative implant rod angle of curvature was used to evaluate the degree

of rod deformation. In order to establish whether it is possible to predict the clinical outcome from the intial rod shape, the relationship between the degree of rod deformation and preoperative implant rod angle of curvature was determined. The over or under correction of the sagittal curve was also evaluated using the postoperative implant rod angle of curvature.

6.3 Methods

6.3.1 Scoliosis surgical procedure

Upon approval of the university hospital research ethics committee on the use of human subjects, twenty (20) scoliosis patients (average age: 14 years, range: 10-20 years) diagnosed as severe Adolescent Idiopathic Scoliosis (AIS) were enrolled in this study and underwent surgical operation. A proper informed consent was thoroughly explained and obtained from all patients. Six mm diameter (Ø6 mm) titanium implant rods and polyaxial pedicle screws (USS II Polyaxial, Synthes GmbH, Switzerland) were implanted to correct the scoliosis deformity. The implant rod curvature and length were decided by the spine surgeons depending on the severity and type of each case. All implant rods were pre-bent only at a single plane. Implant rods and screws were surgically implanted following the double rod rotation technique procedure (Ito et al., 2010). In this technique, two implant rods used for the concave and convex side of the deformity were inserted into the polyaxial screw heads (Fig 6.1(a)). To allow the rods to rotate and translate freely inside the screw head, the polyaxial screw heads remained untightened until the completion of rod rotation procedure. The correction maneuver started when a torque was applied to the rod rotating device to simultaneously rotate the rods (about 90 degrees). This action transfers the previous curvature of rod at the coronal plane to the sagittal plane thereby creating a curve on the sides. Additional in-situ bending or other reduction maneuvers were not done in all the cases involved in this study. The amount of rod contouring was based on the amount of the desired kyphosis in the thoracic spine.

6.3.2 Implant rod angle of curvature

The implant rod angle of curvature at the corresponding extreme ends was measured using the preoperative and postoperative geometry of implant rod during the surgical operation to evaluate implant rod deformation in Fig. 6.1(b). The preoperative geometry of implant rod was measured from the actual implant rod used before surgical implantation by a conventional scanner.

The postoperative implant rod geometry was obtained within a week after the surgical operation using CT scanner (Aquilion 64 CT Scan, Toshiba Medical Systems Corporation, Japan). The slice thickness was set at 0.5 mm. The implant rod geometry was fitted by least square method using quintic polynomial functions having a minimum R^2 value of 0.99 (Salmingo et al., 2012b). Arbitrary points (7 points minimum) were selected for curve fitting. These points were obtained from the inferior to superior endpoint along the central axis of the implant rod. Medical image analysis was performed using computer software (MATLAB R2010b, Massachusetts, USA). The implant rod angle of curvature defined as the angle between the two tangent vectors was computed using the first derivative of the quintic polynomial function evaluated at the implant rod ends (Kanayama et al., 1996; Tadano et al., 1996).

There were three trials for each measurement. The average of the three trials was obtained as the preoperative and postoperative implant rod angle of curvature, θ_1 or θ_2 of each patient, respectively (Table 6.1). Since the implant rod curvature constitutes also the sagittal curve of the spine after surgery, the postoperative implant rod angle of curvature θ_2 was used to evaluate the sagittal curve correction of each scoliosis patient. The degree of rod deformation $\Delta\theta$ was defined as the difference between the preoperative and postoperative implant rod angle of curvature ($\theta_1 - \theta_2$). The relationship between the degree of rod deformation $\Delta\theta$ and preoperative implant rod angle of curvature θ_1 was sought to determine whether it is possible to predict the postoperative clinical outcome from the initial implant rod shape.

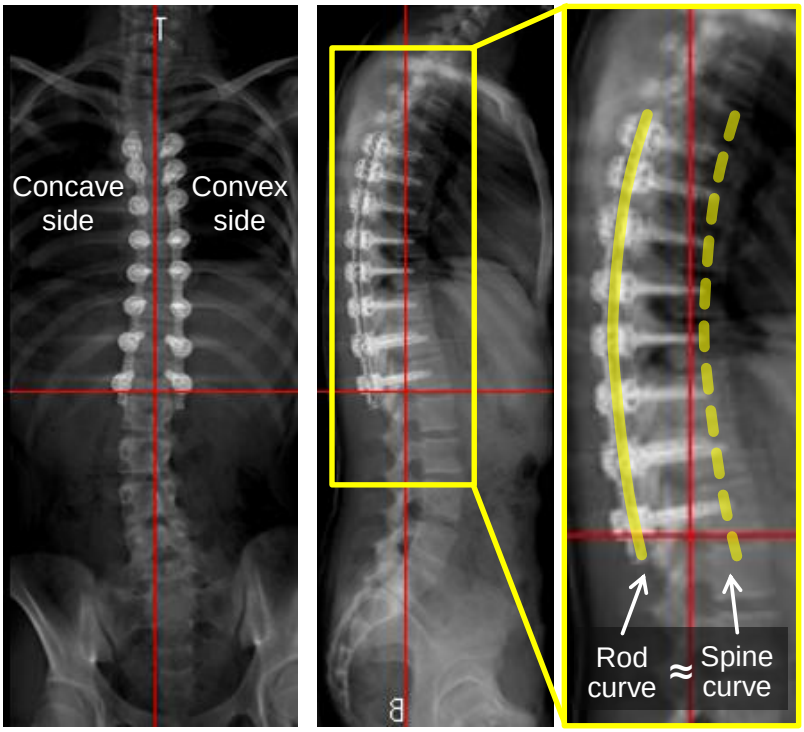

Frontal radiograph Sagittal radiograph

(a)

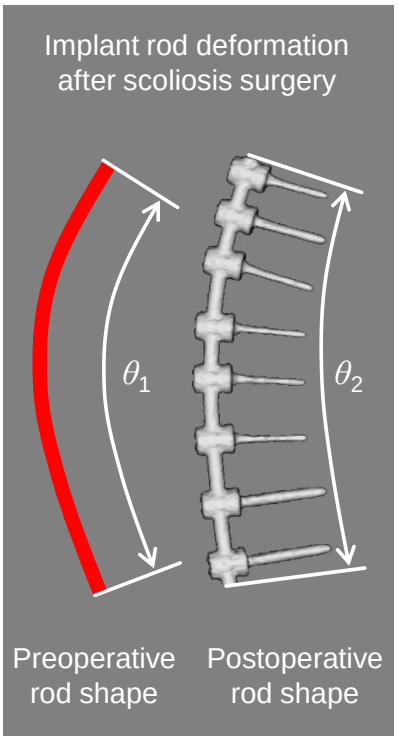

Implant rod angle of curvature

(b)

Figure 6.1 (a) Frontal and sagittal radiographs of the spine after surgery. (b) Preoperative and postoperative implant rod angle of curvature.

Table 6.1 Implant rod angle of curvature at the concave and convex side of deformity of each patient.

Patient	Concave side (deg.)			Convex side (deg.)		
	θ_1	θ_2	$\Delta\theta$	θ_1	θ_2	$\Delta\theta$
1	44.6	25.1	19.5	35.2	33.4	1.9
2	38.1	30.6	7.6	20.3	23.3	-3.0
3	43.4	19.7	23.7	34.7	27.3	7.4
4	18.5	10.6	8.0	20.6	16.3	4.3
5	19.1	5.0	14.1	19.7	24.6	-4.9
6	28.3	13.6	14.7	26.3	23.5	2.7
7	46.5	9.7	36.8	26.2	23.4	2.9
8	56.6	35.3	21.3	34.4	34.8	-0.4
9	18.0	6.1	11.9	11.7	7.0	4.7
10	37.0	18.3	18.7	25.3	26.6	-1.3
11	15.8	3.3	12.5	15.8	19.8	-4.0
12	28.8	13.6	15.3	20.1	14.2	5.9
13	18.1	5.7	12.4	12.8	14.5	-1.7
14	45.6	36.8	8.8	29.6	28.4	1.2
15	22.3	19.3	3.0	22.1	18.0	4.1
16	25.9	12.5	13.4	20.5	15.5	5.0
17	42.9	18.1	24.9	36.5	27.1	9.4
18	48.6	29.0	19.6	38.5	33.0	5.5
19	33.2	20.2	13.0	24.2	28.1	-3.9
20	41.3	23.4	17.9	34.7	39.5	-4.8

6.3.3 Normal spine sagittal curvature

The average thoracolumbar spine sagittal angle of curvature of healthy adolescents obtained by previous study was used to evaluate the sagittal correction (Mac-Thiong et al., 2007). The corresponding sagittal angle of curvature of each vertebra level was also determined since the instrumented or fixation level of each patient differs from each other. The angle of sagittal curvature of each vertebra level was approximated by the ratio of each height of vertebra (Kunkel et al., 2011). The normal spine sagittal angle of curvature between the corresponding fixation level θ_{FL} (FL = most superior and inferior fixation level) of each patient is listed in Table 6.2. Since the extreme fixation levels were the same for both sides of all scoliosis patients, the normal spine sagittal angle of curvature of each patient was the same for the concave and convex side.

Desirable correction of scoliosis deformity is achieved when the deformed spine is brought back to its original shape and fixed using implant rods and screws. Scoliosis correction is preferably attained when the postoperative implant rod angle of curvature θ_2 equals to the sagittal angle of curvature θ_{FL} of healthy adolescents at the corresponding fixation level. Thus, over or under correction of the sagittal curve could be determined using the difference. In this study, over correction was defined when the postoperative implant rod angle of curvature θ_2 is greater than the sagittal angle of curvature θ_{FL}; value of the difference is positive.

6.4 Results

Figure 6.2 shows the preoperative θ_1 and postoperative θ_2 implant rod angle of curvatures at the concave and convex sides of the deformity (Table 6.1, Fig. 6.2). The concave side was significantly deformed and the curvature tended to straighten after the surgical treatment of scoliosis. On the other hand, the rod at the convex side did not have significant deformation after the surgical treatment of scoliosis. The average preoperative and postoperative implant rod

Table 6.2 Normal spine sagittal curvature at the corresponding fixation level obtained from previous studies (Mac-Thiong et al., 2007; Kunkel et al., 2011).

Patient	Fixation level (FL)	Spine sagittal curve θ_{FL} (deg.)
1	T5-L2	12.3
2	T6-T12	27.7
3	T6-L1	18.4
4	T2-L3	12.5
5	T2-L3	12.5
6	T6-L2	8.9
7	T5-L1	21.8
8	T2-T12	41.1
9	T5-L3	2.6
10	T5-L1	21.8
11	T4-L3	6.0
12	T6-L2	8.9
13	T3-L3	9.4
14	T5-T12	31.1
15	T2-T11	36.6
16	T5-L2	12.3
17	T6-T12	27.7
18	T4-L1	25.3
19	T4-T12	34.5
20	T2-T11	36.6

angle of curvature at the concave and convex side of all patients is shown in Fig. 6.3. The average preoperative and postoperative implant rod angle of curvature at the concave side were 33.6 degrees (range 15.8 - 56.6 degrees) and 17.8 degrees (range 3.3 - 36.8 degrees), respectively. The average preoperative and postoperative implant rod angle of curvature at the convex side were 25.5 degrees (range 11.7 - 38.5 degrees) and 23.9 degrees (range 7.0 - 39.5 degrees), respectively.

A significant positive correlation was found between the degree of rod deformation $\Delta\theta$ and preoperative implant rod angle of curvature θ_1 at the concave side ($r = 0.60$, $p < 0.005$) in Fig. 6.4. This means that the greater the implant rod was bent, the higher degree of rod deformation could be obtained. There was no significant correlation on the implant rods at the convex side ($r = 0.26$, $p > 0.05$). However, the deformation behavior of the implant rods at the convex side is still predictable because it did not have significant deformation during scoliosis surgery. The results indicate that the postoperative implant rod curvature consequently the sagittal outcome could be predicted from the initial implant rod shape.

Desirable sagittal correction of scoliosis deformity is attained when the postoperative rod angle of curvature θ_2 equals to the sagittal curvature θ_{FL} at the corresponding fixation level. The difference between these parameters indicates over or under correction of the sagittal curvature. Figure 6.5 shows the difference between the postoperative rod angle of curvature θ_2 at the concave and convex side of deformity and sagittal curvature θ_{FL} of the corresponding fixation level ($\theta_2 - \theta_{FL}$). The positive region shows over correction and the negative region shows under correction. The results show that eight out of twenty patients (40%) had 5 degrees or lesser difference (i.e. Patients 2, 4, 9, 10, 12, 13, 14, 16). Seven patients (35%) had 10 degrees or lesser difference (i.e. Patient 3, 5, 6, 8, 11, 17, 18). Five patients had more than 10 degrees curvature difference (i.e. Patient 1, 7, 15, 19, 20).

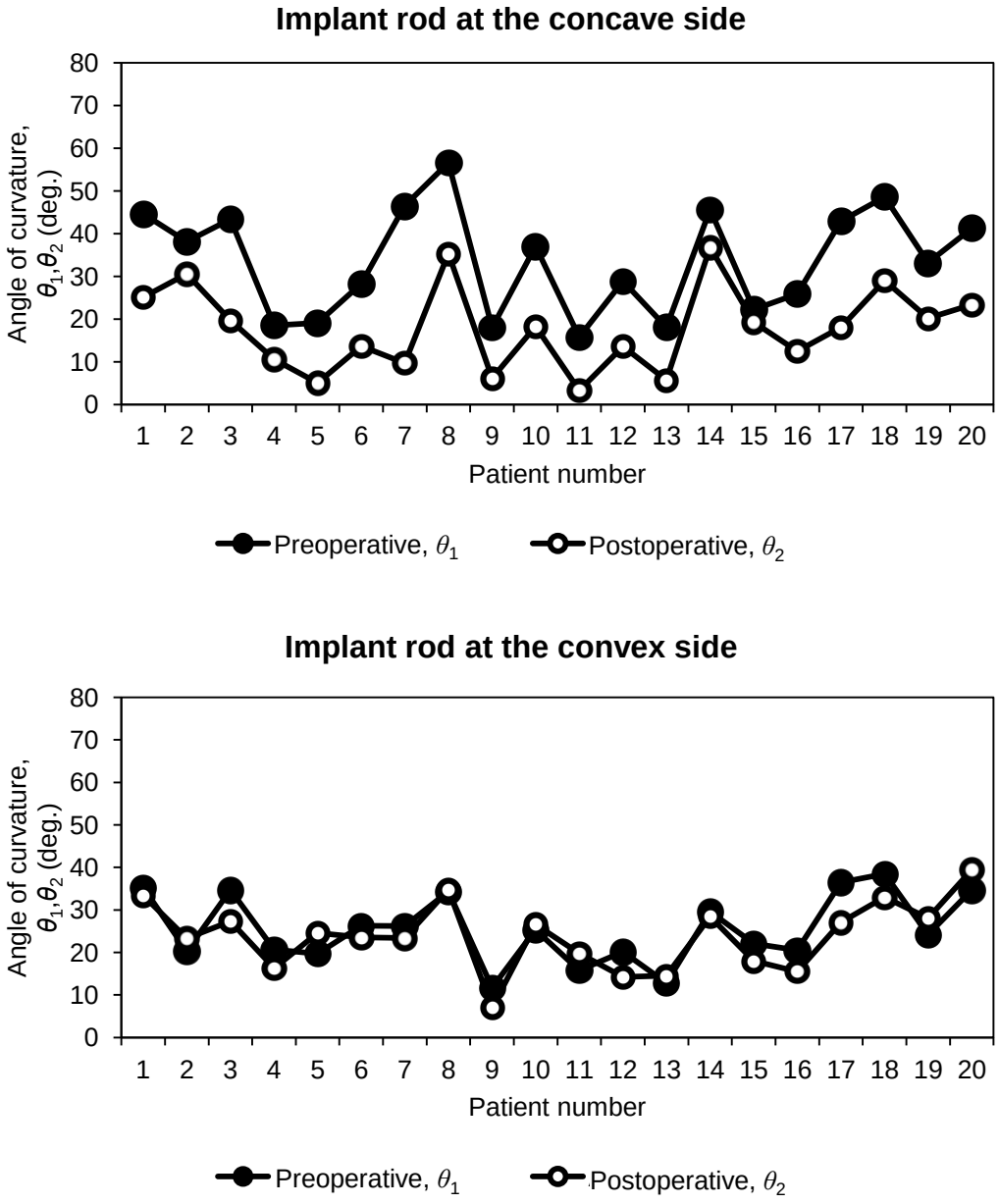

Figure 6.2 Preoperative and postoperative implant rod angle of curvature at the concave and convex side of deformity.

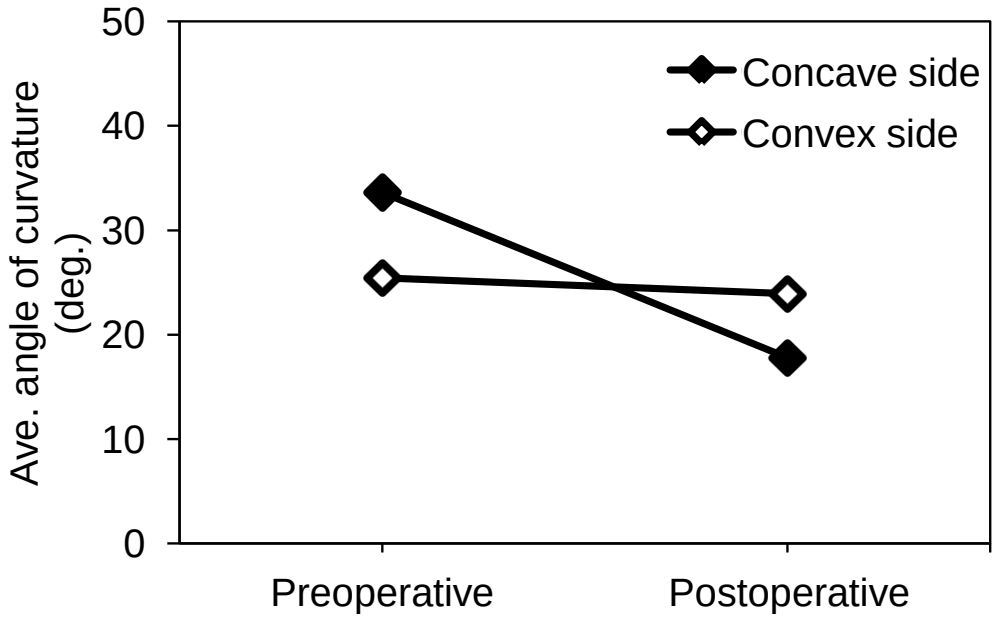

Figure 6.3 Average implant rod angle of curvature measured preoperatively and postoperatively.

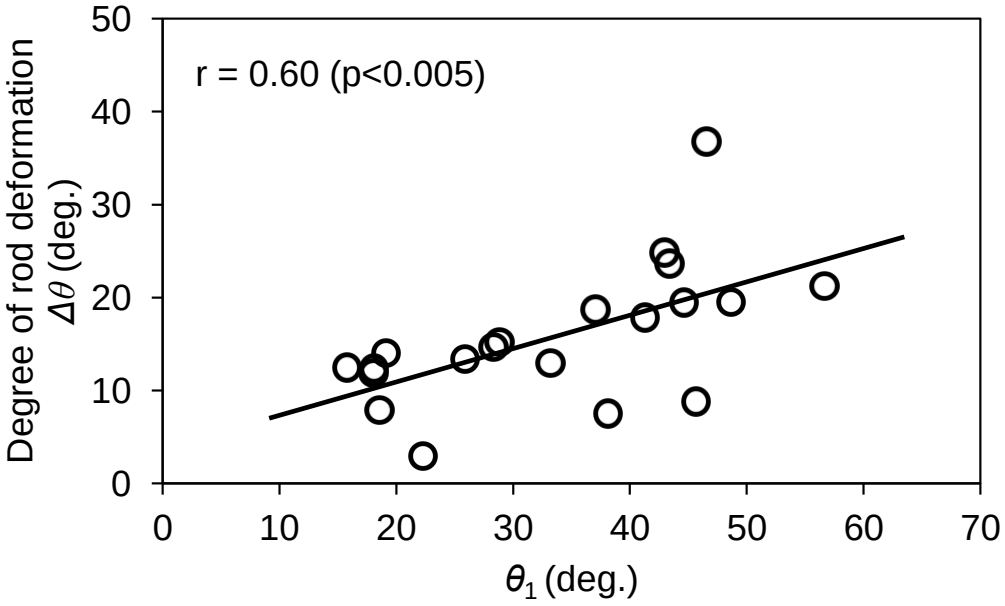

Figure 6.4 Relationship between the preoperative implant rod angle of curvature and degree of rod deformation at the concave side.

6.5 Discussion

Preservation of sagittal balance or alignment of the spine has been well studied. However, these studies were mainly focused on the postoperative results or the clinical outcome already. The primary factors (such as the initial rod shape) which are influencing the postoperative or sagittal outcome are not yet well studied. In fact, even until now, there is no consensus or scientific basis on what possible initial shape of rod could result into a certain sagittal outcome. Decision-making on the parameters to be used during surgery is always based on individual surgeons' preferences and experience (Desroches et al., 2007; Aubin et al., 2008; Majdouline et al., 2009). We have found a positive trend between the degree of rod deformation $\Delta\theta$ and preoperative implant rod angle of curvature θ_1 at the concave side. The significant relationship found in this study ($r = 0.60$, $p < 0.005$) suggests that estimation of the postoperative outcome from the preoperative implant rod shape is possible. A study involving more patients to find the optimal implant rod shape for certain scoliosis patients shall be done in the future. Until now, difficulties in visualizing the key anatomical landmarks from planar radiographs are still being reported. Intra and inter-observer studies were performed to determine the accuracy and reliability of computer methods. The advent of the digital radiographs enables the adjustment of image contrast and brightness. In effect, the anatomical landmarks can be highlighted which were not possible in conventional radiographs. Previous studies were successful in increasing the accuracy and reliability of sagittal profile measurement using computer-assisted programs (Berthonnaud et al., 2005b; Dimar et al., 2008). However, these methods still need many anatomical landmarks (i.e. requiring additional information input or computational time) which might be obscured in radiographs (Anderst et al., 2008). The dual-camera system is relatively simple because it does not require any anatomical feature which might be obscured in digital radiographs. Furthermore, it is well understood that scoliosis has an inherent morphological asymmetry (such as vertebral wedging and rotation) making it more difficult to visualize the anatomical features in the sagittal plane using just two-dimensional radiographs.

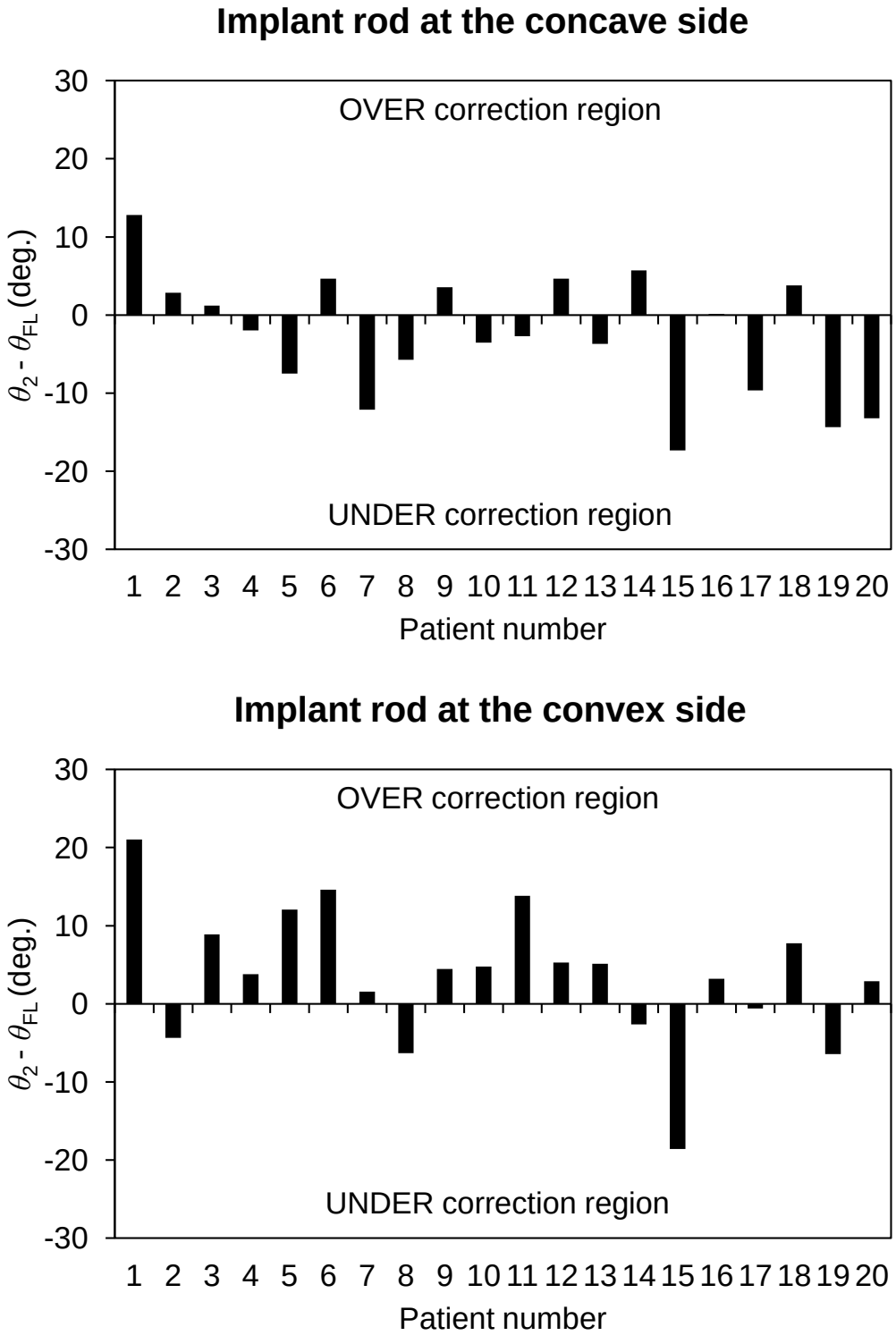

Figure 6.5 Difference between the postoperative implant rod angle of curvature θ_2 and physiological sagittal curvature θ_{FL} at the corresponding fixation level.

The degree of rod deformation indicates the magnitude of corrective forces acting on the rod in vivo. Thus, the results imply that the spine at the concave side was experiencing higher corrective forces than the convex side. This could be explained by the axial rotation and displacement of vertebra during the morphological growth of AIS. Many authors have investigated the cause of axial rotation of vertebrae (White and Panjabi, 1990; Stokes, 1989; Tadano et al., 1996). They have found out that the lateral deviation of the spine shifts the center of axial rotation of vertebra. This shift produces eccentric gravitational loads and moments causing the spinous process to rotate towards the concave side of the scoliosis deformity. As a consequence, the concave side of the deformity always tends to displace anteriorly while posteriorly at the convex side. Hence, the translational and rotational displacement required for the correction of the concave side is always higher than the convex side that could result also to higher corrective forces on that side. The kinematics during simultaneous rotation of rods might have also influenced the deformation behavior of rod. From a mechanical point of view, if torsion occurs on a certain body, the moment/force at the center of rotation is always zero or minimum. It could be hypothesized that the center of rotation of vertebra during simultaneous rotation of rods might be located somewhere around the convex side because the corrective forces acting on that side were negligible as indicated by the degree of rod deformation, theory shown in Fig. 6.6. A future study is required to validate this hypothesis through intraoperative measurement of three-dimensional spinal motion segments during scoliosis surgery.

It is well understood that the interpersonal differences such as height, weight, age, sex and etc. greatly affect the sagittal curvature of scoliosis or even normal subjects. The average physiological sagittal curvature of healthy adolescents obtained by previous studies was used to evaluate the sagittal correction (i.e. whether it was over and under corrected). Thus, it is imperative that a more detailed analysis considering the interpersonal differences will further improve the scoliosis correction assessment using the implant rod curvature.

This study presents the deformation behavior of titanium implant rods during correction of scoliosis deformities. Some stiffer spinal rod materials such as stainless steel and Cobalt-Chrome rods (stiffest of the three) may exhibit lesser implant rod deformation and deliver higher corrective forces than the titanium rods. The stiffer implant rods may provide also greater degree of deformity correction during scoliosis surgery. However, stiffer rods could inhibit bone formation and remodeling because they take too much of the applied loads instead of the spine (Gummerson and Millner, 2010). Likewise, from a mechanical point of view, stiffer rods induce higher corrective force which might be too high and could lead to the pullout of screw from the vertebra. Conversely, we have demonstrated in this study that the degree of deformity correction at the sagittal plane could be also attained or predicted as a function of the preoperative implant rod curvature not only the implant rod stiffness. A recent study has also reported that the magnitude of corrective forces acting on the deformed titanium rods during scoliosis surgery was within the safe level of pullout forces (i.e. 439 N max) (Salmingo et al., 2013)

In this study, we investigated whether we can estimate the postoperative implant rod angle of curvature from the initial implant rod shape. This was attained by measurement of the changes of implant rod geometry before implantation and after surgery (taken by postoperative CT). The postoperative CT was used because the two implant rods (i.e. rod at the concave and convex side) overlap each other at the sagittal plane, as shown in Fig. 6.1(a). Thus, we could not obtain the geometry of each implant rod using just planar sagittal radiograph. Conversely, CT scan can perform image segmentation and obtain the geometry of each rod at both sides postoperatively (Fig. 6.1(b)). In order to prevent the effects of variation of the surgical technique, the same surgeons performed the same surgical technique in all cases.

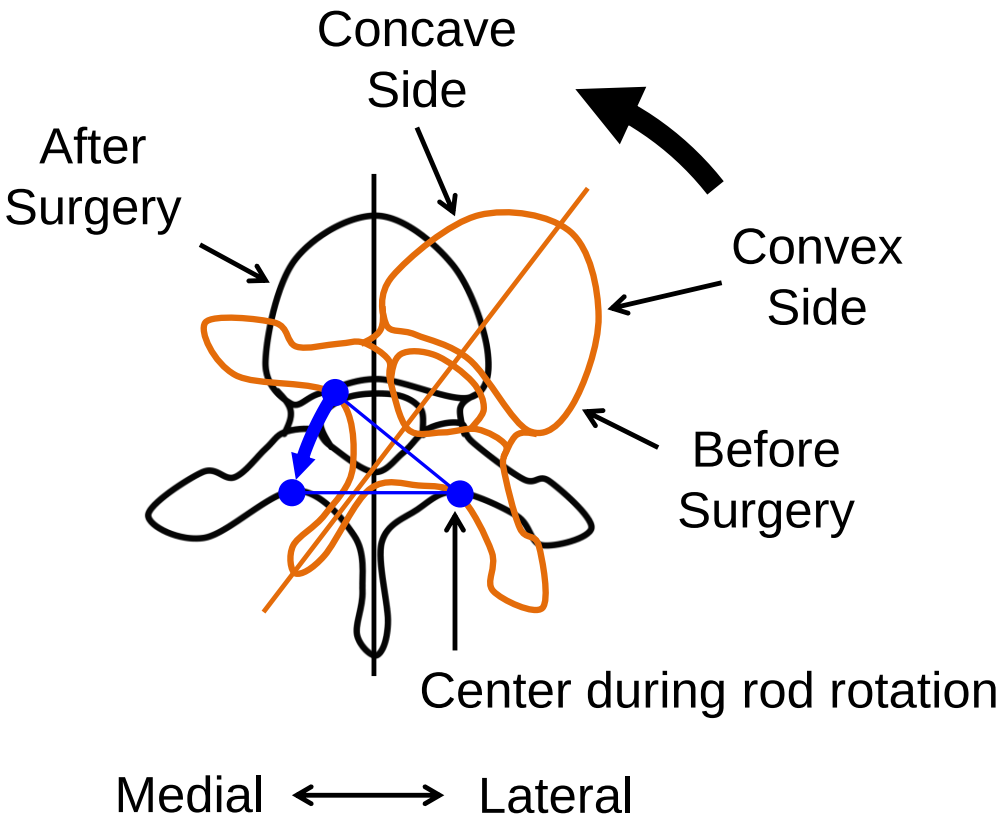

Figure 6.6 Rotation of the vertebra due to scoliosis deformity.

7

Intraoperative Changes of Implant Rod Three-Dimensional Geometry Measured by Dual-Camera System During Scoliosis Surgery

7.1 Abstract

Treatment for severe scoliosis is usually attained when the scoliotic spine is deformed and fixed by corrective rods. However, until now, there is no consensus yet on what implant rod shape could lead into an optimal correction outcome. Investigation of the intraoperative changes of implant rods shape in three-dimensions is necessary to understand the biomechanics of scoliosis correction. The objective of this study was to measure the intraoperative three-dimensional geometry and deformation of implant rod during scoliosis corrective surgery. Two implant rods for the concave and convex side were used to correct the spinal deformity. A pair of images was obtained intraoperatively by the dual-camera system during the surgical operation, i.e. before rotation and after rotation of rod during surgery. The three-dimensional implant rod geometry before implantation was measured directly by the surgeon and after surgery using a Computed Tomography scanner. The images of rods were reconstructed in three-dimensions using quintic polynomial functions. The implant rod deformation was evaluated using the angle between the two three-dimensional tangent vectors measured at the ends of the implant rod. The intraoperative and postoperative corrective forces were also calculated using our previous method. As a result, the deformation of implant rod at the concave side was measured intraoperatively and postoperatively. The maximum rod deformation was found after the rotation of rods. The results indicate that there is a reduction in the corrective forces after scoliosis surgery.

7.2 Introduction

Treatment for severe AIS often requires surgical intervention. Surgical treatment is accomplished when the scoliotic spine is deformed into the desired shape by corrective rods and screws attached to the vertebrae. The introduction of malleable rods and pedicle screws resulted to a more sophisticated system that addressed the scoliosis correction in three-dimensions, however, decision-making has become more complex. The current correction systems require surgeons to plan extensively the amount of rod curvature, length of rod and fixation level of screws to achieve a desirable clinical outcome. Aubin et al. (2007) and Robitaille et al. (2007) reported a large variability of preoperative instrumentation strategies within a group of experienced spine surgeons. Until now, the biomechanics of scoliosis correction is not yet fully understood. There is still a lack of consensus as reflected by the differences of surgical strategies specifically on what implant rod shape, rod length, number of screws and fixation levels should be used to achieve an optimal clinical outcome.

In an attempt to gain better understanding of the biomechanics of scoliosis correction, the effects of instrumentation systems and strategies during scoliosis surgery were investigated. Intraoperative tracking of trunk movement during scoliosis surgery using electromagnetic system and infrared cameras combined with markers that are mounted to the trunk were reported by Mac-Thiong et al. (2000) and Duong et al. (2009), respectively. They monitored the intraoperative motion of the trunk induced by the surgical maneuver during scoliosis surgical correction by posterior instrumentation. Intraoperative tracking of the trunk motion using these methods contributed to a better understanding of the effects of instrumentation systems by studying the movement or deformation correction of the trunk geometry. However, these methods require placement of markers to the trunk leading to increase in time of the surgical procedure. Vertebral motion measurements were also performed using a custom-made spinal instrument with markers attached directly to the vertebra of the spine. The custom-made instrument is drilled and fixed into the vertebral bone during scoliosis surgery (Delorme et al.,

1999; Holly, 2006; Smith et al., 2008). These methods helped the surgeons to understand how effective the various instrumentation systems in correcting the deformity in three-dimensions by evaluating the movements of vertebrae during the correction maneuver. Drilling of vertebral bone, however, became necessary to insert and fix the custom-made instrument in assessing the vertebral motion segments. These systems are complicated which could increase the surgical time and pose surgical operation risks due to additional drilling of bone. A simpler method that could assess the scoliosis correction intraoperatively without significantly affecting or interfering the operation is essential to understand the biomechanical effects of instrumentation systems such as implant rods on scoliosis deformity correction.

Evaluation of scoliosis correction in three-dimensions requires an assessment of both frontal and sagittal planes. Assessment of the frontal plane correction can be perceived easily since this plane is visible during scoliosis surgery (i.e. during posterior approach). Conversely, sagittal plane assessment is difficult because this cannot be seen during the operation and requires imaging tools and methods. The radiographs of many studies indicate that the implant rod curvature constitutes the spine shape (Benli et al., 2007; Lowenstein et al., 2007; Clement et al., 2008; Ito et al., 2010; Patel et al., 2010; Quan and Gibson, 2010; Hwang et al., 2012). This entails that the implant rod geometry can be used also to assess the scoliosis sagittal correction intraoperatively.

The main objective of this study was to measure the intraoperative three-dimensional geometry and deformation of implant rod during scoliosis corrective surgery. Two implant rods for the concave and convex side were used to correct the spinal deformity. A pair of images was obtained intraoperatively by two cameras during the two phases of surgery, i.e. before rotation of rods or when the rods were just inserted into the screw heads, and after rotation of rod (about 90 deg.) when the screws were fully tightened. The implant rod geometries before implantation and after surgery were also measured to compare the changes during the intraoperative phase. The implant rod angle of curvature between the implant rod ends was computed from the

implant rod geometry to quantitatively investigate the deformation of rod. The implant rod angle of curvature was used to assess the scoliosis correction within the implant rod length at the sagittal plane. The intraoperative and postoperative corrective forces acting on rods were also computed. Understanding the rod deformation behavior from the changes of implant rod geometry during the surgical treatment could strengthen our understanding on the biomechanics of scoliosis correction.

7.3 Methods

Upon approval of the university hospital research ethics committee on human subjects, three severe Adolescent Idiopathic Scoliosis (AIS) patients underwent surgical correction. Informed consent was thoroughly explained and obtained from each patient. The titanium implant rods of six mm in diameter (Ø6 mm) and polyaxial pedicle screws (USS II Polyaxial, Synthes GmbH, Switzerland) were implanted to the concave side (left rod) and convex side (right rod) of the scoliosis deformity (Fig. 7.1(left)). The implant rod shape and length vary with each patient and were decided by the attending surgeon (Fig. 7.1(right)). The implant rods were pre-bent at a single plane.

The screws and rods were surgically implanted following the simultaneous double-rod derotation technique. The procedure is briefly discussed here and the full details of the surgical technique are described in the previous paper of Ito et al. (2010). Two rods for the concave and convex side of the deformity were inserted into the polyaxial screw heads. The polyaxial screws were not yet fully tightened, i.e. to allow the rod to rotate and move freely inside the screw head until the completion of the rotation maneuver. The rods were simultaneously rotated (about 90 degrees) thereby transferring the previous curvature of the implant rod from the coronal plane to the sagittal plane.

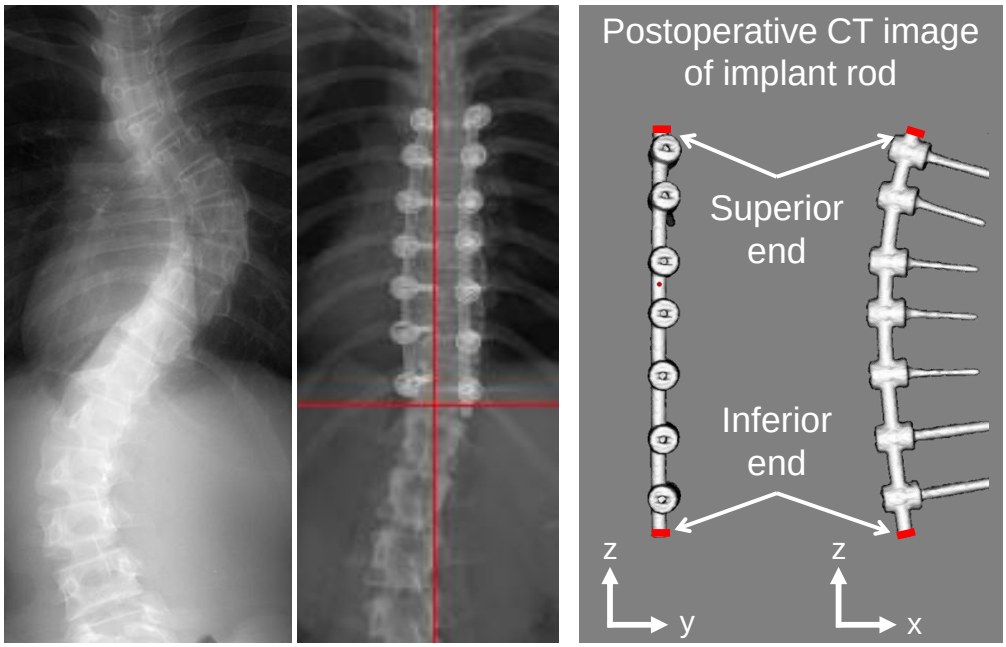

Figure 7.1 Scoliotic spine before surgery and after surgery when fixed by rods at the concave and convex side of the deformity (middle). Implant rod geometry obtained by CT scan and the reference three-dimensional coordinate axes.

7.3.1 Implant rod three-dimensional geometry measurement

The numerical method proposed by Salmingo et al. (2012b) to reconstruct the intraoperative three-dimensional geometry of implant rod utilizing two cameras was used. The images were acquired at the two intraoperative phases of scoliosis surgery, i.e. before rotation of rods or when the rods were just inserted into the screw heads, and after the rotation of rod (about 90 deg.) when the screws were fully tightened.

The image processing algorithm was programmed using computer software (MATLAB R2010b, Massachusetts, USA). The bases of the two cameras were set coplanar. The optical axes were obliquely positioned to each other at an included angle. The included angle (41-42 deg.) was adjusted intraoperatively to attain better image coverage. The intraoperative pairs of images at different views were obtained by the dual camera system, i.e. before rotation of rods (just inserted into the screw heads) and after rotation of rods as shown in Fig. 7.2. The rod at the left side of each image was the spinal rod at the concave side of the deformity. The rod at the right side of each image was the implant rod at the convex side of the deformity. Points $(n = \text{no. of points})$ measured in pixels, i.e. crosses, were selected from the most inferior to the most superior endpoint along the central axes of the implant rods as $(u_{1\to n}, v_{1\to n})$ and $(w'_{1\to n}, h'_{1\to n})$, for left and right images, respectively. Since v-axis and h-axis are parallel because the bases of the both cameras are coplanar to each other, the height of v_n should be equal to h'_n. However, this does not perfectly result into this relation because of the differences in the intrinsic parameters of each camera (e.g. camera focus, positioning error). A scaling factor $f_s = v_n / h'_n$ was introduced to transform the location of points in the right image as

$$h_n = v_n = f_s h'_n \tag{7.1a}$$

$$w_n = f_s w'_n \tag{7.1b}$$

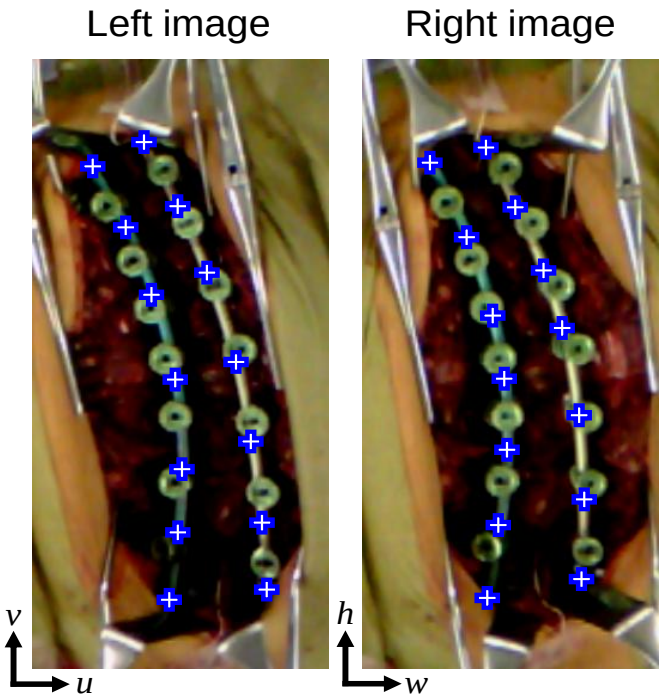

Before rod rotation
(a)

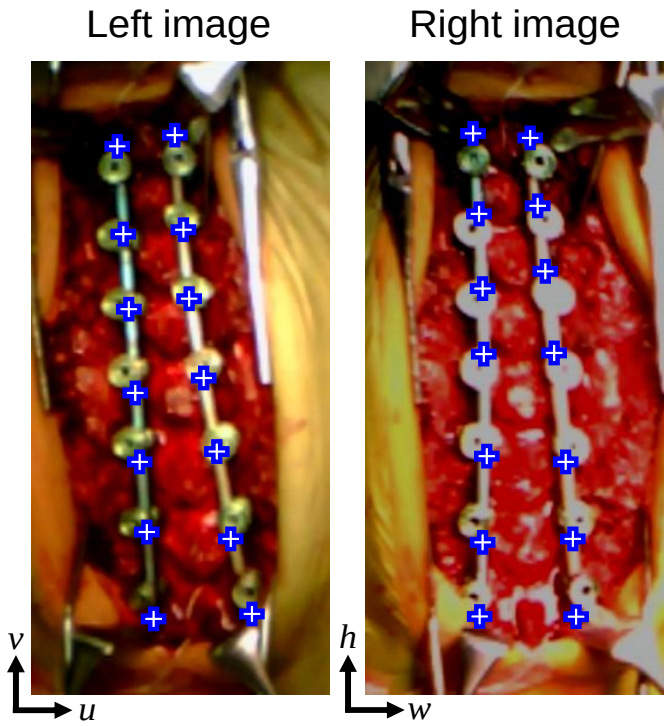

After rod rotation
(b)

Figure 7.2 Intraoperative images obtained by the dual-camera system during scoliosis surgery. The left and right rod of each image was the implant rod at the concave side and convex side, respectively.

The implant rod curvature on left and right pair of images represented by points $(u_{1\to n}, v_{1\to n})$ and $(w_{1\to n}, h_{1\to n})$ was fitted by quintic polynomial functions using least-square method as

$$u(v) = a_1 v + a_2 v^2 + a_3 v^3 + a_4 v^4 + a_5 v^5 \quad (7.2a)$$

$$w(h) = b_1 h + b_2 h^2 + b_3 h^3 + b_4 h^4 + b_5 h^5 \quad (7.2b)$$

The coordinate system was established for the three-dimensional geometry of implant rod (Fig. 7.1(right)). The implant rod is always pre-bent only at a single plane. The *x*-*z* plane was set as the principal bending plane. This plane also corresponds to the sagittal plane after rotation of rod. The *y*-*z* plane is orthogonal to the *x*-*z* plane. The most inferior end of the implant rod was set as the origin (0,0,0). Since the three-dimensional rod geometry could be oriented in various directions, 3D coordinate rotation was performed to translate the most superior end of the implant rod such that it coincides with the *z*-axis and to transform correspondingly the reference coordinate axes or planes. The three-dimensional implant rod geometry was computed using the generalized matrix

$$\begin{bmatrix} x_n \\ y_n \\ z_n \end{bmatrix} = \begin{bmatrix} -1/\tan\beta & 1/\sin\beta & 0 \\ 1 & 0 & 0 \\ 0 & 0 & 1 \end{bmatrix} \begin{bmatrix} u(v_{\max}/n) \\ w(h_{\max}/n) \\ v_{\max}/n \quad \text{or} \quad h_{\max}/n \end{bmatrix} \quad (7.3)$$

The three-dimensional geometry of implant rod can be represented by parametric equations in terms of unit vector *t* as

$$x(t) = c_1 t + c_2 t^2 + c_3 t^3 + c_4 t^4 + c_5 t^5 \quad (7.4a)$$

$$y(t) = d_1 t + d_2 t^2 + d_3 t^3 + d_4 t^4 + d_5 t^5 \quad (7.4b)$$

$$z(t) = t \quad (7.4c)$$

The actual length of rod L_{actual} in mm before bending was used for calibration because its length can be measured before surgical implantation. From a mechanical viewpoint, we know that the deformation of rod caused by bending does not significantly change the length of rod measured at the neutral axis. The actual rod length was measured before surgical implantation and the curve length of rod in pixels was numerically integrated as

$$L_{pixel} = \int_0^t \sqrt{\left(x'(t)\right)^2 + \left(y'(t)\right)^2 + \left(z'(t)\right)^2}\, dt \tag{7.5}$$

The calibration scale k was computed using Eq. (7.6). This parameter is also equal to the resolution of the measurement expressed in mm/pixel.

$$k = L_{actual} / L_{pixel} \tag{7.6}$$

The previous parametric equations Eqs. (7.4) can be represented as a vector function in pixels where (**i**, **j**, **k**) are the unit vectors for *x*, *y*, and *z* directions respectively as

$$\mathbf{r}_p = x(t)\mathbf{i} + y(t)\mathbf{j} + z(t)\mathbf{k} \tag{7.7}$$

The three-dimensional coordinates of implant rod in millimeters can be computed by equation

$$\mathbf{r} = \mathbf{r}_p \cdot k \tag{7.8}$$

The implant rod geometry before implantation was also measured by a conventional flatbed scanner. The implant geometry after surgery (one week maximum) was obtained postoperatively by CT scanner (Aquilion 64 CT Scan, Toshiba Medical Systems Corporation, Japan).

7.3.2 Implant rod deformation measurement

The three-dimensional geometry of spinal rod was obtained to quantitatively evaluate the implant deformation. The magnitude of implant rod deformation was evaluated using the angle of curvature between the most inferior and superior ends of the implant rod (Fig. 7.3). The angle of curvature was calculated using the three-dimensional implant rod geometry functions.

The tangent vector at the most inferior (*i* = inferior) and superior (*s* = superior) ends of the implant rod was computed as

$$\dot{\mathbf{r}}_i = \left(\frac{\partial x}{\partial t}, \frac{\partial y}{\partial t}, \frac{\partial z}{\partial t}\right)_i = \left(x'(z), y'(z), 1\right)_i \tag{7.9a}$$

$$\dot{\mathbf{r}}_s = \left(\frac{\partial x}{\partial t}, \frac{\partial y}{\partial t}, \frac{\partial z}{\partial t}\right)_s = \left(x'(z), y'(z), 1\right)_s \tag{7.9b}$$

The implant rod angle of curvature was calculated as the angle between the two three-dimensional tangent vectors formed normal to the implant rod ends (Fig. 7.3). The angle θ_{is} between the three-dimensional tangent vectors was obtained by $\dot{\mathbf{r}}_i$ and $\dot{\mathbf{r}}_s$ at the most inferior and superior implant rod ends, respectively as

$$\theta_{is} = \cos^{-1}\left(\frac{\dot{\mathbf{r}}_i \cdot \dot{\mathbf{r}}_s}{\left|\dot{\mathbf{r}}_i\right|\left|\dot{\mathbf{r}}_s\right|}\right) \tag{7.10}$$

7.3.3 Scoliosis correction assessment

It has already been shown that the implant rod curvature constitutes also the postoperative sagittal curve of the spine within its length. Thus, the implant rod angle of curvature can be used to evaluate scoliosis curvature correction postoperatively. The implant rod angle of curvature obtained in this study and the average thoracolumbar curvature of healthy adolescents at the sagittal plane established by previous studies were used for comparison. Mac-Thiong et al. (2007) measured the physiological thoracolumbar curvature of healthy adolescents at the sagittal plane. The individual curvature of each vertebra level was also determined because the instrumented level of each patient differs from each other. The individual curvature for each vertebra level was approximated using the ratio of each height of vertebra reported by Kunkel et al. (2011). The normal spine sagittal curvature between the corresponding fixation levels of each patient is listed in Table 7.1. The same angle was used for both sides for each patient because the extreme fixation level of the concave and convex side was also the same for both sides. The desirable correction is attained when the postoperative implant rod angle of curvature is the same with the normal spine sagittal curvature at the corresponding fixation level. Hence, assessment of over or under correction of the sagittal curve could be determined by the difference. In this study, under correction is defined when the postoperative implant rod angle of curvature was lower than the normal sagittal curvature of healthy adolescents. Likewise, over correction is

defined when the postoperative implant rod angle of curvature was higher than the normal sagittal curvature.

7.3.4 Intraoperative and postoperative force analysis

The intraoperative and postoperative forces were also computed using the changes of implant rod geometry after the rotation of rod and after surgery, respectively. The method proposed by Salmingo et al. (2013) was performed using ANSYS 11.0 software (ANSYS, Inc., Pennsylvania, USA). The elasto-plastic finite element model of the implant rod before surgery was reconstructed using 10 node tetrahedral solid elements. The forces were applied iteratively to the location of the screws such that the rod was deformed the same after surgery. The corrective forces acting on the implant rod were obtained after series of iterations. The material model was based from the implant manufacturer specifications. The elasto-plastic material properties were elastic modulus (E), yield stress (σ_Y), yield strain (ε_Y) and hardening coefficient (H) equal to 105 GPa, 900 MPa, 8.57×10^{-3} and 2.41 GPa, respectively.

7.4 Results

7.4.1 Implant rod three-dimensional geometry

The implant rod curvature images were obtained before implantation, before rotation of rod, after rotation of rod, and after surgery for each scoliotic patient. The implant rod length at the concave side of each patient was 218 mm, 188 mm and 215 mm for Patient 1, Patient 2 and Patient 3, respectively. The implant rod length at the convex side of each patient was 232 mm, 188 mm and 239 mm for Patient 1, Patient 2 and Patient 3, respectively (Table 7.1). The images were analyzed to measure the three-dimensional implant rod geometry. Figure 7.4 shows the three-dimensional implant rod geometry of the three patients during scoliosis surgery. To standardize and better understand the three-dimensional geometry and deformation of spinal rod, 3D coordinate

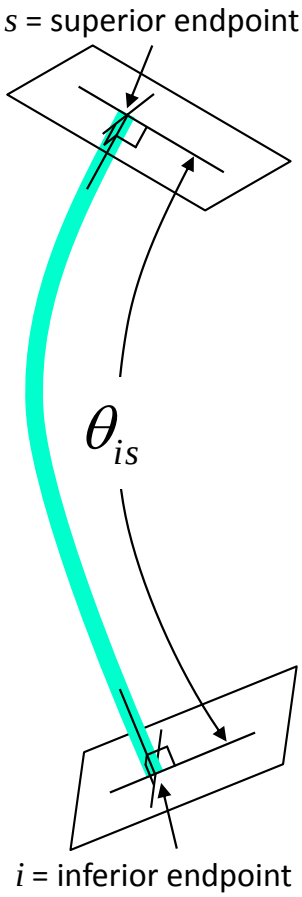

Figure 7.3 Rod deformation expressed as **i**mplant rod angle of curvature.

Table 7.1 Range of fixation, normal curvature of the spine, location of rod, length of rod and implant rod degree of curvature of each scoliosis patient.

Patient	Fixation range	Normal curve* (deg.)	Location	Rod length (mm)	Before implantation (deg.)	Before rotation (deg.)	After rotation (deg.)	After surgery (deg.)
1	T5-L1	22	Concave	218	52	55	5	26
			Convex	232	32	39	14	24
2	T6-T12	28	Concave	188	45	40	9	29
			Convex	188	31	32	26	30
3	T5-T12	31	Concave	215	50	40	31	36
			Convex	239	33	35	36	36

* Mac-Thiong et al. (2007) and Kunkel et al. (2011)

rotation was performed to translate the most superior end of the implant rod such that it coincides with the *z*-axis and to transform the planes to the corresponding reference coordinate axes or planes. The figures at the left side show the three-dimensional implant rod geometry at the concave side of deformity. The three-dimensional geometry of the implant rods at the convex side of deformity are shown at the right side. The 3D implant rod geometry was measured at different phases of scoliosis surgery, i.e. before implantation, before rotation of rod, after rotation of rod, and after surgery. All rods were not significantly deformed in *y*-*z* planes, i.e. the deformation was very small to be detected.

The *x*-*z* plane shows significant changes of rod geometry at the different phases of the surgical procedure. There was a slight difference between the geometry of implant rod before implantation and before rotation of rod. This is when the rod was just inserted into the heads of the implant screws. The rods tended to straighten during and after the surgical operation. The highest deformation occurred after rotation of rod and regained its curvature after the surgery. The curvature regain indicates that the kyphosis curve recovered after surgery or postoperatively. The deformation of rod indicates that the amount of corrective forces were significant as indicated by the changes of rod geometry in three-dimensions.

7.4.2 Implant rod deformation

The implant rod angle of curvature was used to evaluate implant rod deformation. The implant rod angle of curvature was computed as the angle between the two three-dimensional tangent vectors evaluated at the most inferior and most superior ends of the rod (Figs. 7.3 and 7.5). This corresponds also to the angle of curvature between the most inferior and most superior fixation level of the scoliosis patient. The unit of angle is expressed in degrees. The implant rod angles of curvature before implantation, before rotation of rod,

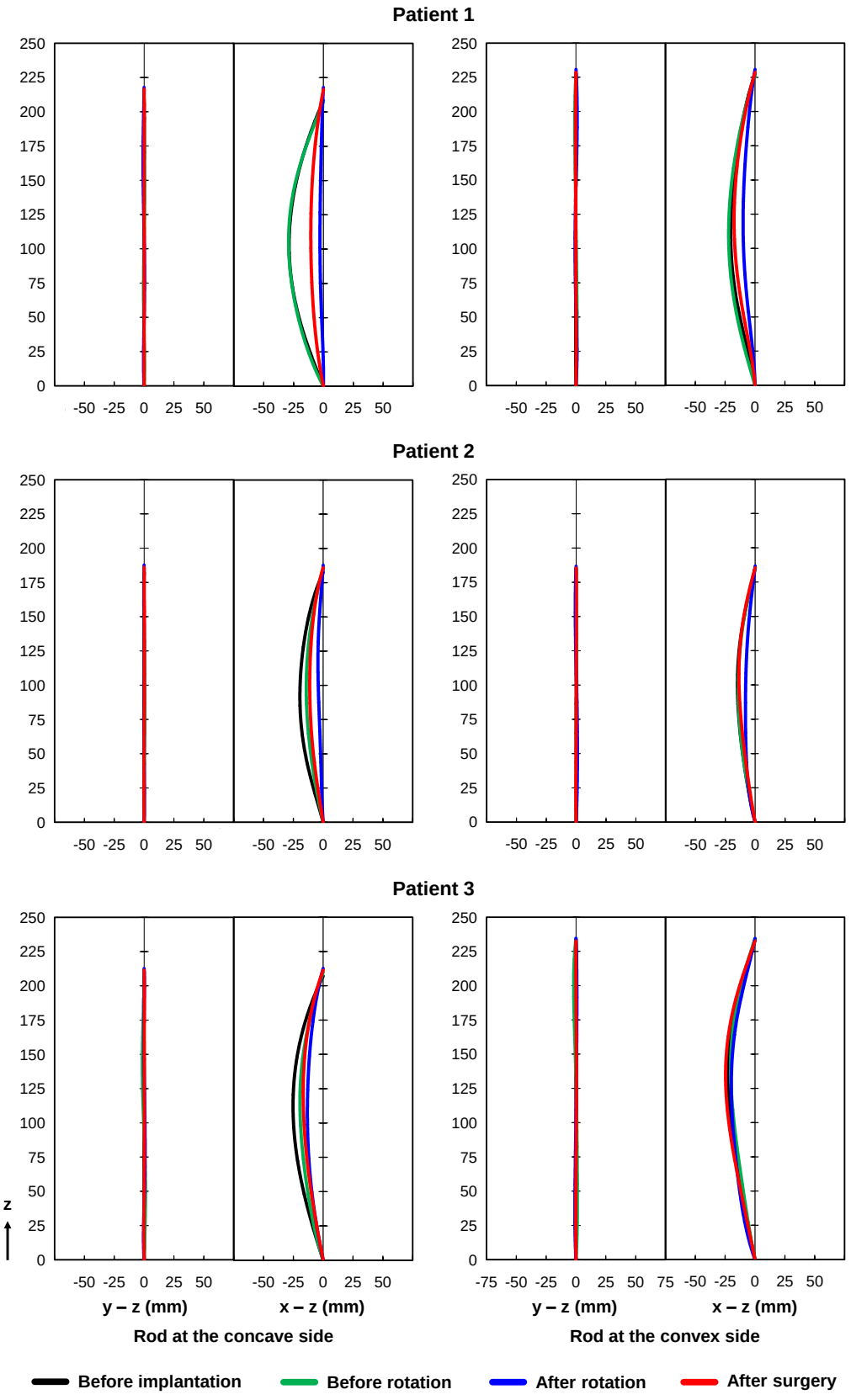

Figure 7.4 Three-dimensional implant rod geometry during and after surgery.

after rotation of rod, and after surgery of each scoliosis patient for the concave and convex sides are listed in Table 7.1.

Figure 7.5 shows the rod angle of curvature of each patient. The angle of curvature of the implant rod at the convex side did not have significant deformation except on Patient 1 during after rotation of rod. The difference between the implant rod angle of curvature before implantation to before rotation of rod for both concave and convex side was 0.4 deg. in average (range: -7.0 deg. to 10.0 deg.). For all patients, the highest deformation or a decrease in the implant rod angle of curvature was observed during after rotation of rod (degree of deformation was 50 deg.). Likewise, the implant rod angle of curvature at the concave side recovered after surgery in all scoliotic patients. The implant rod angle of curvature increased or regained by 9.9 deg. in average (range: 0.3 deg. to 20.7 deg.).

7.4.3 Scoliosis sagittal correction assessment

Since the implant rod curvature at the sagittal plane constitutes also the postoperative sagittal curve of the spine within the rod length. Ideal correction is achieved when the implant rod angle of curvature is the same with the thoracolumbar curvature of normal or healthy adolescents. The normal thoracolumbar curvature of healthy adolescents obtained by previous studies at the corresponding fixation level of each patient is listed in Table 7.1. The normal curvature for the comparison of the concave and convex side was the same since the most inferior and superior fixation level of each patient was also the same for both sides. For all patients, there was a small deviation or a slight over correction (maximum was 5.0 deg., convex side of Patient 3) from the normal curvature for both concave and convex sides (Fig. 7.6). The results indicate that the regain of implant rod curvature after rotation of rod were beneficial for obtaining the normal kyphosis of scoliosis patients. Thus, careful decision making on the shape or curvature of implant rod during scoliosis surgery is extremely important to prevent over or under correction of the spine sagittal curve.

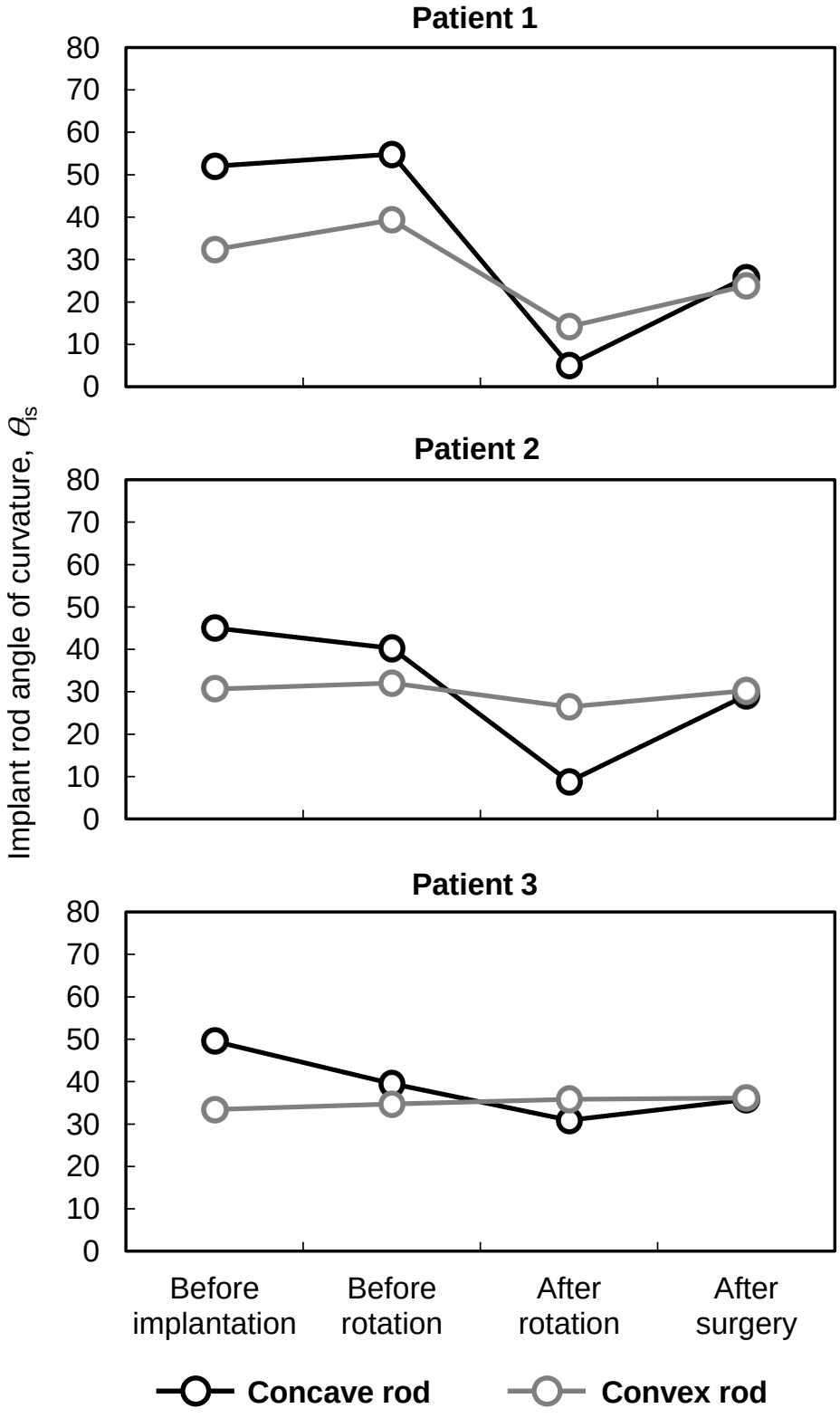

Figure 7.5 Implant rod angle of curvature of each patient.

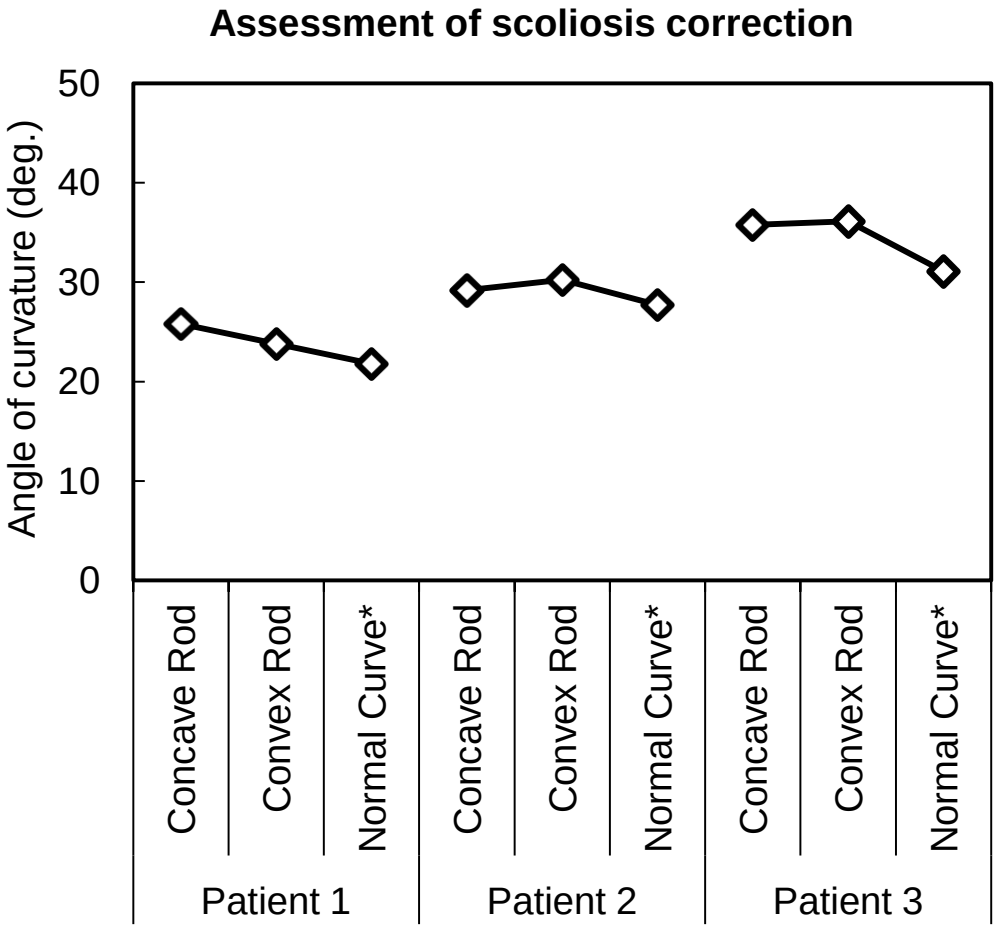

Angle of curvature (deg.) = angle of curvature after surgery θ_{is} of the implant rod at the concave and convex side, and normal spine curvature of healthy adolescents

Figure 7.6 Assessment of scoliosis correction using implant rod angle of curvature compared to normal curvature of the spine obtained by Mac-Thiong et al. (2007) and Kunkel et al. (2011)

7.4.4 Intraoperative and postoperative force

The magnitude of corrective forces obtained by FEA acting on each screw is shown in Fig. 7.7. The highest corrective force was acting at the extreme ends while the corrective forces along the apical vertebra tended to increase. This shows that the apical vertebra needs higher corrective forces than the other vertebra. The results show that the forces at the convex side were lower than the concave side. Apparently, in Patient 2 (convex-postoperative), the forces were minimal because the implant rod completely regained after surgery; returned to previous shape. Likewise, we could not detect significant amount of rod deformation and forces in the rod at the convex side of Patient 3. The results also indicate that the intraoperative corrective forces were significantly higher than the postoperative forces.

7.5 Discussion

Understanding of the biomechanics of scoliosis correction is important because until now optimal scoliosis correction is still difficult to attain. Surgical parameters specifically what shape and length of rod, location of fixation levels and surgical technique still vary dependently with the surgeons' experiences and preferences. There is no consensus yet on what surgical strategy can be applied to a certain scoliosis case to achieve an optimal clinical outcome. Furthermore, in vivo implant rod deformation could alter the correction outcome primarily at the sagittal plane. Thus, it is imperative that the three-dimensional changes of implant rod geometry at the different phases of shall be measured during scoliosis surgery.

The results show that the three-dimensional geometry of implant rod can be measured intraoperatively during scoliosis surgery. For all cases, there was a small difference between the geometry of implant rod before implantation and before rotation (Fig. 7.5). This suggests that the corrective forces acting on the rods were minimal. This is because the rods were just inserted into the screw heads and the correction maneuver or rotation of rod

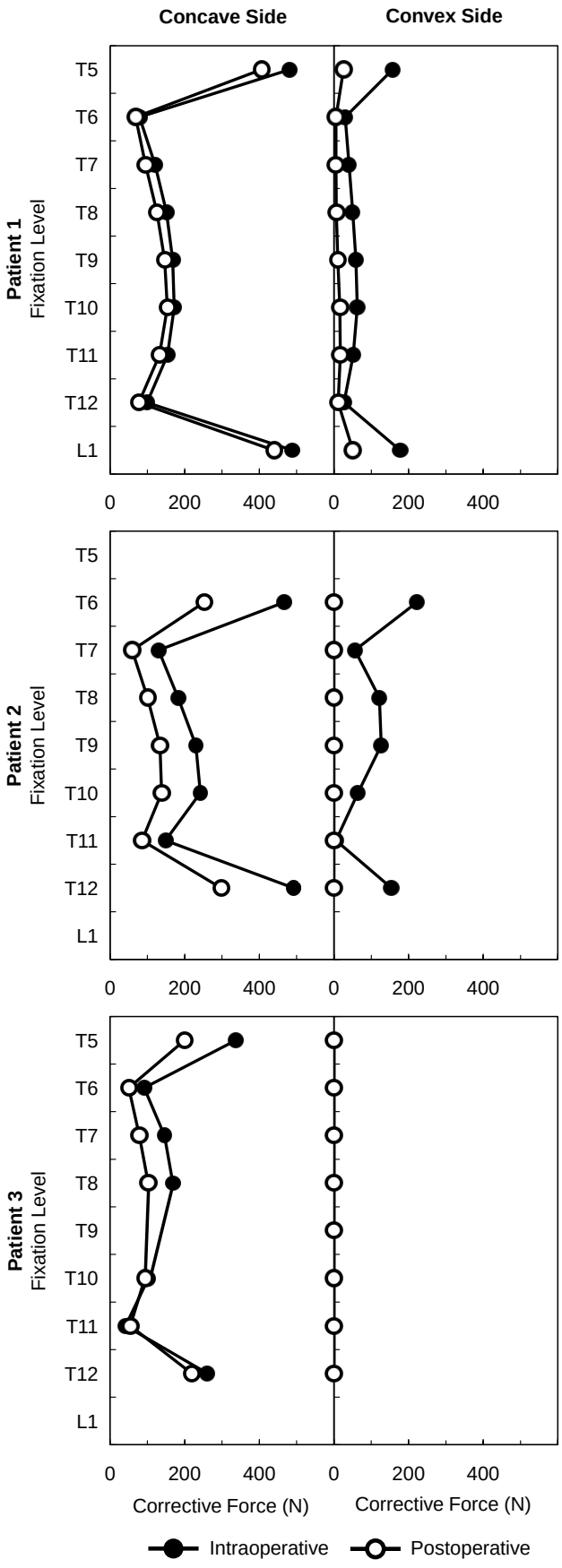

Figure 7.7 Intraoperative and postoperative corrective forces of each patient.

has not been initiated yet. Conversely, the rods specifically at the concave side tended to straighten after rotation of rod. The significant decrease in the implant rod curvature indicates that the corrective forces carried by the spinal rod were also high. The goal of scoliosis correction was to transfer the previous curvature of implant rod at the coronal plane to the sagittal plane by rod rotation (approx. 90 deg). Thus, a significant amount of corrective forces is required to displace the spine structure to the desired location. The rod curvature tended to regain after surgery (one week maximum) which subsequently increased the kyphosis curve. The increase in the implant rod curvature might be due to the effects of body weight after surgery wherein patients began doing postoperative activities such as standing, walking and etc. It is well established that the body weight increases the curvature of the spine (Janssen et al., 2010 and Little et al., 2012).

The angle of curvature revealed that the implant rod at the concave and convex side was the same after surgery even though it was pre-bent at a different curvature. Furthermore, it can be also noticed that despite of the various degree of deformation, i.e. before rotation and after rotation of each case, the angle of curvature on both sides tended to converge after surgery. These results reveal that there is a compensatory mechanism that attempt to equalize the changes in both sides. This is beneficial during scoliosis surgery because this could help us estimate the postoperative sagittal curvature since the deformation of rod at the convex side was minimal.

To the best of our knowledge, this is the first time that the intraoperative three-dimensional geometry of implant rod was measured quantitatively during scoliosis surgery. Previous studies performed finite element modeling of the scoliosis surgical procedure (Aubin et al., 2008; Lafon et al., 2009; Wang et al., 2011a). However, rod deformation was not considered in their analyses. This study showed a significant magnitude of implant rod deformation during the different phases of surgery. From a mechanical point of view, if rod deformation is not considered in finite element analysis or being a rigid body model, the magnitude of computed forces will be high and thus unrealistic. Indeed the maximum force obtained

by Aubin et al. (2008) was 956 N that is apparently high enough to deform the implant rod during scoliosis surgery. Salmingo et al. (2012a) reported the magnitude of corrective forces acting on the deformed implant rods after surgery. The maximum corrective force obtained was 439 N. Deformation of implant rod should not be neglected in order to obtain more accurate results. The intraoperative and postoperative corrective forces were also computed. The implant rod deformation is directly related to the magnitude of corrective forces acting on the spine in vivo. The highest corrective force occurred after the rotation of rod and decreased after surgery (Fig. 7.7). The magnitudes of corrective forces imply that the intraoperative phase requires more attention for preventing implant rod breakage or screw pullout during scoliosis surgery. Thus, careful intraoperative rod maneuver and planning is important to achieve a safe and optimal clinical outcome.

8

Conclusions

8.1 Summary of findings

The distribution of corrective forces acting at the deformed implant rod was analyzed using just the rod geometry at different phases of scoliosis treatment, i.e. during surgery and after surgery. These forces are carried by the implant rod as a result of the inherent resistance of the spine to correction. This work helps to understand the magnitude of corrective forces acting at the vertebrae of the spine during scoliosis treatment.

The proposed numerical method using the dual-camera system to measure the intraoperative three-dimensional geometry of implant rod during scoliosis surgery was validated using the actual implant rod used for scoliosis treatment. The accuracy of the method (within 0.32 to 0.45 mm) is sufficient enough to measure the intraoperative deformation of implant rod during scoliosis corrective surgery. The proposed method is useful because it requires only the actual length of implant rod for calibration and does not employ any calibration markers and additional devices which could interfere the scoliosis surgical procedure.

Scoliosis correction mechanism does not only depend on the number of screws and corrective forces acting on implants but also associated with screw the placement configuration. The findings of this study suggest that scoliosis deformity can be easily manipulated with higher screw density. However, increasing screw density alone does not ensure safe clinical outcome as indicated by the magnitude of forces. Moreover, the increase in total number of screws tended to reduce the magnitude of corrective forces. The forces tended to be more distributed when more screws are used but also may depend on the screw placement configuration.

The positive correlation between the degree of rod deformation and preoperative implant rod curvature implies that the postoperative implant rod shape or clinical outcome can be predicted from the initial implant rod geometry. It was clearly shown that the implant rod curvature greatly influenced the sagittal correction of scoliosis deformity. Careful planning of the preoperative implant rod curvature is necessary to prevent over or under

correction of spine deformity. The deformation of implant rod indicates that the corrective forces required at the concave side are higher than the convex side of deformity.

To the best of our knowledge, this is the first time that the intraoperative three-dimensional geometry of implant rod was measured quantitatively during scoliosis surgery. The magnitude of intraoperative corrective forces was higher than the postoperative forces. This suggests that extensive planning of the implant rod shape to be used for scoliosis treatment is important because bone and implant fracture might occur intraoperatively as indicated by the magnitude of forces.

In this study, we presented the magnitude of corrective forces acting on the deformed implant rod and vertebra during scoliosis surgery. This study provides new insights on the effects of screw placement configuration on the corrective forces and deformation behavior of the implant rod during scoliosis treatment.

8.2 Future works

The optimal implant rod geometry which could attain the best clinical outcome could be investigated using patient-specific finite element model of the spine and implants. Using patient-specific models, it is possible to investigate the effects of instrumentation and outcome of the surgical procedure.

Another important issue during the surgical treatment is the loss of feeling of the surgeon to feel the resistance of each corrected level (i.e. located at each screw). This is because the rod rotating device is attached to the rod at a single location only. It will be more meaningful in future studies if we can directly establish the relation of the required force to rotate the rod and the forces acting on each screw or vice versa because the corrective forces occurring at each screw might be excessive. From this, the surgeons can decide intraoperatively whether the applied force during the rod rotation maneuver is safe or not.

The reconstruction of implant rod three-dimensional geometry was conducted after the images had been obtained. These images were analyzed using a custom program in Matlab by manually selecting the points along the neutral axis for curve fitting of the implant rod shape. Thus, the three-dimensional reconstruction of implant rod geometry is not conducted in real-time. The real-time reconstruction is difficult because of image artifacts (e.g. blood surrounds the rod, implant screw head covers the rod). Hence, it will be more useful in the future to develop an image processing algorithm that will automatically segment the implant rod shape and remove the image artifacts. Furthermore, we could also analyze the real-time corrective forces from the implant rod deformation during scoliosis corrective surgery.

References

Aaro, S., Dahlborn, M. (1982) Estimation of vertebral rotation and the spinal and rib cage deformity in scoliosis by computer tomography. Spine 6:460-467.

Adair, I., Van Wijk, M., Armstrong, G. (1977) Moiré topography in scoliosis screening. Clinical Orthopaedics and Related Research 129:165-171.

Akbarnia, B. (2007) Management themes in early onset scoliosis. Journal of Bone and Joint Surgery 89:42-54.

Anderst, W., Vaidya, R., Tashman, S. (2008) A technique to measure three-dimensional in vivo rotation of fused and adjacent lumbar vertebrae. Spine Journal 8:991-997.

Angevine, P., Kaiser, M. (2008) Radiographic measurement techniques. Neurosurgery 63:40-45.

Asher, M., Lai, S., Burton, D. (2010) Analysis of instrumentation/fusion survivorship without reoperation after primary posterior multiple anchor instrumentation and arthrodesis for idiopathic scoliosis. Spine Journal 10:5-15.

Aubin, C., Petit, Y., Stokes, I., Poulin, F., Gardner-Morse, M., Labelle, H. (2003) Biomechanical modeling of posterior instrumentation of the scoliotic spine. Computer Methods in Biomechanics and Biomedical Engineering 6:27-32.

Aubin, C., Labelle, H., Ciolofan, O. (2007) Variability of spinal instrumentation configurations in adolescent idiopathic scoliosis. European Spine Journal 16:57-64.

Aubin, C., Labelle, H., Chevrefils, C., Desroches, G., Clin, J., and Boivin, A. (2008) Preoperative planning simulator for spinal deformity surgeries. Spine 33:2143-2152.

Benli, I., Ates, B., Akalin, S., Citak, M., Kaya, A., Alanay, A. (2007) Minimum 10 years follow-up surgical results of adolescent idiopathic scoliosis patients treated with TSRH instrumentation. European Spine Journal 16:381-391.

Berthonnaud, E., Dimnet, J., Roussouly, P., Labelle, H. (2005a) Analysis of the sagittal balance of the spine and pelvis using shape and orientation parameters. Journal of Spinal Disorders and Techniques 18:40-47.

Berthonnaud, E., Labelle, H., Roussouly, P., Grimard, G., Vaz, G., Dimnet, J. (2005b) A variability study of computerized sagittal spinopelvic radiologic measurements of trunk balance. Journal of Spinal Disorders and Techniques 18:66-71.

Berven, S., Bradford, D. (2002) Neuromuscular scoliosis: causes of deformity and principles for evaluation and management. Seminars in Neurology 22:167-178.

Bilgiç, S., Ersen, O., Sehirlioglu, A. (2010) Brace treatment in adolescent idiopathic scoliosis. Journal of Clinical and Analytical Medicine. (open access).

Boulay, C., Tardieu, C., Hecquet, J., Benaim, C., Mouilleseaux, B., Marty, C., Prat-Pradal, D., Legaye, J., Duval-Beaupère, G., Pélissier, J. (2006) Sagittal alignment of spine and pelvis regulated by pelvic incidence: standard values and prediction of lordosis. European Spine Journal 15:415-422.

Bunnell, W. (2005) Selective screening for scoliosis. Clinical Orthopaedics and Related Research 434:40-45.

Cheng, J., Lebow, R., Schmidt, M., Spooner, J. (2008) Rod derotation techniques for thoracolumbar spinal deformity. Neurosurgery 63:149-156.

Clement, J., Chau, E., Kimkpe, C., Vallade, M. (2008) Restoration of thoracic kyphosis by posterior instrumentation in adolescent idiopathic scoliosis: comparative radiographic analysis of two methods of reduction. Spine 33:1579-1587.

Clements, D., Betz, R., Newton, P., Rohmiller, M., Marks, M., Bastrom, T. (2009) Correlation of scoliosis curve correction with the number and type of fixation anchors. Spine 34:2147-2150.

Cotrel, Y., Dubousset, J., Guillaumat M. (1988) New universal instrumentation in spinal surgery. Clinical Orthopaedics and Related Research 227:10-23.

Daruwalla, J., Balasubramaniam, P. (1985) Moire topography in scoliosis - its accuracy in detecting the site and size of the curve. Journal of Bone and Joint Surgery 67:211-213.

De Jonge, T., Dubousset, J., Illes, T. (2002) Sagittal plane correction in idiopathic scoliosis. Spine 27:754-760.

Delorme, S., Labelle, H., Aubin, C., de Guise, J., Rivard, C., Poitras, B., Coillard, C., Dansereau, J. (1999) Intraoperative comparison of two instrumentation techniques for the correction of adolescent idiopathic scoliosis. Rod rotation and translation. Spine 24:2011-2017.

Delorme, S., Labelle, H., Aubin, C., de Guise, J., Rivard, C., Poitras, B., Dansereau, J. (2000) A three-dimensional radiographic comparison of Cotrel-Dubousset and Colorado instrumentations for the correction of idiopathic scoliosis. Spine 25:205-210.

Desroches, G., Aubin, C., Sucato, D., Rivard, C. (2007) Simulation of an anterior spine instrumentation in adolescent idiopathic scoliosis using a flexible multi-body model. Medical and Biological Engineering and Computing 45:759-768.

Di Silvestre, M., Parisini, P., Lolli, F., Bakaloudis, G. (2007) Complications of thoracic pedicle screws in scoliosis treatment. Spine 32:1655-1661.

Dickson, R., Weinstein, S. (1999) Bracing and screening - yes or no? Journal of Bone and Joint Surgery 81:193-198.

Dimar, J., Carreon, L., Labelle, H., Djurasovic, M., Weidenbaum, M., Brown, C., Roussouly, P. (2008) Intra- and inter-observer reliability of determining radiographic sagittal parameters of the spine and pelvis using a manual and a computer-assisted methods. European Spine Journal 17:1373-1379.

Doody, M., Lonstein, J., Stovall, M., Hacker, D., Luckyanov, N., Land, C. (2000) Breast cancer mortality after diagnostic radiography. Spine 25. 2052- 2063.

Drerup, B. (1984) Principles of measurement of vertebral rotation from frontal projections of the pedicles. Journal of Biomechanics 17:923-935.

Duong, L., Mac-Thiong, J., Labelle, H. (2009) Real time noninvasive assessment of external trunk geometry during surgical correction of adolescent idiopathic scoliosis. Scoliosis 4:5.

Erol, B., Kusumi, K., Lou, J., Dormans, J. (2002) Etiology of congenital Scoliosis. University of Pennsylvania Orthopaedic Journal 15:37-42.

Freedman, L., Houghton, G., Evans, M. (1986) Cadaveric study comparing the stability of upper distraction hooks used in Harrington instrumentation. Spine 11:579-582.

Gertzbein, S., Macmichael, D., Tile, M. (1982) Harrington instrumentation as a method of fixation in fractures of the spine-A critical analysis of deficiencies. Journal of Bone and Joint Surgery 64:526-529.

Goldberg, C., Kaliszer, M., Moore, D., Fogarty, E., Dowling, F. (2001) Surface topography, Cobb angles, and cosmetic change in scoliosis. Spine 26:55-63.

Grossman, T., Mazur, J., Cummings, R. (1995) An evaluation of the Adams forward bend test and the scoliometer in a scoliosis screening setting. Journal of Pediatric Orthopaedics 15:535-538.

Guidera, K., Hooten, J., Weatherly, W., Highhouse, M., Castellvi, A., Ogden, J., Pug, L., Cook, S. (1993) Cotrel-Dubousset instrumentation: results in 52 patients. Spine 18:427-431.

Gummerson, N., Millner, P. (2010) Spinal fusion for scoliosis, clinical decision-making and choice of approach and devices. Skeletal Radiology 39:939-942.

Harrington, P. (1962) Treatment of scoliosis, correction and interna1 fixation by spine instrumentation. Journal of Bone and Joint Surgery 44:591-610.

Hartley, R., Zisserman, A. (2003) Multiple view geometry in computer vision, 2nd Edition, Cambridge University Press, United Kingdom, 10-12.

Hattori, T., Sakaura, H., Iwasaki, M., Nagamoto, Y., Yoshikawa, H., Sugamoto, K. (2011) In vivo three-dimensional segmental analysis of adolescent idiopathic scoliosis. European Spine Journal 20:1745-1750.

Hirsch, C., Waugh, T. (1968) The introduction of force measurements guiding instrumental correction of scoliosis. Acta Orthopaedica Scandinavica 39:136-144.

Holly, L. (2006) Image-guided spinal surgery. The International Journal of Medical Robotics and Computer Assisted Surgery 2:7-15.

Hwang, S., Samdani, A., Gressot, L., Hubler, K., Marks, M., Bastrom, T., Betz R., Cahill, P. (2012) Effect of direct vertebral body derotation on the sagittal profile in adolescent idiopathic scoliosis. European Spine Journal 21:31-39.

Illés, T., Tunyogi-Csapó, M., Somoskeöy, S. (2011) Breakthrough in three-dimensional scoliosis diagnosis: significance of horizontal plane view and vertebra vectors. European Spine Journal 20:135-143.

Ito, M., Abumi, K., Kotani, Y., Takahata, M., Sudo, H., Hojo, Y., Minami, A. (2010) Simultaneous double-rod rotation technique in posterior instrumentation surgery for correction of adolescent idiopathic scoliosis. Journal of Neurosurgery Spine 12:293-300.

Janssen, M., Vincken, K., Kemp, B., Obradov, M., de Kleuver, M., Viergever, M., Castelein, R., Bartels, L. (2010) Pre-existent vertebral rotation in the human spine is influenced by body position. European Spine Journal 19:1728-1734.

Kanayama, M., Tadano, S., Kaneda, K., Ukai, T., Abumi, K. (1996) A mathematical expression of three-dimensional configuration of the scoliotic spine. ASME Journal of Biomechanical Engineering 118:247-252.

Kim, Y., Lenke, L., Kim, J, Bridwell, K., Cho, S., Cheh, G., Sides, B. (2006) Comparative analysis of pedicle screw versus hybrid instrumentation in posterior spinal fusion of adolescent idiopathic scoliosis. Spine 31:291-298.

Knott, P., Mardjetko, S., Techy, F. (2010) The use of the T1 sagittal angle in predicting overall sagittal balance of the spine. Spine Journal 10:994-998.

Kumar, K. (1996) Spinal deformity and axial traction. Spine 21:653-655.

Kunkel, M., Herkommer, A., Reinehr, M., Bockers, T., Wilke, H. (2011) Morphometric analysis of the relationships between intervertebral disc and vertebral body heights: an anatomical and radiographic study of the thoracic spine. Anatomy 219:375-387.

Labelle, H., Dansereau, J., Bellefleur, C., Jequier, J. (1995) Variability of geometric measurements from three-dimensional reconstructions of scoliotic spines and rib cages. European Spine Journal 4:88-94.

Lafon, Y., Lafage, V., Dubousset, J., Skalli, W. (2009) Intraoperative three-dimensional correction during rod rotation technique. Spine 34:512-519.

Lafon, Y., Lafage, V., Steib, J., Dubousset, J., Skalli, W. (2010) In vivo distribution of spinal intervertebral stiffness based on clinical flexibility tests. Spine 35:186-193.

Lee, S., Suk, S., Chung, E. (2004) Direct vertebral rotation: a new technique of three-dimensional deformity correction with segmental pedicle screw fixation in adolescent idiopathic scoliosis. Spine 29:343-349.

Legaye, J., Duval-Beaupere, G., Hecquet, J., Marty, C. (1998) Pelvic Incidence: A fundamental pelvic parameter for three-dimensional regulation of spinal sagittal curves. European Spine Journal 7:99-103.

Liljenqvist, U., Hackenberg, L., Link, T., Halm, H. (2001) Pullout strength of pedicle screws versus pedicle and laminar hooks in the thoracic spine. Acta Orthopaedica Belgica 67:157-163.

Liljenqvist, U., Allkemper, T., Hackenberg, L., Link, T., Steinbeck, J., Halm, H. (2002) Analysis of vertebral morphology in idiopathic scoliosis with use of magnetic resonance imaging and multiplanar reconstruction. Journal of Bone Joint Surgery 84:359-368.

Little, J., Adam, C. (2010) Development of a computer simulation tool for application in adolescent spinal deformity surgery. Lecture Notes in Computer Science 5958:90-97.

Little, J., Izatt, M., Labrom, R., Askin, G., Adam, C. (2012) Investigating the change in three dimensional deformity for idiopathic scoliosis using axially loaded MRI. Clinical Biomechanics 27:415-421.

Lou, E., Hill, D., Raso, J., Moreau, M., Mahood, J. (2002) Instrumented rod rotator system for spinal surgery. Medical and Biological Engineering and Computing 40:376-379.

Lou, E., Raso, V., Martin, B., Schile, D., Epper, M., Mahood, J., Moreau, M., Hill, D. (2005) Wireless surgical tools for mechanical measurements during scoliosis surgery. IEEE Engineering in Medicine and Biology Society 7:7131-7134.

Lowe, T., Edgar, M., Margulies, J., Miller, N., Raso, V., Reinker, K., Rivard, C. (2000) Etiology of idiopathic scoliosis: current trends in research. Journal of Bone and Joint Surgery 82:1157-1168.

Lowenstein, J., Matsumoto, H,. Vitale, M., Weidenbaum, M., Gomez, J., Lee, F., Hyman, J., Roye, D. (2007) Coronal and sagittal plane correction in adolescent idiopathic scoliosis: a comparison between all pedicle screws versus hybrid thoracic hook lumbar screw constructs. Spine 32:448-452.

Mac-Thiong, J., Labelle, H., Vandal, S., Aubin, C. (2000) Intra-operative tracking of the trunk during surgical correction of scoliosis: a feasibility study. Computer Aided Surgery 5:333-342.

Mac-Thiong, J., Labelle, H., Berthonnaud, E., Betz, R., Roussouly, P. (2007) Sagittal spinopelvic balance in normal children and adolescents. European Spine Journal 16:227-234.

Majdouline, Y., Aubin, C., Sangole, A., Labelle, H. (2009) Computer simulation for the optimization of instrumentation strategies in adolescent idiopathic scoliosis. Medical and Biological Engineering and Computing 47:1143-1154.

Maruyama, T., Takeshita, K. (2008) Surgical treatment of scoliosis: a review of techniques currently applied. Scoliosis 3:6.

Matsumoto, T., Kitahara, H., Minami, S., Takahashi, K., Yamagata, M., Moriya, H., Tamaki, T. (1997) Flexibility in the scoliotic spine: three-dimensional analysis. Journal of Spinal Disorders and Techniques 10: 125-131.

McAfee, P., Bohlman, H. (1985) Complications following Harrington instrumentation for fractures of the thoracolumbar spine. Journal of Bone and Joint Surgery 67:672-685.

McKenna, C., Wade, R., Faria, R., Yang, H., Stirk, L., Gummerson, N., Sculpher, M., Woolacott, N. (2012) EOS 2D/3D X-ray imaging system: a systematic review and economic evaluation. Health Technology Assessment 16:1-188

McLain, R., Sparling, E., Benson, D. (1993) Early failure of short-segment pedicle instrumentation for thoracolumbar fractures. A preliminary report. Journal of Bone and Joint Surgery 75:162-167.

Mehta, J., Gibson, M. (2003) The treatment of neuromuscular scoliosis. Current Orthopaedics 17:313-321.

Mehta, H., Santos, E., Ledonio, C., Sembrano, J., Ellingson, A., Pare, P., Murrell, B., Nuckley, D. (2012) Biomechanical analysis of pedicle screw thread differential design in an osteoporotic cadaver mode. Clinical Biomechanics 27:234-240.

Nachemson, A., Elfström, G. (1969) A force indicating distractor for the Harrington rod procedure. Journal of Bone and Joint Surgery 51:1660-1662.

Nachemson, A., Elfström, G. (1971) Intravital wireless telemetry of axial forces in Harrington distraction rods in patients with idiopathic scoliosis. Journal of Bone and Joint Surgery 53:445-465.

North American Spine Society, http://www.spine.org/.

Ondra, S., Marzouk, S. (2007) Principles of sagittal plane deformity. In: Heary, R., Albert, T. (eds). Spinal deformites: the essentials. Thieme, New York, 59-65.

Pangea System Technique Guide, www.synthes.com.

Patel, A., Schwab, F., Ungar, B., Farcy, J., Lafage, V. (2010) Analysis of sagittal plane deformity and correction. Current Orthopaedic Practice 21:356-363.

Patwardhan, A., Bunch, W., Meade, K., Vanderby, R., Knight, G. (1986) A biomechanical analog of curve progression and orthotic stabilization in idiopathic scoliosis. Journal of Biomechanics 19:103-117.

Paxinos, O., Tsitsopoulos, P., Zindrick, M., Voronov, L., Lorenz, M., Havey, R., Patwardhan, A. (2010) Evaluation of pullout strength and failure mechanism of posterior instrumentation in normal and osteopenic thoracic vertebrae. Journal of Neurosurgery Spine 13:469-476.

Perdriolle, R., Vidal, J. (1987) Morphology of scoliosis: three-dimensional evolution. Orthopedics 10:909-915.

Pierre, C., Kreitz, B., Cassidy, J., Dzus, A. (1998) A study of the diagnostic accuracy and reliability of the scoliometer and Adam's forward bend test. Spine 23:796-802.

Quan, G., Gibson, M. (2010) Correction of main thoracic adolescent idiopathic scoliosis using pedicle screw instrumentation: does higher implant density improve correction. Spine 35:562-567.

Rajwani, T., Bagnall, K., Lambert, R., Videman, T., Kautz, J., Moreau, M., Mahood, J., Raso, V., Bhargava, R. (2004) Using magnetic resonance imaging to characterize pedicle asymmetry in both normal patients and patients with adolescent idiopathic scoliosis. Spine 29:145-152.

Rhee, J., Bridwell, K., Won, D., Lenke, L., Chotigavanichaya, C., Hanson, D. (2002) Sagittal plane analysis of adolescent idiopathic scoliosis: the effect of anterior versus posterior instrumentation. Spine 27:2350-2356.

Riseborough, E., Davies, R. (1973) A genetic survey of idiopathic scoliosis in Boston, Massachusetts. Journal of Bone and Joint Surgery 55:974-982.

Robitaille, M., Aubin, C., Labelle, H. (2007) Intra and interobserver variability of preoperative planning for surgical instrumentation in adolescent idiopathic scoliosis. European Spine Journal 16:1604-1614.

Ronckers, C., Doody, M., Lonstein, J., Stovall, M., Land, C. (2008) Multiple diagnostic x-rays for spine deformities and risk of breast cancer. Cancer Epidemiology Biomarkers and Prevention 17:605-613.

Rose, P., Lenke, L., Bridwell, K., Mulconrey, D., Cronen, G., Buchowski, J., Schwend, R., Sides, B. (2009) Pedicle screw instrumentation for adult idiopathic scoliosis: an improvement over hook/hybrid fixation. Spine 34:852-857.

Roussouly, P., Nnadi, C. (2010) Sagittal plane deformity: an overview of interpretation and management. European Spine Journal 19:1824-1836.

Salehi, L., Mangino, M., De Serio, S., De Cicco, D., Capon, F., Semprini, S., Pizzuti, A., Novelli, G., Dallapiccola, B. (2002) Assignment of a locus for autosomal dominant idiopathic scoliosis (IS) to human chromosome 17p11. Human Genetics 111:401-404.

Salmingo, R., Tadano, S., Fujisaki, K., Abe, Y., Ito, M. (2012a) Corrective force analysis for scoliosis from implant rod deformation. Clinical Biomechanics 27:545-550.

Salmingo, R., Tadano, S., Fujisaki, K., Abe, Y., Ito, M. (2012b) A simple method for in vivo measurement of implant rod three-dimensional geometry during scoliosis surgery. ASME Journal of Biomechanical Engineering 134:054502.

Salmingo, R., Tadano, S., Fujisaki, K., Abe, Y., Ito, M. (2013) Relationship of forces acting on implant rods and degree of scoliosis correction. Clinical Biomechanics 28:122-128.

Schlenk, R., Kowalski, R., Benzel, E. (2003) Biomechanics of spinal deformity. Neurosurgical Focus 14:1-6.

Schlenzka, D., Poussa, M., Muschik, M. (1993) Operative treatment of adolescent idiopathic thoracic scoliosis: Harrington - DTT versus Cotrel-Dubousset instrumentation. Clinical Orthopaedics and Related Research 297:155-160.

Schroth, C. (1992) Introduction to the three-dimensional scoliosis treatment according to Schroth. Physiotherapy 78:810-815.

Seller, K., Wahl, D., Wild, A., Krasupe, R., Schneider, E., Linke, B. (2007) Pullout strength of anterior spinal instrumentation: a product comparison of seven screws in calf vertebral bodies. European Spine Journal 16:1047-1054.

Smith, J. (2001) Adult deformity: management of sagittal plane deformity in revision adult spine surgery. Current Opinion in Orthopedics 12:206-215.

Smith, H., Welsch, M., Sasso, R., Vaccaro, A. (2008) Comparison of radiation exposure in lumbar pedicle screw placement with fluoroscopy vs computer-assisted image guidance with intraoperative three-dimensional imaging. Journal of Spinal Cord Medicine 31:532-537.

Steinmetz, M., Rajpal, S., Trost, G. (2008) Segmental spinal instrumentation in the management of scoliosis. Neurosurgery 63:131-138.

Stokes, I., Bigalow, L., Moreland, M. (1987) Three-dimensional spinal curvature in idiopathic scoliosis. Journal of Orthopaedic Research 5:102-113.

Stokes, I. (1989) Axial rotation component of thoracic scoliosis. Journal of Orthopaedic Research 7:702-708.

Stokes, I. (1994) Three-dimensional terminology of spinal deformity. Spine 19:236-248.

Storer, S., Vitale, M., Hyman, J., Lee, F., Choe, J., Roye, D. (2005) Correction of adolescent idiopathic scoliosis using thoracic pedicle screw fixation versus hook constructs. Journal of Pediatric Orthopedics 25:415-419.

Tadano, S., Kanayama, M., Ukai, T., and Kaneda, K. (1996) Morphological modeling and growth simulation of idiopathic scoliosis. In: Hayashi, K., Ishikawa, H. (eds.), Computational biomechanics, Springer, Tokyo, 67-87.

Tribus, C. (2003) Degenerative lumbar scoliosis: evaluation and management. Journal of the American Academy of Orthopaedic Surgeons 11:174-183.

van den Hout, J., van Rhijn, L., van den Munckhof, R., van Ooy, A. (2002) Interface corrective force measurements in Boston brace treatment. European Spine Journal 11:332-335.

Vialle, R., Levassor, N., Rillardon, L., Templier, A., Skalli, W., Guigui, P. (2005) Radiographic analysis of the sagittal alignment and balance of the spine in asymptomatic subjects. Journal of Bone and Joint Surgery 87:260-267.

Vrtovec, T., Janssen, M., Likar, B., Castelein, R., Viergever, M., Pernus, F. (2012) A review of methods for evaluating the quantitative parameters of sagittal pelvic alignment. Spine Journal 12:433-446.

Wade, R., Yang, H., McKenna, C., Faria, R., Gummerson, N., Woolacott, N. (2012) A systematic review of the clinical effectiveness of EOS 2D/3D X-ray imaging system. European Spine Journal 22:296-304.

Wang, X., Aubin, C., Crandall, D., Labelle, H. (2011a) Biomechanical comparison of force levels in spinal instrumentation using monoaxial versus multi degree of freedom postloading pedicle screws. Spine 36:95-104.

Wang, X., Aubin, C., Crandall, D., Labelle, H. (2011b) Biomechanical modeling and analysis of a direct incremental segmental translation system for the instrumentation of scoliotic deformities. Clinical Biomechanics 26:548-555.

Weiss, H., Wekmann, M., Stephan, C. (2007) Correction effects of the ScoliOlogiC® "Cheneau light" brace in patients with scoliosis. Scoliosis 2:2.

White, A., Panjabi, M. (1990) Clinical biomechanics of the spine, 2nd Edition, Lippincott, Philadelphia, 30-342.

Willers, U., Hedlund, R., Aaro, S., Normelli, H., Westman, L. (1993) Principles, indications, and complications of spinal instrumentation. Spine 18:713-717.

Yeung, A., Ottaviano, D., Lee, D., Haher T. (2003) Spine testing modalities. In: DeWald, R., Arlet, V., Carl, A., O'Brien, M. (eds.), Spinal deformities the comprehensive text, Thieme, New York, 176-186.

Zielke, K. (1982) Ventral derotation spondylodesis. Results of treatment of cases of idiopathic lumbar scoliosis. Zeitschrift für Orthopädie und ihre Grenzgebiete 120:320-329.

List of Publications

Peer-Reviewed Scientific Journals:

1. Salmingo RA, Tadano S, Fujisaki K, Abe Y, Ito M (2013) Relationship of Forces Acting on Implant Rods and Degree of Scoliosis Correction. Clinical Biomechanics (28)2:122-128.
2. Salmingo R, Tadano S Fujisaki K, Abe Y, Ito M (2012) Corrective Force Analysis for Scoliosis From Implant Rod Deformation. Clinical Biomechanics (27)6:545-550.
3. Salmingo RA, Tadano S, Fujisaki K, Abe Y, Ito M (2012) A Simple Method for In Vivo Measurement of Implant Rod Three-Dimensional Geometry During Scoliosis Surgery. ASME Journal of Biomechanical Engineering (134)5:054502.1-054502.5.

Currently Under Revision:

4. Salmingo RA, Tadano S, Abe Y, Ito M (2012) Influence of Implant Rod Curvature on Sagittal Correction of Scoliosis Deformity. [Minor Revisions Submitted on June 27, 2013, Submitted on August 30, 2012, The Spine Journal].

Currently in Preparation for Submission:

5. Salmingo RA, Tadano S, Abe Y, Ito M. (2013) Intraoperative Implant Rod Three-Dimensional Geometry Measured by Dual Camera System During Scoliosis Surgery. (in preparation for Journal of Biomechanics)

Other Publications (in Japanese):

1. 安倍雄一郎, 伊東学, 鐙邦芳, 藤崎和弘, Remel Salmingo, 但野茂, 久田雄一郎, 高畑雅彦, 須藤英毅, 長濱賢, 中原誠之 (2013) 側弯症矯正手術における内固定金属の力学分担:クロスリンクによる応力分散効果. Journal of Spine Research 4(3):750.
2. 伊東学, 安倍雄一郎, 鐙邦芳, 藤崎和弘, Remel Salmingo, 但野茂, 小谷善久, 須藤英毅, 長濱賢, 岩田玲, 三浪明男 (2011) 特発性側弯症後方矯正手術時における脊椎インプラントの応力評価. Journal of Spine Research 2(3):609.

Conference Proceedings:

1. Salmingo RA, Tadano S, Abe Y, Ito M (2013) Influence of Spinal Rod Curvature on Scoliosis Sagittal Correction. Transactions of the 2013 Orthopaedic Research Society Annual Meeting. January 26-29, 2013 in San Antonio, Texas, USA.
2. Salmingo R, Tadano S, Abe Y, Ito M (2013) Scoliosis Sagittal Correction Dependence on Implant Rod Curvature. In Proceedings of the 25th JSME Bioengineering Conference. January 9-11, 2013 in Tsukuba, JAPAN.

3. Salmingo RA, Tadano S, Fujisaki K, Abe Y, Ito M (2012) Corrective Force in Rods During Scoliosis Treatment. Transactions of the 2012 Orthopaedic Research Society Annual Meeting. February 3-7, 2012 in San Francisco, California, USA.
4. Salmingo R, Fujisaki K, Tadano S, Abe Y, Ito M (2012) Effect of Screw Placement Configurations to the Corrective Forces in Rods During Scoliosis Surgery. In Proceedings of the 24th JSME Bioengineering Conference. January 7-8, 2012 in Osaka, JAPAN.
5. Salmingo R, Fujisaki K, Tadano S, Abe Y, Ito M (2011) Relationship Between the Force on Implant Screw and the Corrective Angle of Scoliosis Deformity. In Proceedings of the 38th Annual Meeting of the Japanese Society for Clinical Biomechanics. November 18-19, 2011 in Kobe, JAPAN
6. Salmingo R, Fujisaki K, Tadano S, Abe Y, Ito M (2011) Corrective Forces Acting on Implant Rods in Scoliosis Surgery. In Proceedings of the 50th Japanese Society for Medical and Biological Engineering part of 91st Hokkaido Medical Congress. October 8, 2011 in Sapporo, JAPAN. Received the "Best Research Presentation Award".
7. Fujisaki K, Salmingo RA, Tadano S, Abe Y, Ito M (2011) Corrective Force Analysis in Spinal Rods Fixation for Scoliosis Deformity. Transactions of the 2011 Orthopaedic Research Society Annual Meeting. January 13-16, 2011 in Long Beach, California, USA.
8. Salmingo R, Fujisaki K, Tadano S, Abe Y, Ito M (2010) Force Analysis of Corrective Rod for Scoliosis Treatment. In Proceedings of the 21st JSME Conference on Frontiers in Bioengineering. November 12-13, 2010 in Kanazawa, JAPAN.
9. [In Japanese] 安倍 雄一郎, 伊東 学, 鐙 邦芳, 藤崎 和弘, Remel Salmingo, 小谷 善久, 須藤 英毅, 三浪 明男 (2010) Finite Element Deformation Analysis of Spinal Rod During Scoliosis Corrective Surgery. In Proceedings of the 37th Annual Meeting of the Japanese Society for Clinical Biomechanics. November 1-2, 2010 in Kyoto, JAPAN.
10. Salmingo R, Giri B, Fujisaki K, Takao S, Tadano S, Abe Y, Ito M (2010) Scoliosis Corrective Force Estimation From the Implant Rod Deformation. In Proceedings of the 2010 JSME Conference on Robotics and Mechatronics. June 13-16, 2010 in Asahikawa, JAPAN.

Acknowledgements

Many people have been a part of my graduate education, as friends, family, teachers and colleagues.

First and foremost, I would like to express my deep and sincere gratitude to my academic supervisor, Professor Shigeru Tadano who gave me the opportunity to work in his laboratory. I appreciate his continuous guidance and encouragement. His support helped me in all the time of research and writing of this thesis. I am deeply grateful with Assoc. Professor Masahiro Todoh for his kind support and guidance which have been of great value in this study. He had inspired me not only in doing research but also to live in a foreign country. I wish to convey my sincere gratitude to Assoc. Professor Kazuhiro Fujisaki, currently in Hirosaki University, for devoting his precious time, most especially for giving me valuable suggestions and untiring help.

Special thanks to the collaborating orthopaedic surgeons Dr. Yuichiro Abe and Dr. Manabu Ito of the Department of Orthopaedic Surgery for providing me the CT images and clinical insights of scoliosis. Their medical expertise had challenged me to do research in scoliosis. I greatly appreciate their hard work through our meaningful discussions.

I wish to express my warm and sincere thanks to my senior lab mate, Dr. B Giri for his personal guidance and assistance that he had given me especially in my first few months here in Japan. I consider him not only my senior lab mate but also a dear friend of mine. I also thank my official tutor Dr. R Takeda for helping me a lot during my first year in Japan. I am truly indebted for his continuous support and guidance even up to now. I warmly thank my other senior lab mates, Dr. S Takao for introducing ANSYS, Dr. Y Nakajima and Dr. S Yamada for their excellent advices and friendly help which have been of great value in this study. I want to thank my fellow lab members Dr. Y Zhang, Mr. S Keeratihattayakorn, Mr. H Suzuki and Dr. K Endo, I wish you all the best in your future research endeavors.

I also thank our laboratory technical official Mr. Toshiaki Takada for his technical support not to mention his sincere kindness towards me and our usual long conversations over a cup of Japanese green tea. I would like to thank our secretary Ms. Yumi Yamazaki for helping me a lot during my travels and in facilitating the official procedures in Hokkaido University. I also appreciate her kindness during my stay in the laboratory.

I thank the professors in the Division of Human Mechanical Systems and Design. Their efforts during the coursework had been a great value in completing my graduate studies in Hokkaido University. I would like to convey my special thanks to Professor Toshiro Ohashi and Professor Itsuro Kajiwara who were the examiners during the oral examination and for giving me valuable advices that helped me prepare for the final defense. I would like to thank the professors in our division who were also the examiners during the final defense, Professor Katsuhiko Sasaki, Professor Takashi Nakamura,

Professor Kazuaki Sasaki, Professor Yukinori Kobayashi and Professor Yoshihiro Narita. I would like to thank Professor Ryutaro Himeno and Professor Hideo Yokota of RIKEN, and Professor Kikuo Umegaki who were also the examiners of this dissertation.

I also wish to extend my appreciation to the previous and current graduate and undergraduate students whom I met at Hokkaido University. Thank you for the friendship and for making me feel welcome.

I would like to acknowledge the Monbukagakusho (MEXT) of the Japanese Government for providing me this intangible scholarship grant.

The road to my graduate degree has been long and winding. I would like to thank some people from the early days who had inspired me to pursue research in orthopaedic biomechanics. To my former boss at Orthopaedic Innovations Manufacturing Incorporated, Ramon B. Gustilo, MD, world-class orthopaedic surgeon, one of the top-cited clinical orthopaedics researcher, very famous but humble man, thank you for giving me my first opportunity to conduct research in orthopaedic implants. I look up to you with so much admiration and respect. Likewise to Sir Bobby and Sir Jude, it was an honor to be working with two great bioengineers like you. They had remarkably influenced my entire career in the field of orthopaedic research.

Sincere thanks to the HAFS (Hokkaido Association of Filipino Students) family for their support and also for never letting me feel that I am away from home.

I owe my loving thanks to my tooth fairy and wife, Dr. Joanna Grace T. Salmingo. She helped me to concentrate on completing this dissertation and supported me mentally during the course of this work. Most of all, for temporarily giving up her dental practice in the Philippines, without her help, inspiration and encouragement, this study would not have been completed. I also thank my daughter Reanna Airi for giving me great motivation to achieve my goals in life.

I would like to thank my parents Dr. Renato Salmingo and Melba Salmingo, my parents-in-law Chief Eng'r. Juanito Tabalina and Diana Tabalina, my brothers, sister and my wife's family, thank you for their absolute confidence in me and for their unflagging love and support; this dissertation is simply impossible without them.

To the almighty one, I thank GOD for all the graces he bestowed upon me especially for the gift of knowledge, love, family and friends. I thank you for giving me strength and courage to surpass every trial that comes my way. May your name be exalted, honored and glorified.

Remel Alingalan Salmingo
Sapporo, Hokkaido, Japan
September 2013